Electronic Supporting Information

1 Synthesis

1.1 Experimental. All reagents were analytical grade and used as received. Column chromatography was performed with silica gel 60 (particle size 35-70 µm, 230-400 mesh, Merck). NMR and mass spectra were measured by the Department of Organic Chemistry, University of Münster. NMR spectra were recorded on an DPX/Avance 300 or an Avance 400 from Burker Analytische Messtechnik (Karlsruhe, Germany) for some of the Pt(II) complexes, the ligands and their precursors and on an DD2 600 from Agilent for the Pt(II) complexes. The ^{1}H NMR chemical shifts (δ) of the signals are given in parts per million and referenced to residual protons in the deuterated solvents: DMSO-d_6 (2.50 ppm), CD_2Cl_2-d_2 (5.32 ppm), $CDCl_3$-d (7.26 ppm) or THF-d_8 (3.58 ppm). The ^{19}F NMR chemical shifts are referenced to $CFCl_3$ as an internal standard, the ^{195}Pt NMR chemical shifts are referenced to Na_2PtCl_6 and the ^{31}P NMR chemical shifts are referenced to phosphoric acid as an external standard. The signal multiplicities are abbreviated as follows: s, singlet; d, doublet; t, triplet; q, quartet; m, multiplet. All coupling constants (J) are given in Hertz. High resolution mass spectrometry (HRMS) was performed via electrospray ionization (ESI) on a Bruker Daltonics MicroTof with loop injection.

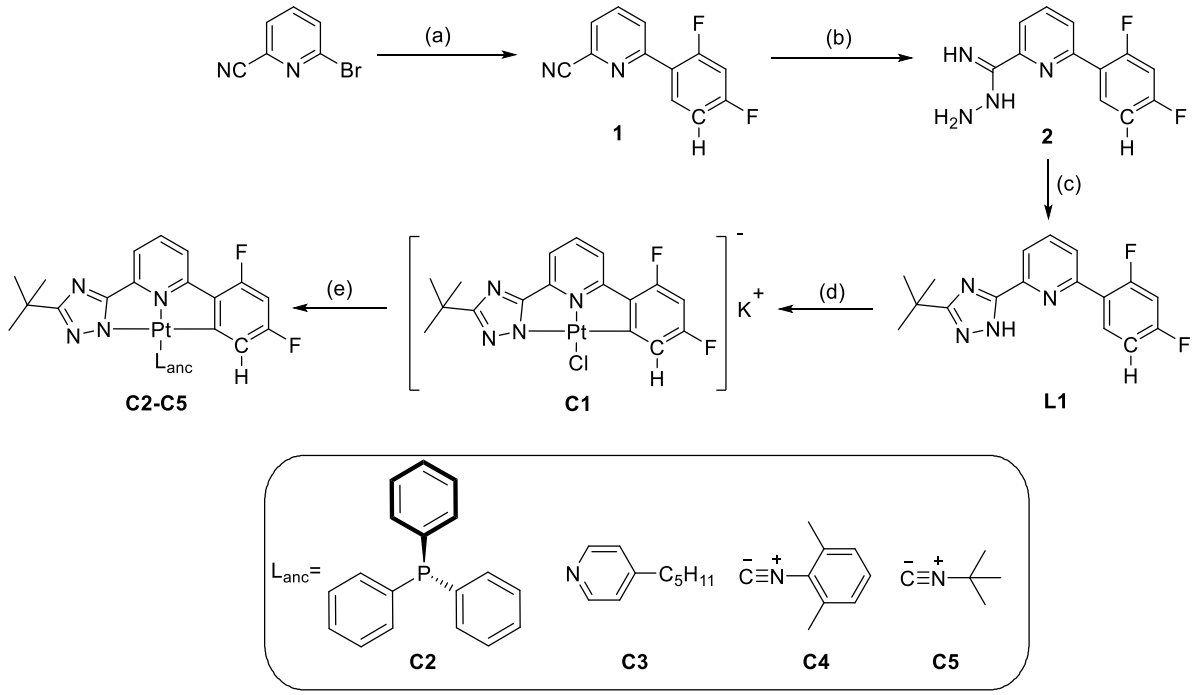

Scheme S1. *Synthetic route towards the C^N^N ligand and the corresponding Pt(II) complex. (a) 2,4-Difluorophenylboronic acid, $Pd(PPh_3)_4$, K_2CO_3, THF, N_2, reflux, 24 h. (b) N_2H_4 x H_2O, EtOH, rt. (c) 1) tBuC(O)Cl, K_2CO_3, DMF, 0°C to rt, 2) ethylene glycol, 160°C. (d) K_2PtCl_4, acetic acid, reflux. (e) L_{anc}, THF*

*6-(2,4-Difluorophenyl)picolinonitrile (**1**)*

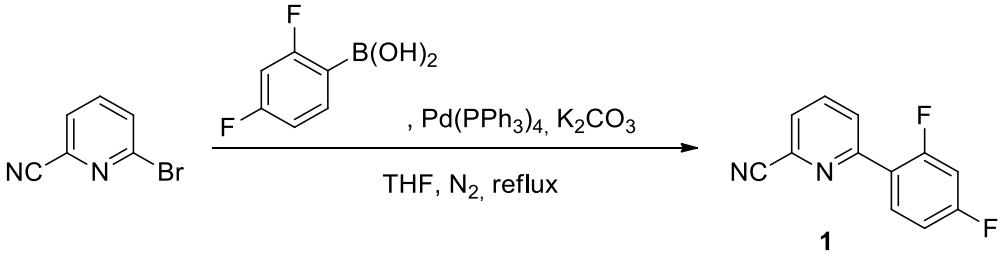

2-Bromo-6-cyanopyridine (2 g, 11.04 mmol), $Pd(PPh_3)_4$ (1.275 g, 1.104 mmol) and $K_2CO_{3(aq)}$ (2 M, 16 mL) are combined in THF (200 mL) and degassed by nitrogen bubbling. 2,4-Difluorophenylboronic acid (2.085 g, 13.2 mmol) is added and the reaction mixture was degased again and refluxed for 12 h to yield a yellow solution. Next, the solvent was removed under reduced pressure and the occurring precipitate was dissolved in ethyl acetate. Residual salt was removed by solvent extraction with brine. The combined organic phases were dried with $MgSO_4$, filtered, concentrated and the crude compound was adsorbed onto silica gel. This was loaded onto a column packed with silica gel to perform a column chromatography separation with hexane / ethyl acetate as eluent (8:2) to yield a white solid (1.69 g, 71%). ^{1}H NMR (300 MHz, CD_2Cl_2) δ 8.08 (td, *J* = 8.9, 6.6 Hz, 1H), 8.01 (ddd, *J* = 8.2, 1.9, 1.1 Hz, 1H), 7.98 – 7.86 (m, 1H), 7.68 (dd, *J* = 7.6, 1.1 Hz, 1H), 7.14 – 7.03 (m, 1H), 6.98 (ddd, *J* = 11.4, 8.8, 2.5 Hz, 1H). ^{19}F NMR (282 MHz, CD_2Cl_2): δ -107.90, -112.49. HRMS (ESI+, MeOH, *m/z*) calcd. for $[M + H]^+$, 217.0577; found, 217.0575 ($[M + H]^+$); calcd. for $[M + Na]^{+,}$ 239.0391; found, 239.0391 ($[M + Na]^+$).

*6-(2,4-Difluorophenyl)picolinimidohydrazide (**2**).*

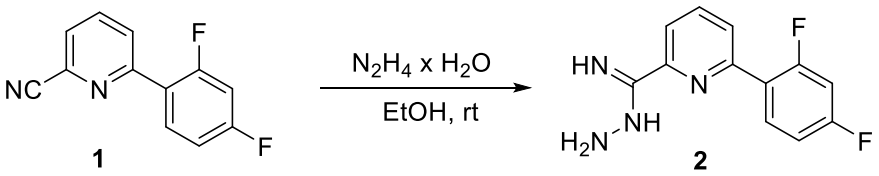

To a solution of **1** (1.03 g, 4.7 mmol) in EtOH (30 mL) hydrazine monohydrate (2.4 mL, 47 mmol) was added. The reaction mixture was stirred at room temperature overnight. The solvent was removed to a minimum at reduced pressure and water was added to give a white precipitate, which was filtered off and washed thoroughly with water to give the final product (0.75 g, 65%). ^{1}H NMR (300 MHz, DMSO-d_6) δ 8.24 (td, *J* = 9.0, 6.9 Hz, 1H), 7.90 (dd, *J* = 8.0, 1.4 Hz, 1H), 7.85 (t, *J* = 7.6 Hz, 1H), 7.70 (ddd, *J* = 7.3, 2.4, 1.4 Hz, 1H), 7.40 (ddd, *J* =

11.8, 9.3, 2.5 Hz, 1H), 7.30 – 7.16 (m, 1H), 5.84 (s, 2H), 5.40 (s, 1H). ^{19}F NMR (282 MHz, DMSO) δ -109.27, -112.26. HRMS (ESI+, MeOH, *m/z*) calcd. for $[M + H]^+$, 249.0946; found, 249.0952 ($[M + H]^+$).

*2-(3-(tert-butyl)-1H-1,2,4-triazol-5-yl)-6-(2,4-difluorophenyl)pyridine (**3**).*

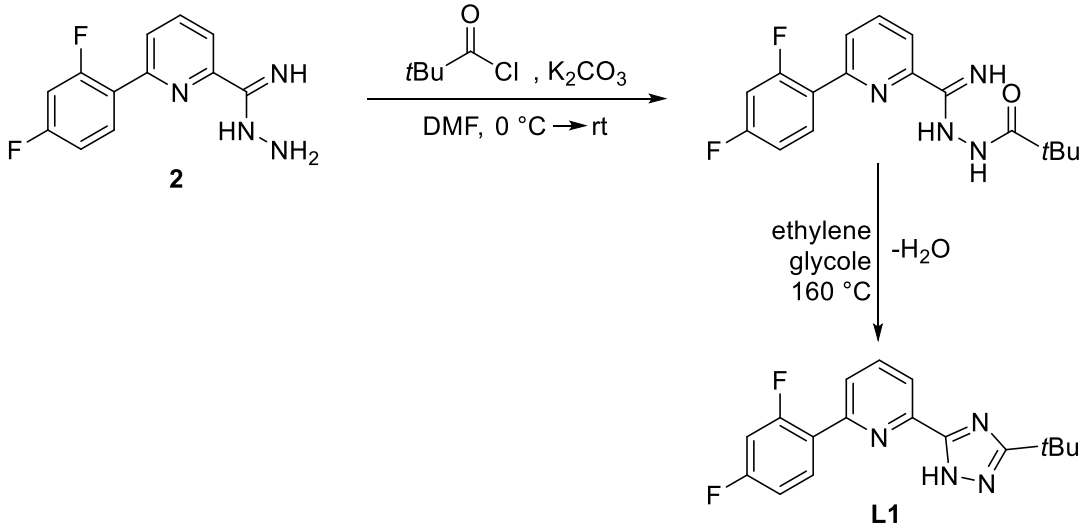

A flame-dried, nitrogen-purged Schlenk tube was loaded with **2** (1.8 g, 7.25 mmol) and sodium carbonate (1.1 g, 7.98 mmol), evacuated, gently heated, and refilled with nitrogen after being cooled to room temperature. Next, dry N,N-DMF (50 mL) was added, and the suspension was cooled to 0 °C. In a separately prepared Schlenk tube, trimethylacetyl chloride was handled the same way as above (918 mg, 7.61 mmol) in N,N-DMF (60 mL). This solution was then slowly added to the cooled suspension under strong stirring. A precipitate was formed overnight while the reaction mixture was allowed to warm up to room temperature. After adding a small amount of water, the suspension was stirred strongly for one hour and then filtered and washed with few water. This intermediate was dried under vacuum and used without further purification for the next step, where it is suspended in ethylene glycol (0.5 mL / 100 mg ratio). The suspension was then heated to 160 °C for 2 h, during which all material is dissolved. After cooling to room temperature, the volume is doubled by adding water, causing the product **L1** to precipitate. The suspension is stirred for another hour, filtered, and the solid is washed with water. Column chromatography was performed on silica gel with hexane / ethyl acetate as eluent, to yield a white solid (1.93 g, 85 %). ^{1}H NMR (300 MHz, CD_2Cl_2) δ 8.20 (m, 1H), 8.06 (d, *J* = 7.6 Hz, 1H), 7.89 (t, *J* = 7.8 Hz, 1H), 7.79 (d, *J* = 8.1 Hz, 1H), 7.10 – 6.88 (m, 2H), 1.42 (s, 9H). ^{19}F NMR (282 MHz, CD_2Cl_2) δ -107.93, -111.20. ^{13}C NMR (75 MHz, $CDCl_3$) δ 152.44,

147.00, 137.88, 132.39, 132.26, 125.25, 125.12, 120.67, 112.10, 111.87, 104.89, 104.55, 104.19, 32.96, 29.54. HRMS (ESI+, MeOH, *m/z*) calcd. for $[M + H]^+$, 315.14158; found, 315.14148 ($[M + H]^+$); calcd. for $[M + Li]^+$, 321.14979 ; found, 321.14949 ($[M + Li]^+$); calcd. for $[2M + Na]^+$, 651.25783; found, 651.25772 ($[M + Na]^+$).

Synthesis of the Pt(II) Complex ***C1***.

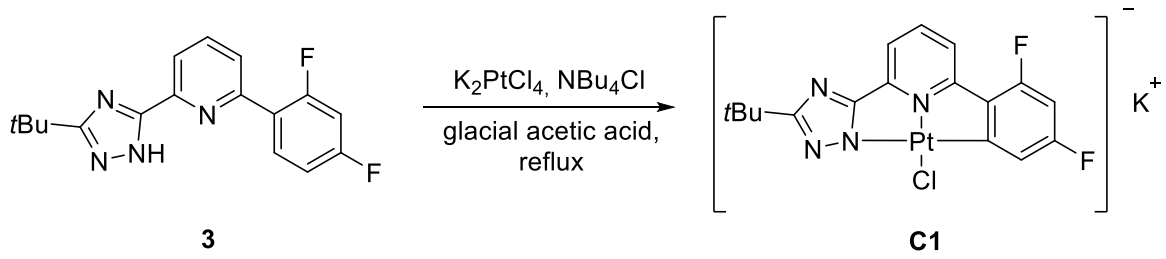

A mixture of the tridentate ligand **L1** (100 mg, 0.31 mmol), K_2PtCl_4 (132 mg, 0.31 mmol) and NBu_4Cl (9 mg, 0.031 mmol) were refluxed in glacial acetic acid (40 mL) for 24 h. After cooling down the yellowish solution to room temperature, the solvent was removed to a minimum and a dark green precipitate was formed which was filtered off and washed several times with water to give the complex **C1**. HRMS (ESI+, MeOH, *m/z*) calcd. for $[M + H + Na]^+$, 566.04945; found, 566.04958 ($[M + H + Na]^+$); calcd. for $[2M + 2H +Na]^{+,}$ 1110.10826; found, 1110.10983 ($[M + Na]^+$). HRMS (ESI-, MeOH, *m/z*) calcd. for $[M]^-$, 543.1; found 543.1 ($[M^-]$); calcd. for $[2M + H]^{-,}$ 1086.1; found, 1085.6 ($[2M + H]^-$); calcd. for $[2M + 2H + Cl]^{-,}$ 1123.1; found, 1122.7 ($[2M + 2H + Cl]^-$).

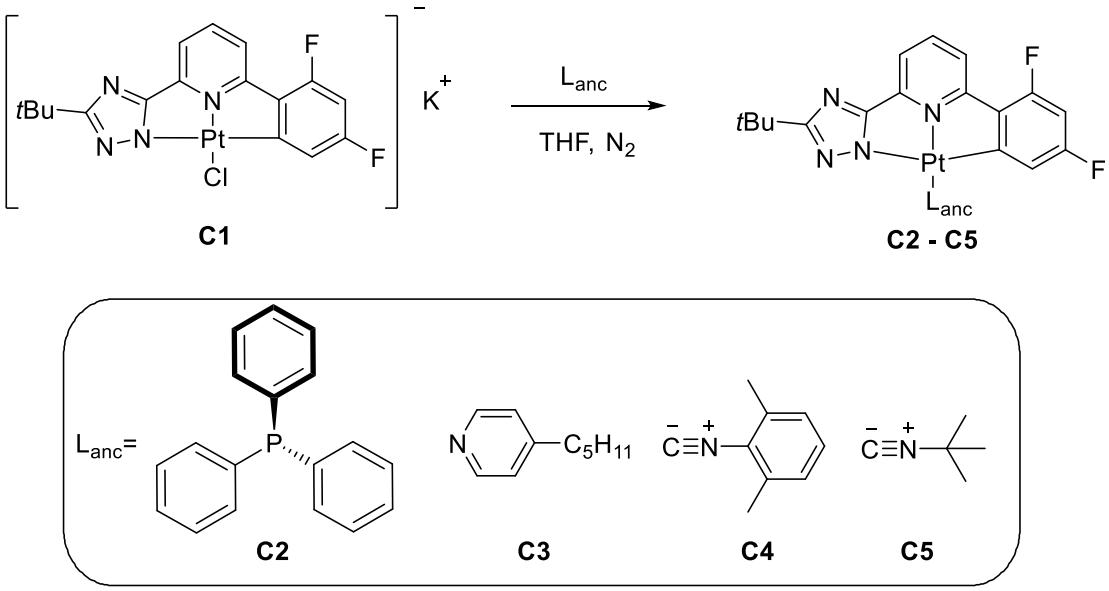

Scheme S2. *General Procedure for the Synthesis of the Pt(II) Complexes **C2-C5***.

The dark-green Pt(II) precursor **C1** was dissolved in THF to give a yellow solution. Next, a slight excess of the ancillary ligand L_{anc} (1.1 eq.) was brought into the reaction vessel. Detailed reaction conditions for each complex are given below. After the reaction is finished the complex was adsorbed onto silica gel and loaded onto a column packed with silica gel, and a column chromatographic separation was performed using the eluent given in the information below to give the final product **C2-C5** as a coloured solid. Crystals were grown for complex **C2** and **C3** by vapour diffusion method using ethylacetate as solvent.

*Detailed reaction conditions and characterization for complexes **C2-C5***

C2

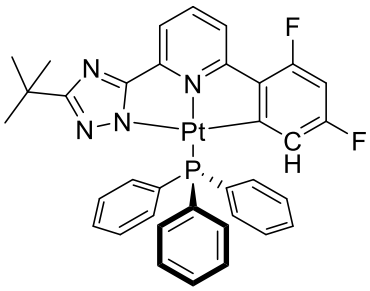

The reaction was thoroughly blubbered with N_2 before P(Phenyl)$_3$ was added. Then the reaction mixture was refluxed in THF overnight. Column chromatography on silica gel was

performed with hexane / ethyl acetate as eluent (8:2) to obtain a green/yellow powder (78 %). ^{1}H NMR (600 MHz, THF-d_8) δ 7.93 (t, *J* = 8.0 Hz, 1H), 7.81 (dd, *J* = 12.1, 7.3 Hz, 6H), 7.76 (d, *J* = 8.2 Hz, 1H), 7.60 (d, *J* = 7.8 Hz, 1H), 7.48 (td, *J* = 7.3, 1.7 Hz, 3H), 7.41 (td, *J* = 7.7, 2.3 Hz, 6H), 6.53 (ddd, *J* = 12.0, 8.8, 2.4 Hz, 1H), 5.99 (d, *J* = 9.7 Hz, 1H), 1.09 (s, 9H). ^{31}P NMR (243 MHz, THF) δ 21.96 (^{1}J(^{31}P, ^{195}Pt) = 4028 Hz)). ^{19}F NMR (564 MHz, THF) δ -108.30, -111.36. ^{195}Pt NMR (107 MHz, THF-d_8) δ -4193.05 (d, *J* = 4021.7 Hz). HRMS (ESI+, MeOH, *m/z*) calcd. for $[M + H]^+$, 770.18213; found, 770.18069 ($[M + H]^+$); calcd. for $[2M+ H]^{+,}$ 1539.35627; found, 1539.35452 ($[2M + H]^+$); calcd. for $[2M+ Na]^{+,}$ 1561.33822; found, 1561.33639 ($[2M + Na]^+$).

C3

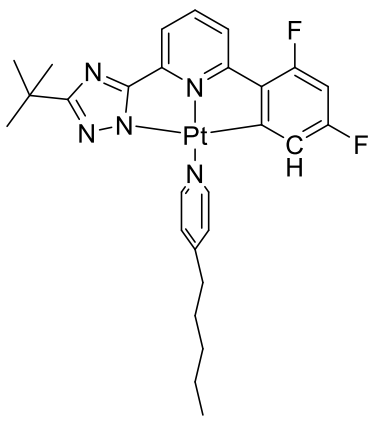

After the addition of 4-pentylpyridine the reaction mixture was refluxed overnight under nitrogen atmosphere. Column chromatography was performed with CH_2Cl_2 / MeOH as eluent (98:2). Recrystallization from CH_2Cl_2 / hexane gave an orange solid which was additional purified by preparative TLC with the same eluent used above to give **C3** (11 %). ^{1}H NMR (600 MHz, THF-d_8) δ 8.95 (d, *J* = 6.5 Hz, 2H), 7.79 (t, *J* = 8.0 Hz, 1H), 7.55 (d, *J* = 8.1 Hz, 1H), 7.46 (d, *J* = 7.8 Hz, 1H), 7.42 (d, *J* = 6.2 Hz, 2H), 6.61 (ddd, *J* = 11.7, 9.2, 2.2 Hz, 1H), 6.19 (dd, *J* = 8.5, 2.2 Hz, 1H), 2.78 – 2.73 (m, 2H), 2.50 (s, 6H), 1.35 (s, 9H), 0.95 (t, *J* = 7.0 Hz, 3H).^{19}F NMR (564 MHz, THF) δ -107.55, -111.69. ^{13}C NMR (151 MHz, THF) δ 173.41, 164.71, 156.35, 154.72, 153.42, 142.27, 127.17, 119.45, 119.34, 116.08, 115.67, 115.57, 100.19, 100.01, 99.84, 36.09, 34.02, 32.63, 30.82, 30.52, 27.93, 23.49, 14.46. HRMS (ESI+, MeOH, *m/z*) calcd. for $[M + H]^+$, 657.21137; found, 657.21157 ($[M + H]^+$); calcd. for $[2M+ H]^{+,}$ 1539.35627; found, 1539.35452 ($[2M + H]^+$) $]^+$); calcd. for $[2M+ Na]^{+,}$ 1561.33822; found, 1561.33639 ($[2M + Na]^+$).

C4

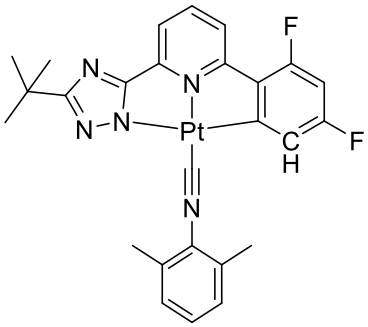

After the addition of 2-isocyano-1,3-dimethylbenzene, the reaction mixture was stirred 3h at room temperature under nitrogen atmosphere. An orange precipitate was formed which was purified by column chromatography using CH_2Cl_2 / MeOH (98:2) as eluent to give complex **C4**. (70 %). ^{1}H NMR (300 MHz, Chloroform-*d*) δ 9.10 (d, *J* = 7.6 Hz, 1H), 8.02 (t, *J* = 8.1 Hz, 1H), 7.90 (d, *J* = 8.3 Hz, 1H), 7.40 – 7.30 (m, 1H), 7.23 (d, *J* = 7.6 Hz, 2H), 6.96 (dd, *J* = 7.9, 2.4 Hz, 1H), 6.65 (ddd, *J* = 11.4, 8.8, 2.4 Hz, 1H), 2.61 (s, 6H), 1.57 (s, 9H).^{19}F NMR (564 MHz, $CDCl_3$) δ -102.88, -107.51. HRMS (ESI+, MeOH, *m/z*) calcd. for $[M + H]^+$, 639.16440; found, 639.16414 ($[M + H]^+$); calcd. for $[M+ Na]^{+,}$ 679.19331; found, 679.19346 ($[M + Na]^+$); calcd. for $[2M+ Na]^{+,}$ 1335.39662; found, 1335.39810 ($[2M + Na]^+$).

C5

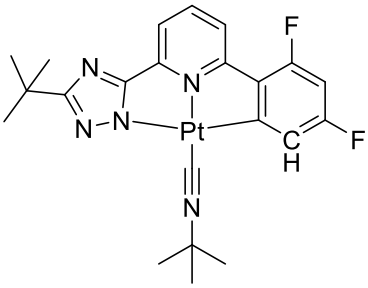

The mixture immediately turned red, after adding *tert*-butyl isocyanide to the reaction vessel. Next, the reaction mixture was stirred for 1h at room temperature under nitrogen atmosphere. After removing the solvent under reduced pressure, a dark-red compound is obtained. Purification was performed by column chromatography on silica gel using CH_2Cl_2 / MeOH (98:2) as eluent to give complex **C5** (78 %). The color of the compound indicates a strong aggregation of complex **C5**, confirmed by the emission properties in solid state. Because of that, NMR spectroscopy was measured temperature dependent with low concentrations (299 K, 323 K, 348 K and 373 K) to get the single molecule signals, with best results at 323 K. ^{1}H NMR

(600 MHz, DMSO-d_6, 323 K) δ 8.25 (s, 1H), 7.96 (d, J = 39.6 Hz, 2H), 7.09 (s, 1H), 6.72 (s, 1H), 1.70 (s, 9H), 1.53 (d, J = 17.5 Hz, 9H). ^{19}F NMR (564 MHz, DMSO, 323 K) δ -103.99, -107.26. HRMS (ESI+, MeOH, *m/z*) calcd. for $[M + H]^+$, 591.16437; found, 591.16362 ($[M + H]^+$).

1.2 NMR spectra.

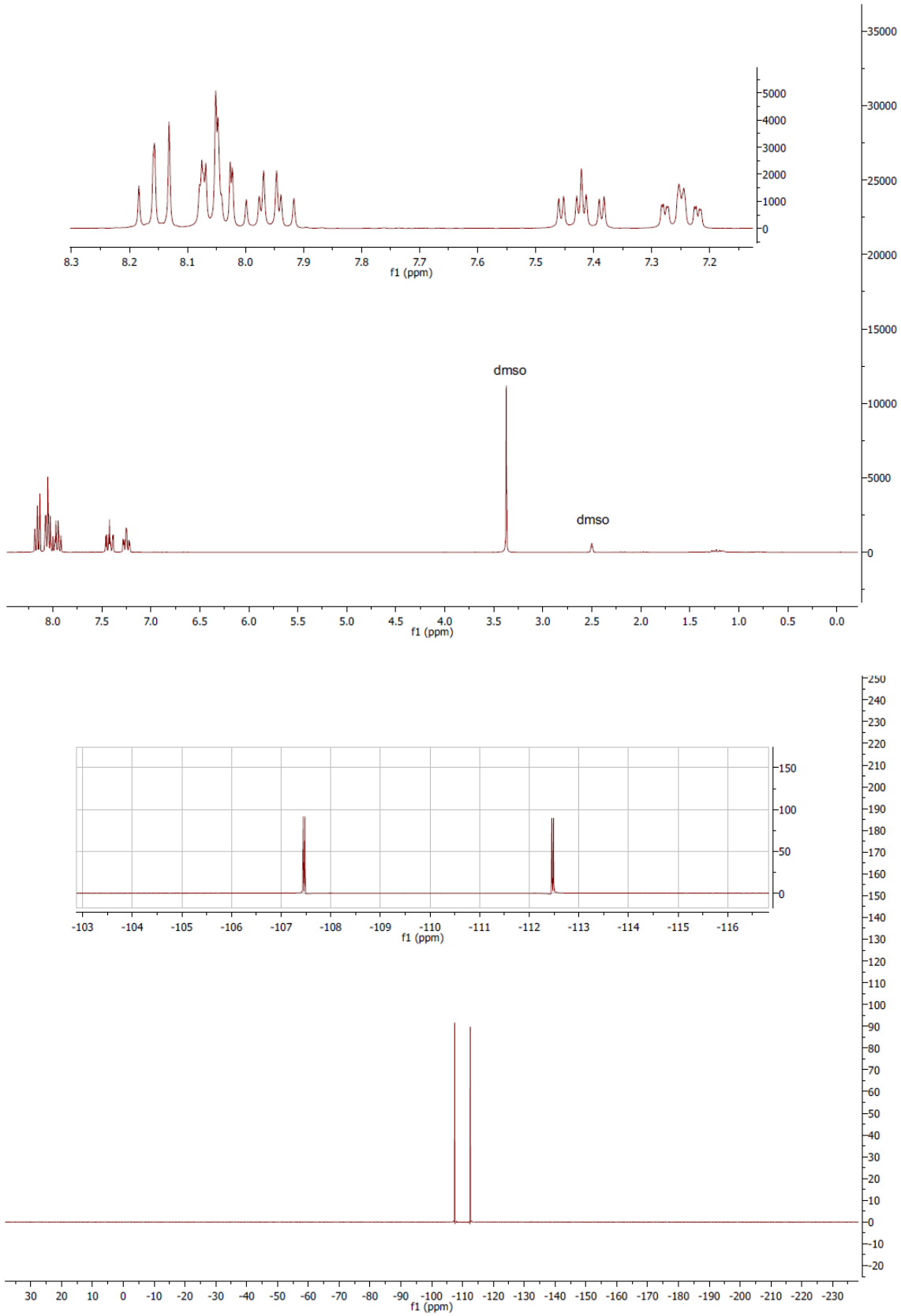

Spectra S1. *NMR spectra of* ***1****. (Top: ^{1}H-NMR Bottom: ^{19}F-NMR)*

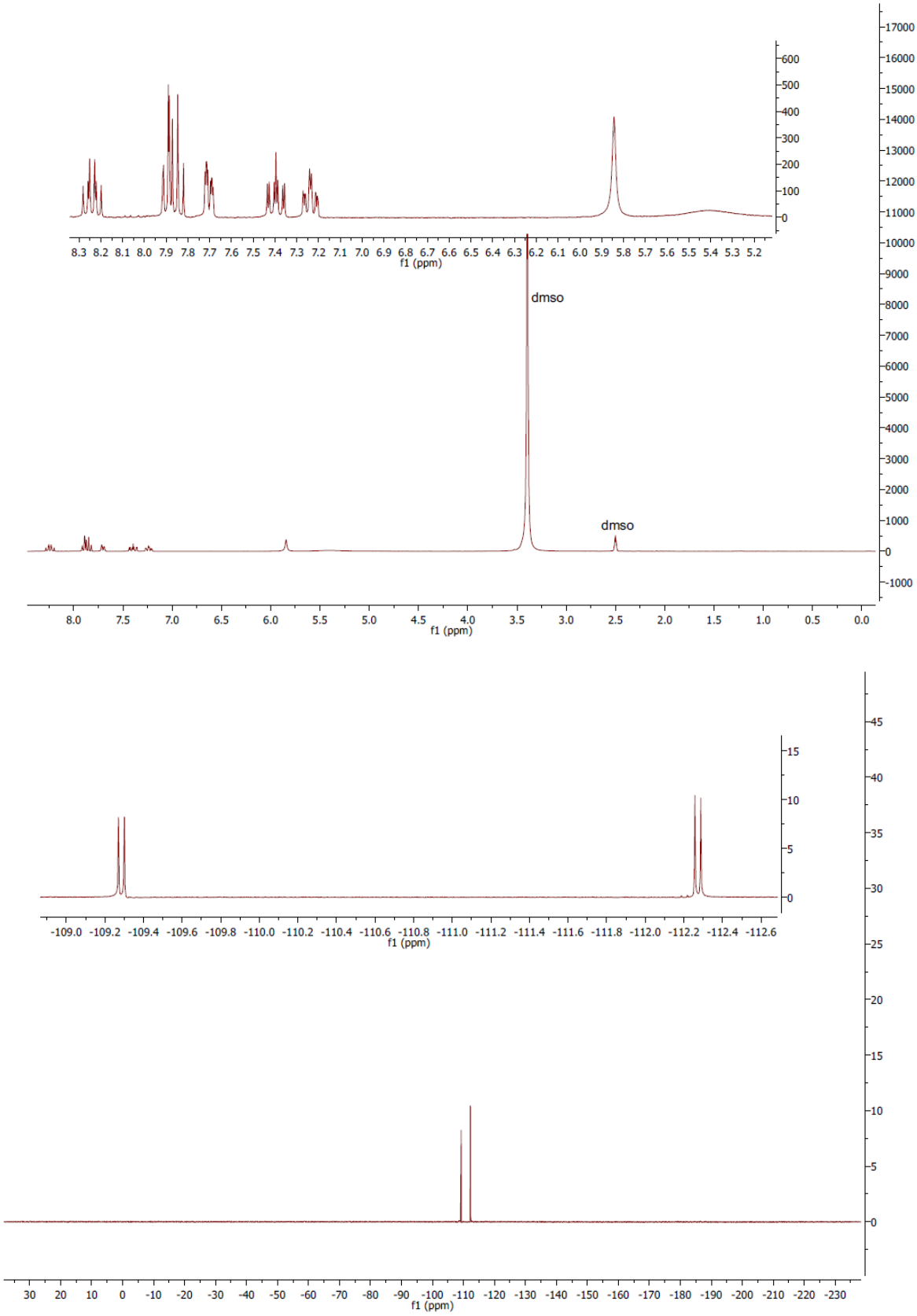

Spectra S2. *NMR spectra of* ***2****. (Top: ^{1}H-NMR Bottom: ^{19}F-NMR)*

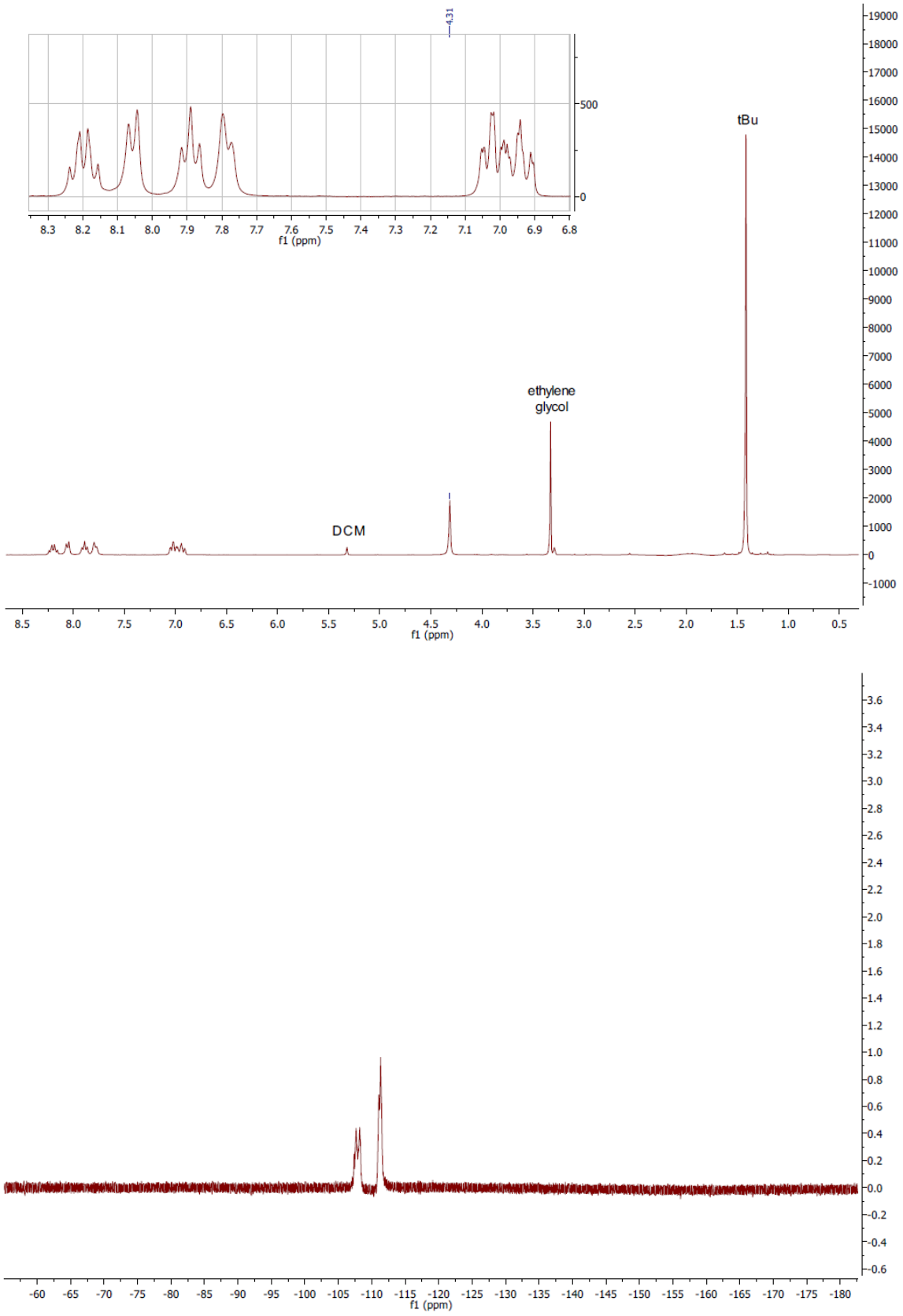

Spectra S3. *NMR spectra of* ***L1****. (Top: ^{1}H-NMR Bottom: ^{19}F-NMR)*

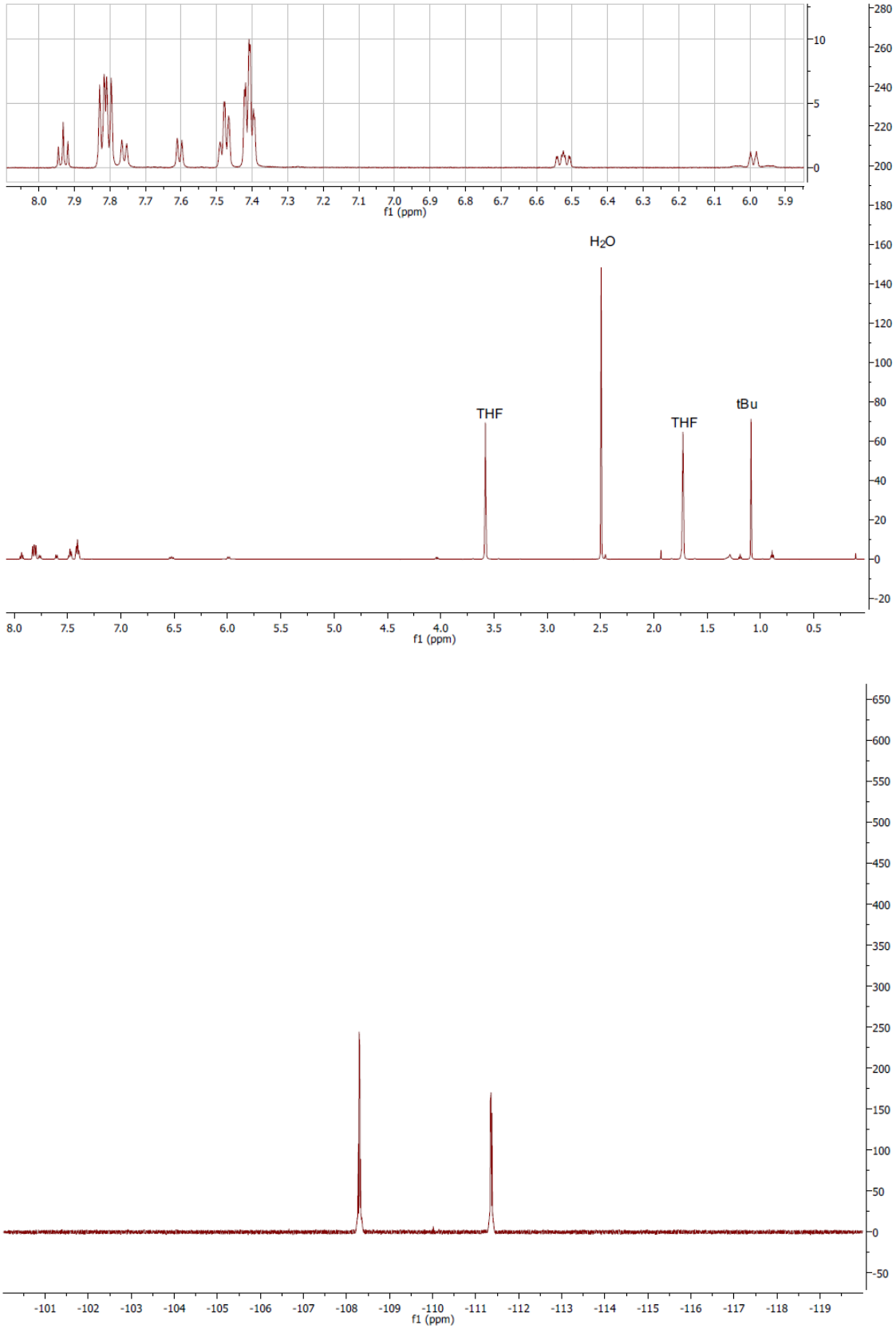

Spectra S4. *NMR spectra of* ***C2****. (Top: ^{1}H-NMR Bottom: ^{19}F-NMR)*

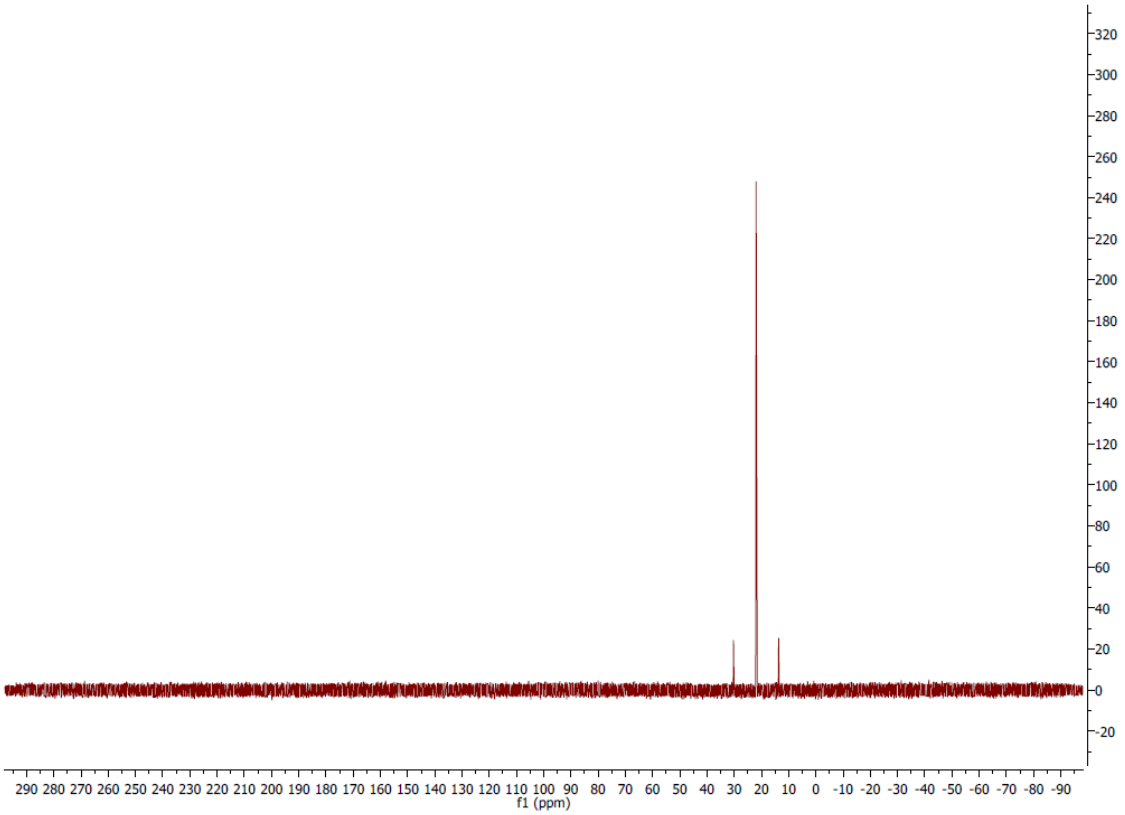

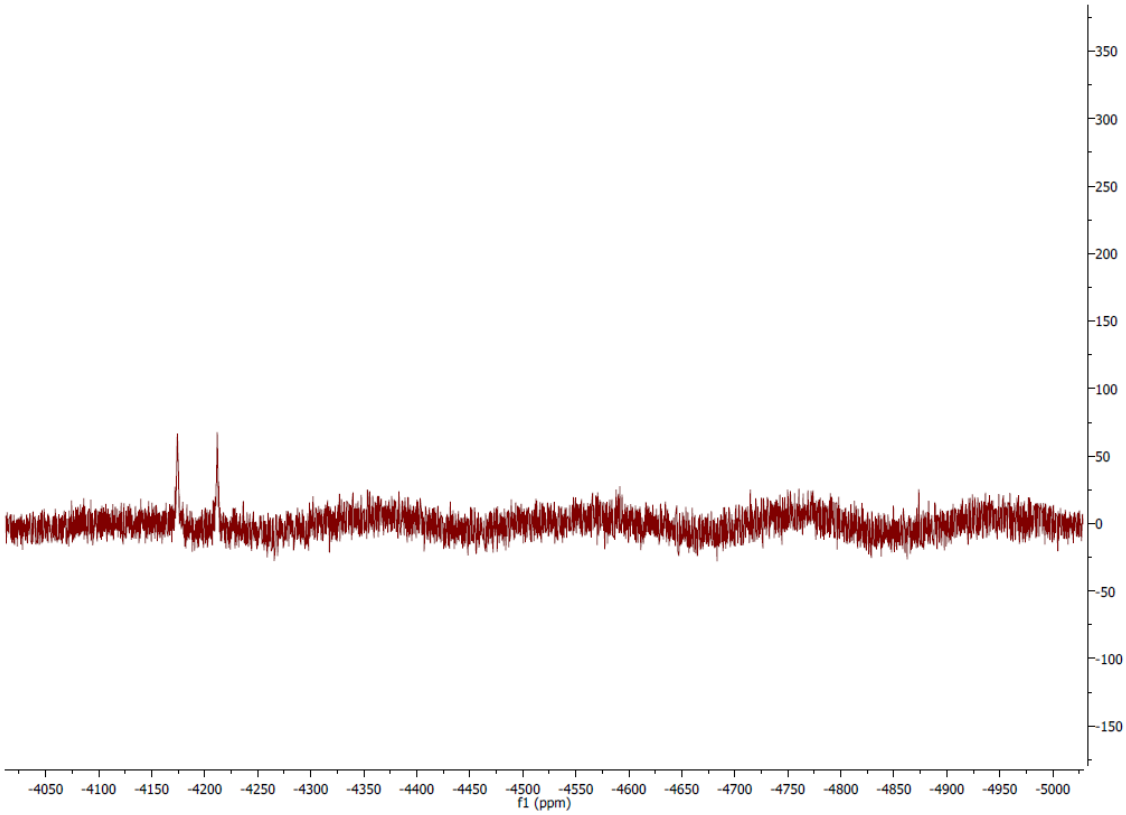

Spectra S5. *NMR spectra of* ***C2****. (Top: ^{31}P-NMR Bottom: ^{195}Pt-NMR)*

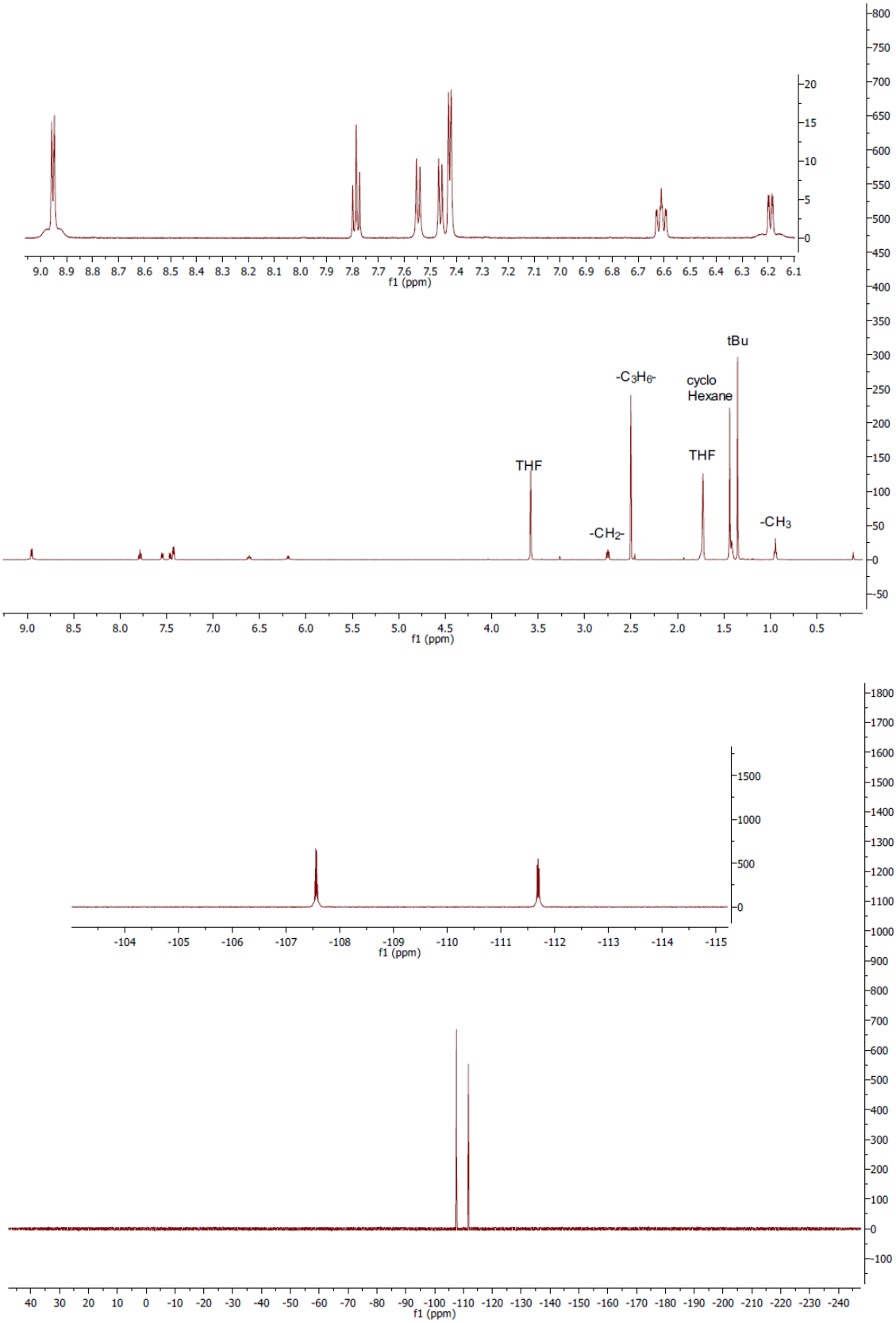

Spectra S6. *NMR spectra of* ***C3****. (Top: ^{1}H-NMR Bottom: ^{19}F-NMR)*

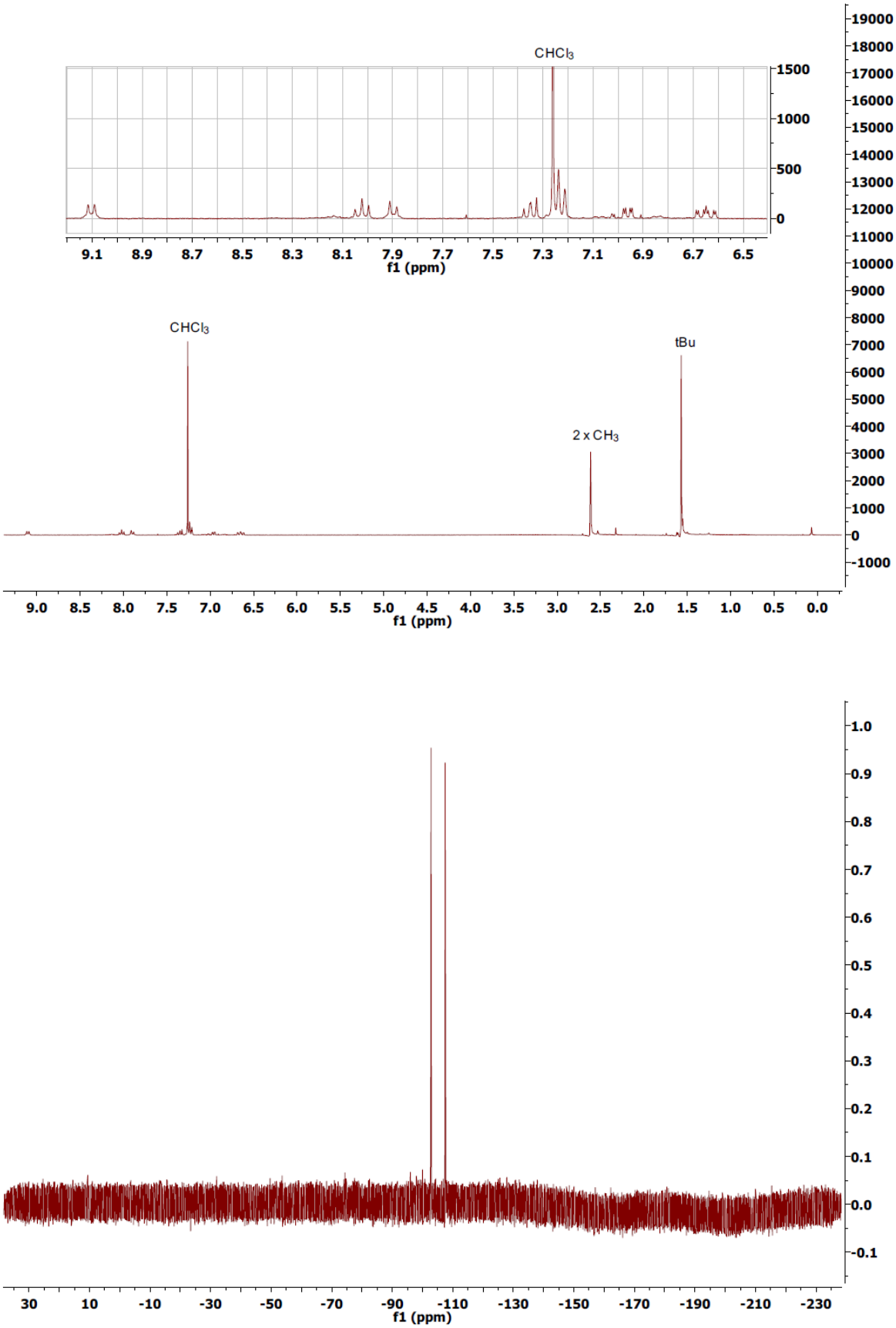

Spectra S7. *NMR spectra of* ***C4****. (Top: ^{1}H-NMR Bottom: ^{19}F-NMR)*

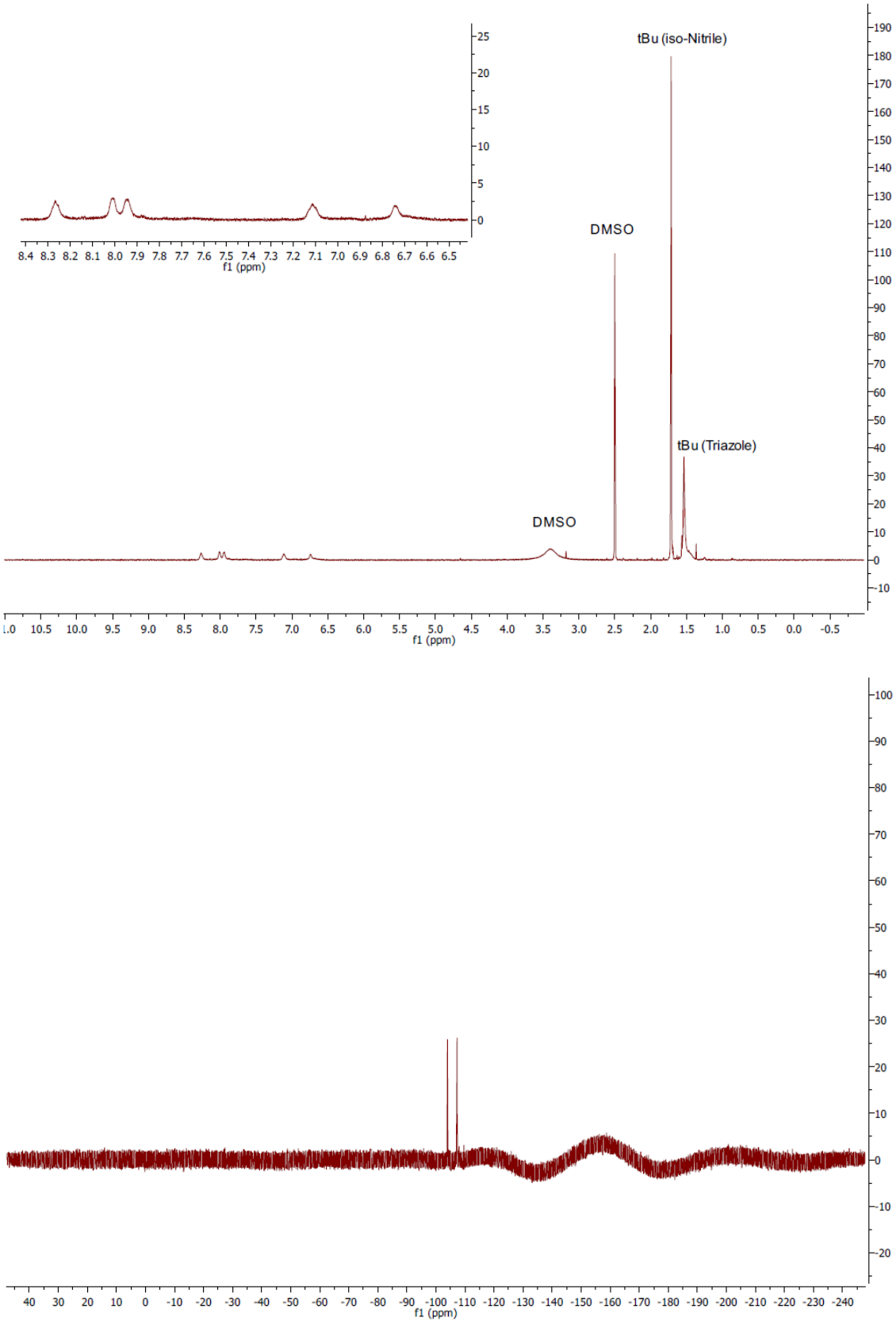

Spectra S8. *NMR spectra of* ***C5****. (Top: ^{1}H-NMR Bottom: ^{19}F-NMR)*

1.3 X-ray crystal structures. For compounds **C2** and **C3** data sets were collected with a Nonius KappaCCD diffractometer. Programs used: data collection, COLLECT (R. W. W. Hooft, Bruker AXS, 2008, Delft, The Netherlands); data reduction Denzo-SMN[1]; absorption correction, Denzo[2]; structure solution SHELXS-97[3]; structure refinement SHELXL-97 and graphics, XP (BrukerAXS, 2000). For compound **1** data sets were collected with a D8 Venture Dual Source 100 CMOS diffractometer. Programs used: data collection: APEX2 V2014.5-0 (Bruker AXS Inc., 2014); cell refinement: SAINT V8.34A (Bruker AXS Inc., 2013); data reduction: SAINT V8.34A (Bruker AXS Inc., 2013); absorption correction, SADABS V2014/2 (Bruker AXS Inc., 2014); structure solution SHELXT-2014 (Sheldrick, 2014); structure refinement SHELXL-2014 (Sheldrick, 2014) and graphics, XP (Bruker AXS Inc., 2014).Thermals ellipsoids are shown with 30% probability for compound **C2** and **C3** and with 50% probability for compound **1**. *R*-values are given for observed reflections, and wR^2 values are given for all reflections.

Exceptions and special features: For the compound **C2** one badly disordered THF molecule was found in the asymmetrical unit and could not be satisfactorily refined. The program SQUEEZE (A. L. Spek J. Appl. Cryst., 2003, 36, 7-13) was therefore used to remove mathematically the effect of the solvent. The quoted formula and derived parameters are not included the squeezed solvent molecules. Compound **C3** present one n-pentyl group and one THF molecule are disordered over two positions. Several restraints (SADI, SAME, ISOR and SIMU) were used in order to improve refinement stability. Compound **1** crystallized with two molecules in the asymmetric unit.

X-ray crystal structure analysis of C2 (dan7095): formula $C_{35}H_{29}F_2N_4PPt$, M = 769.68, yellow crystal, 0.10 x 0.06 x 0.03 mm, a = 10.2152(2), b = 10.8813(2), c = 15.7154(2) Å, α = 96.105(1), β = 104.356(1), γ = 104.287(2)°, V = 1613.6(1) Å^3, ρ_{calc} = 1.584 gcm^{-3}, μ = 4.439 mm^{-1}, empirical absorption correction ($0.665 \leq T \leq 0.878$), Z = 2, triclinic, space group $P\bar{1}$ (No. 2), λ = 0.71073 Å, T = 223(2) K, ω and φ scans, 15571 reflections collected ($\pm h$, $\pm k$, $\pm l$), [(sinθ)/λ] = 0.67 Å^{-1}, 7889 independent (R_{int} = 0.040) and 7212 observed reflections [I>2σ(I)], 391 refined parameters, R = 0.042, wR^2 = 0.097, max. (min.) residual electron density 0.79 (-1.12) e.Å^{-3}, hydrogen atoms were calculated and refined as riding atoms.

X-ray crystal structure analysis of C3 (dan7469): formula $C_{27}H_{29}F_2N_5Pt \cdot C_4H_8O$, M = 728.75, yellow crystal, 0.17 x 0.10 x 0.01 mm, a = 21.2263(2), b = 18.3170(3), c = 16.6102(2) Å, β = 111.060(1) °, V = 6026.7(1) Å^3, ρ_{calc} = 1.606 gcm^{-3}, μ = 4.701 mm^{-1}, empirical absorption correction (0.504 ≤ T ≤ 0.954), Z = 8, monoclinic, space group $C2/c$ (No. 15), λ = 0.71073 Å, T = 223(2) K, ω and φ scans, 19723 reflections collected ($\pm h$, $\pm k$, $\pm l$), [(sinθ)/λ] = 0.62 Å^{-1}, 6061 independent (R_{int} = 0.041) and 5098 observed reflections [I>2σ(I)], 458 refined parameters, R = 0.034, wR^2 = 0.087, max. (min.) residual electron density 0.80 (-0.98) e.Å^{-3}, hydrogen atoms were calculated and refined as riding atoms.

X-ray crystal structure analysis of 1 (dan7901): formula $C_{12}H_6N_2F_2$, M = 216.19, colourless crystal, 0.20 x 0.15 x 0.11 mm, a = 24.0158(10), b = 3.6946(1), c = 24.1833(8) Å, β = 117.592(1) °, V = 1901.7(1) Å^3, ρ_{calc} = 1.510 gcm^{-3}, μ = 0.119 mm^{-1}, empirical absorption correction (0.976 ≤ T ≤ 0.987), Z = 8, monoclinic, space group $P2_1/n$ (No. 14), λ = 0.71073 Å, T = 101(2) K, ω and φ scans, 24584 reflections collected ($\pm h$, $\pm k$, $\pm l$), 3522 independent (R_{int} = 0.057) and 2852 observed reflections [I>2σ(I)], 289 refined parameters, R = 0.036, wR^2 = 0.088, max. (min.) residual electron density 0.26 (-0.22) e.Å^{-3}, hydrogen atoms were calculated and refined as riding atoms.

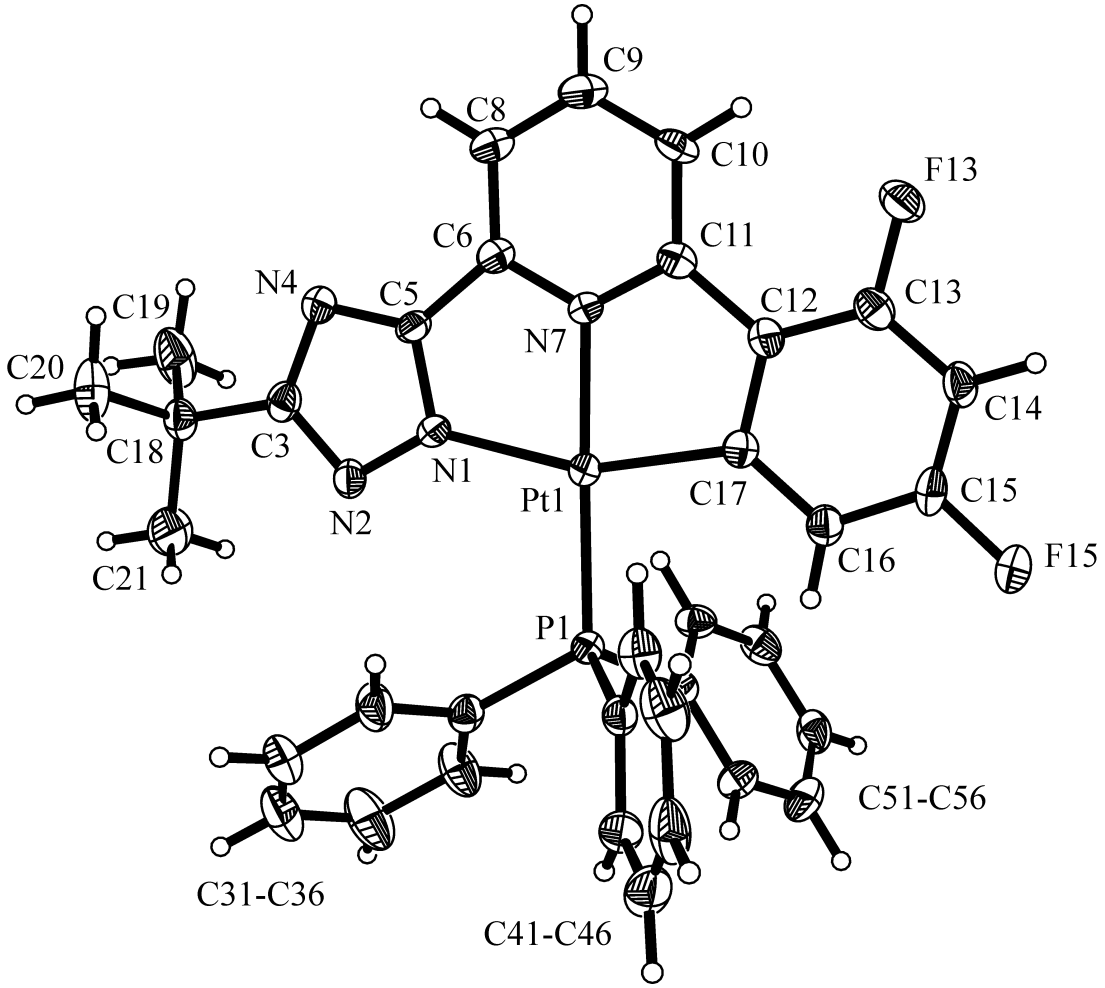

Figure S1a. Crystal structure of compound **C2.** (Thermals ellipsoids are shown with 30% probability.)

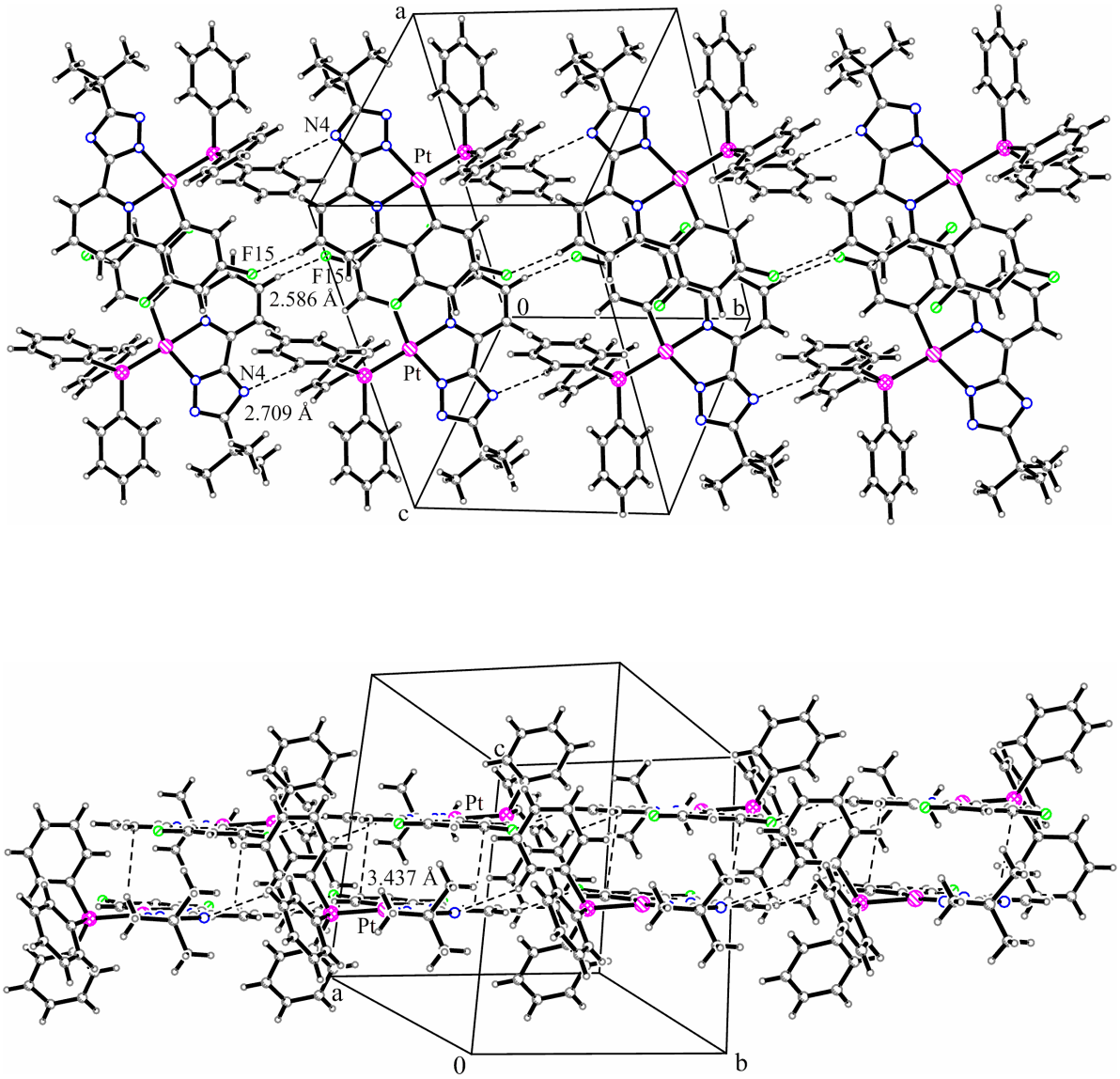

Figure S1b. Top: Packing diagram presenting the C-H···F and C-H···N interactions along the *ac*-plane in complex **C2**. Bottom: π···π stacking involving only the phenylpyridine moiety in complex **C2**

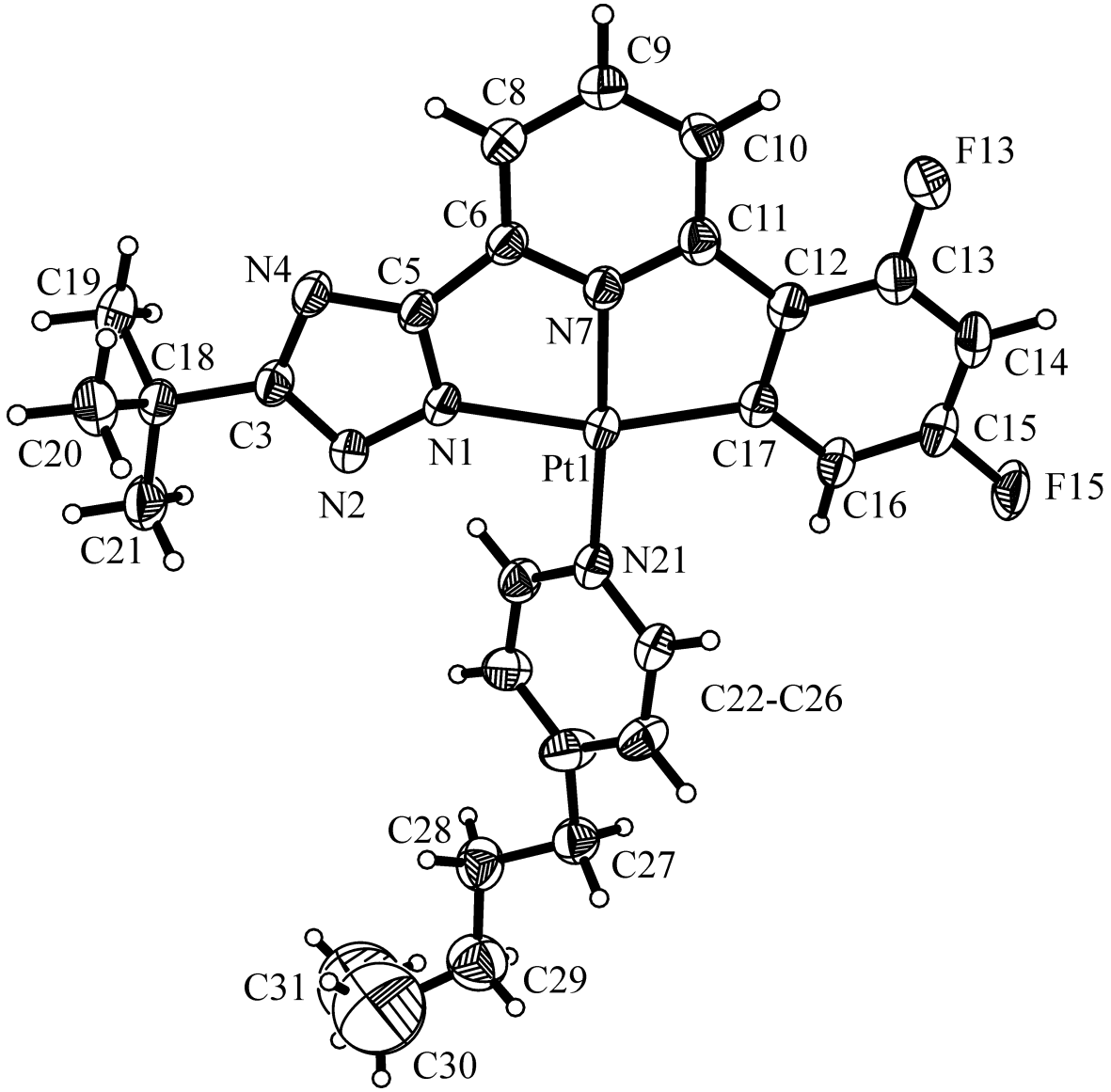

Figure S2a. Crystal structure of compound **C3**. (Thermals ellipsoids are shown with 30% probability.)

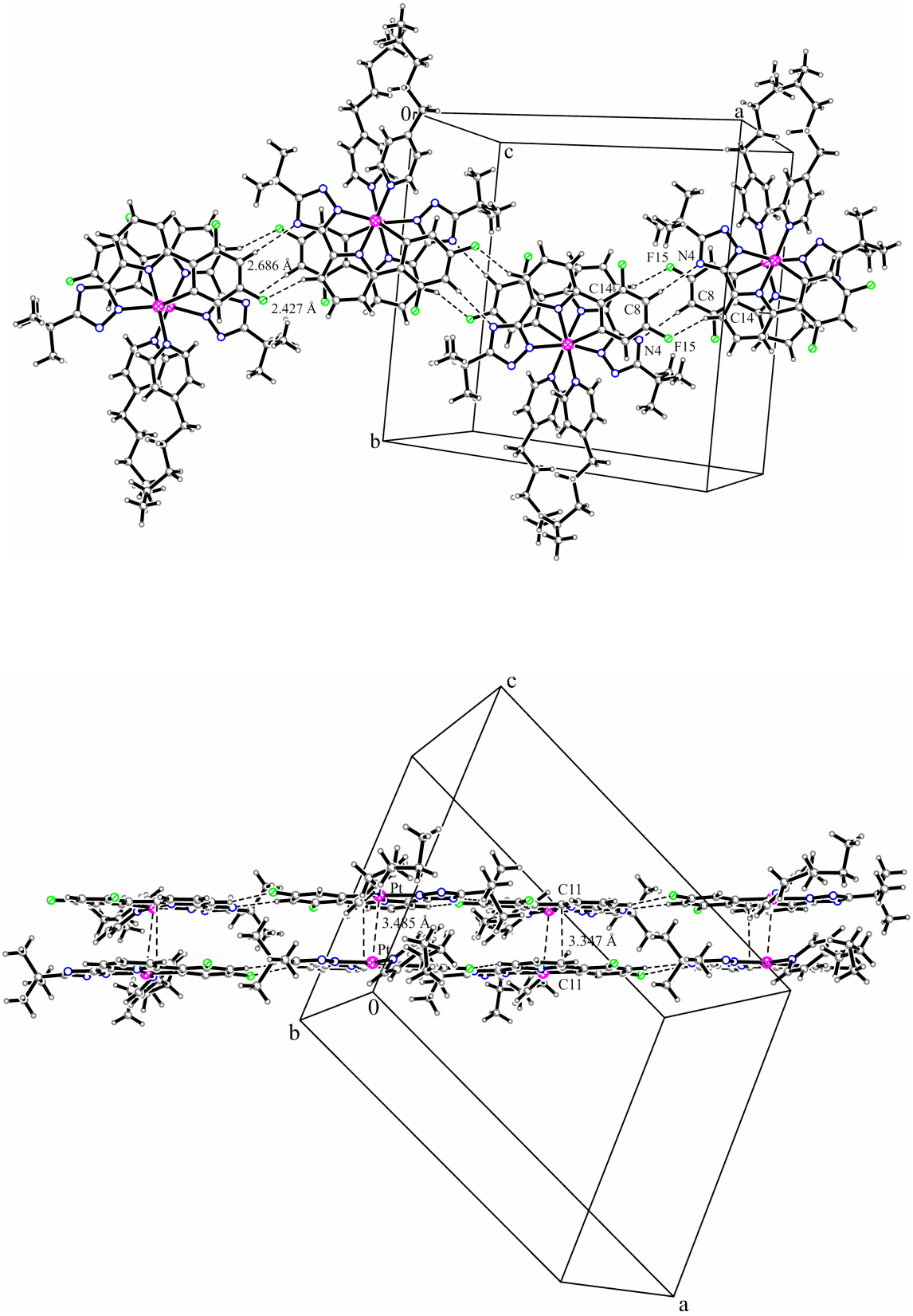

Figure S2b. Top: Packing diagram presenting the C-H···F and C-H···N interactions along the *ac*-plane in complex **C3**. Bottom: Pt···Pt interactions and π···π stacking in complex **C3**.

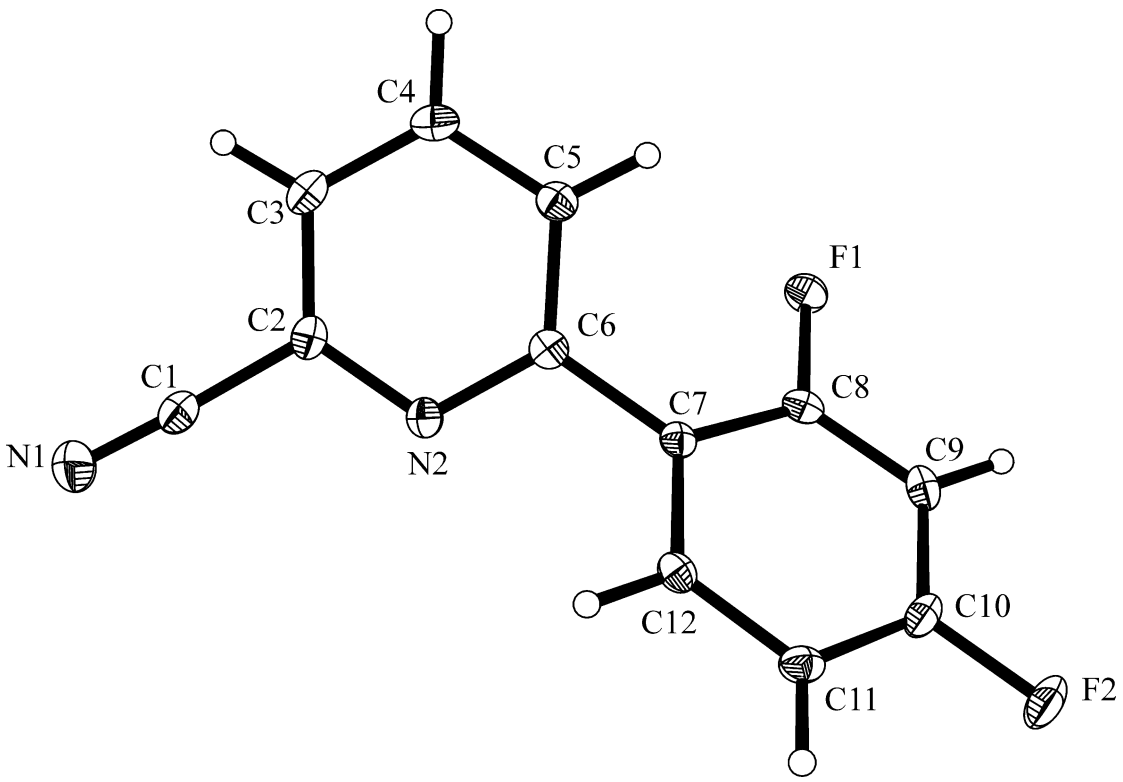

Figure S3. Crystal structure of compound **1**.

Only one molecule of two found in the asymmetric unit is shown.

(Thermals ellipsoids are shown with 50% probability.)

[1] Z. Otwinowski, W. Minor, *Methods Enzymol*. **1997**, *276*, 307 – 326.

[2] Z. Otwinowski, D. Borek, W. Majewski, W. Minor, *Acta Crystallogr. Sect. A* **2003**, *59*, 228 – 234.

[3] G. M. Sheldrick, *Acta Crystallogr. Sect. A* **1990**, *46*, 467 –473 .

[4] G. M. Sheldrick, *Acta Crystallogr. Sect. A* **2008**, *64*, 112 – 122.

2 Scanning tunnelling microscopy

All measurements where performed under ultrahigh vacuum conditions ($p<10^{-10}$ mbar) using a low-temperature scanning tunneling microscope (CreaTec LT-STM) operating at 5K. The sample preparation for the STM experiments is based on *in situ* thermal sublimation of the Platinum complexes from a commercial evaporator (CreaTec TUBOmini) onto a afore cleaned Au(111) single crystal. The STM images were acquired in the constant-current mode. The bias voltage is always given with respect to the sample (i.e. positive sample bias corresponds to electrons tunneling from occupied electronic states of the tip into unoccupied states of the sample).

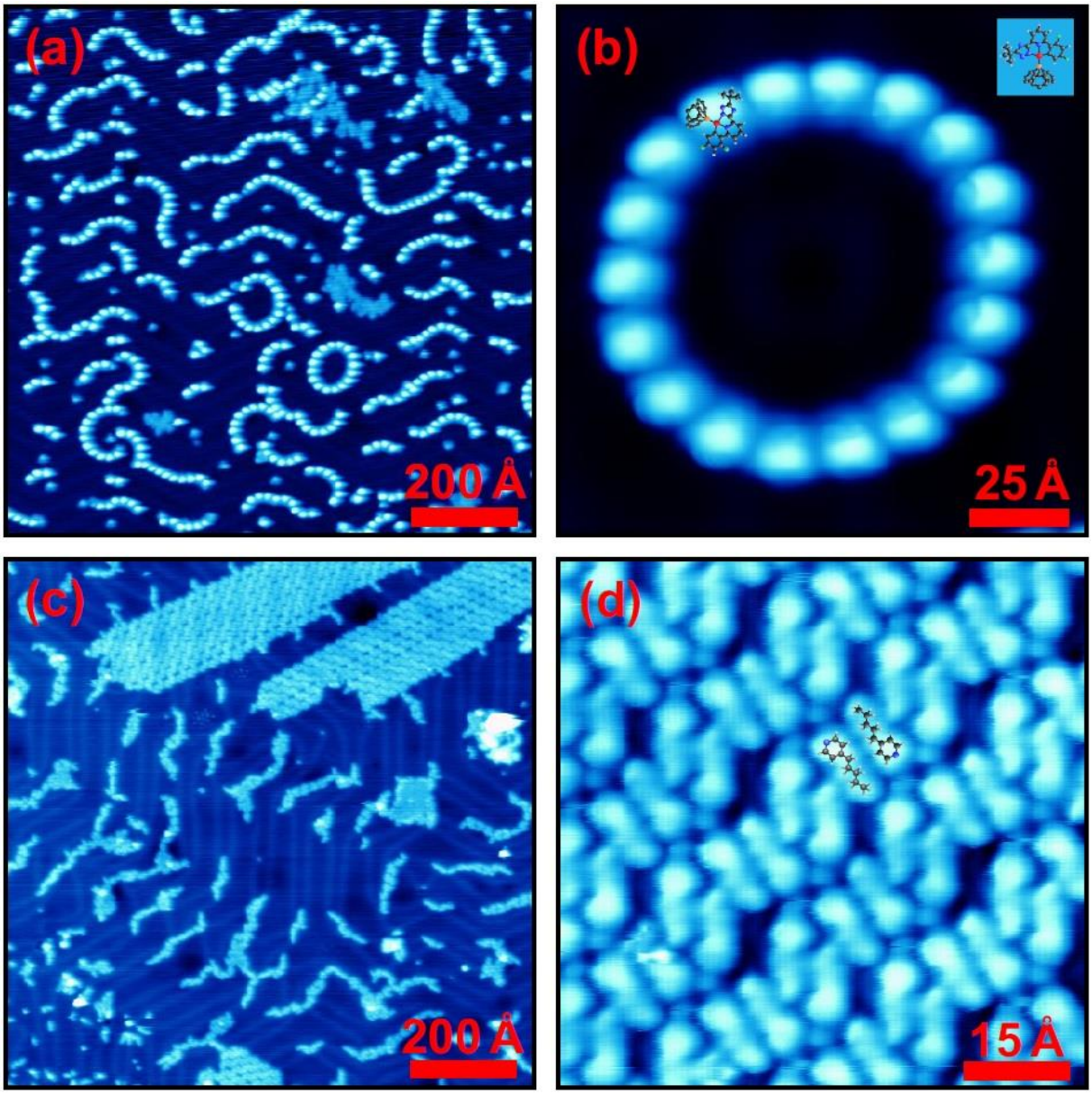

Figure S4. *STM images of complexes **C2** (top) and **C3** (bottom)*

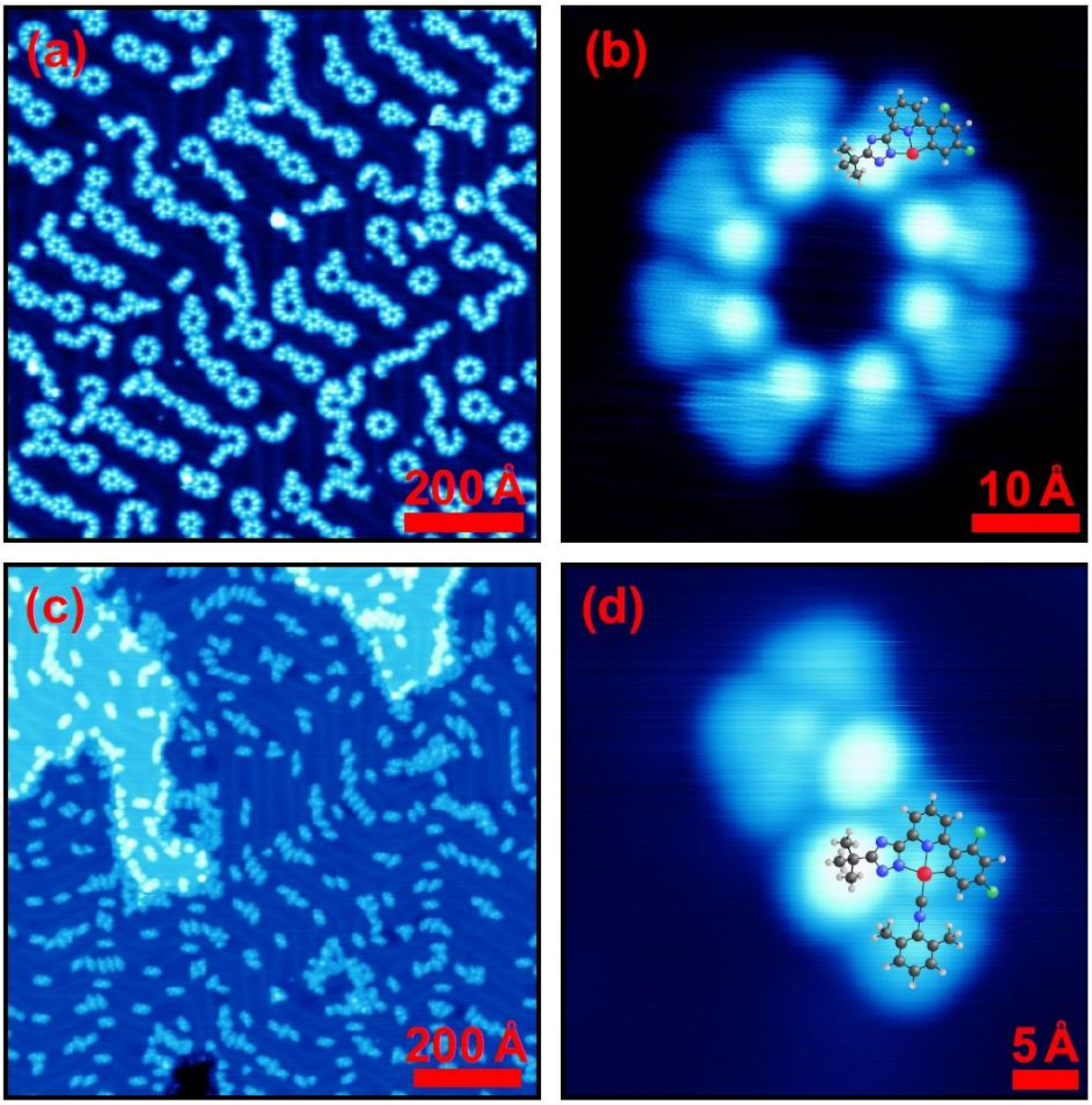

Figure S5. *STM images of complexes **C5** (top) and **C4** (bottom).*

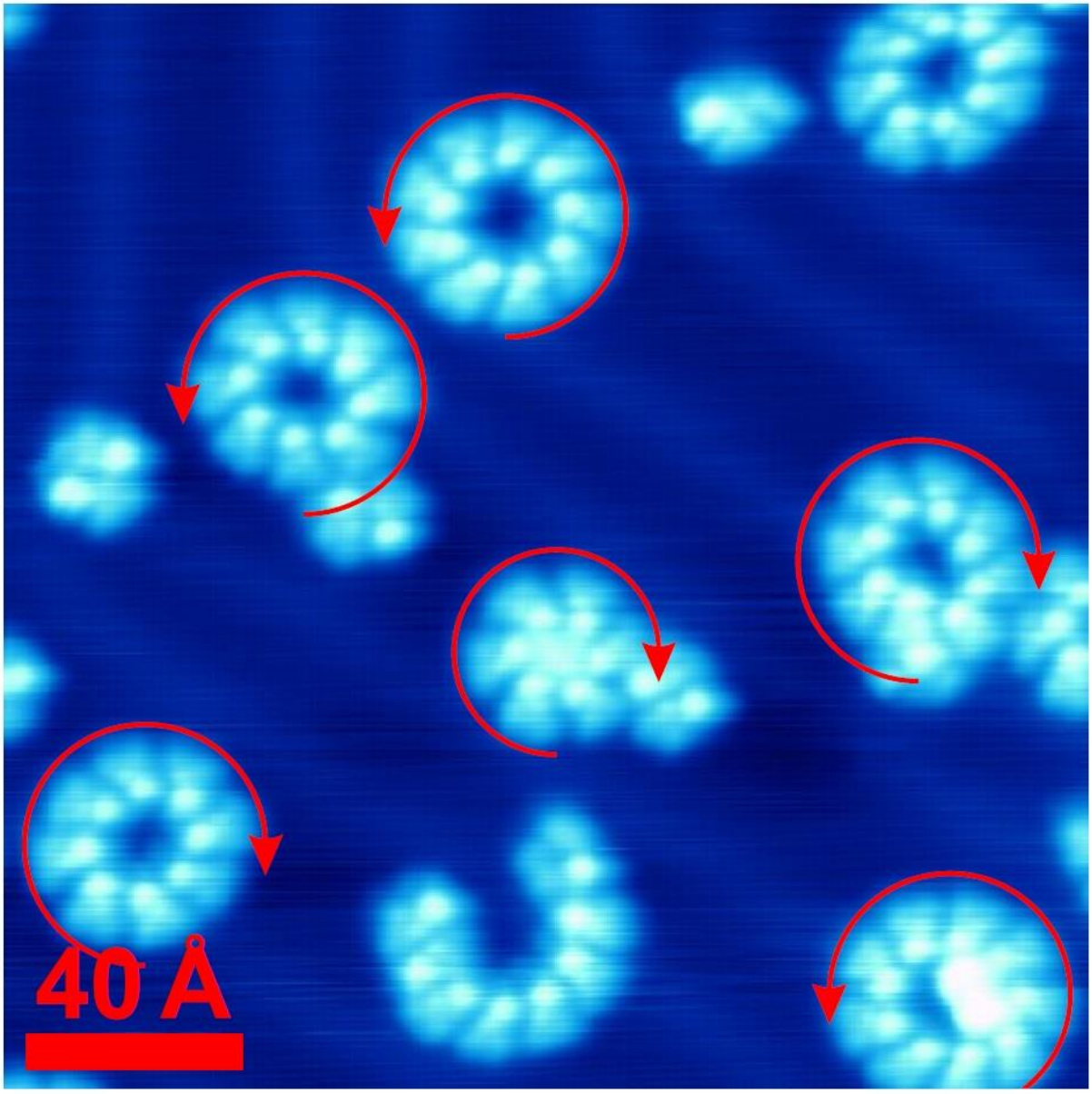

Figure S5(b). Close up *STM images of complexes **C5**. The red arrows indicating the two possible stereoisomers.*

3 Computational Details

All DFT calculations were performed with the Gaussian 09 Rev. D.01 package[5] using the PBE0 hybrid functional[6] and the SDD basis set, which consists of the D95 full double zeta basis set[7] and effective core potentials (ECP)[8] for atoms heavier than Argon. The standard convergence criteria for geometry optimizations and single point calculations were used. To include solvent effects the polarizable continuum model (PCM)[9-11] was employed. The cavity for the molecule was formed based on the Bondi model for atomic radii[12]. For Complex **C2** the vibrationally resolved emission spectrum was obtained by ground state geometry optimizations employing the local spin density approximation and subsequent calculations using the Franck-Condon method[13] in Gaussian 09. The standard parameters were modified to include up to 5000 vibrational states to adequately incorporate temperature effects at 300K and the half width at half maximum for the gaussian peaks was changed from 135 cm^{-1} to 500 cm^{-1}. For the dimers of Complexes **C3**, **C4** and **C5**, optimized geometries differed strongly, so single point calculations in the singlet ground state were performed at the optimized structure from the triplet state optimization using the equilibrated solvent from the triplet calculation, thus correctly emulating a vertical transition. In the figure, the peaks are represented by gaussian functions with a HWHM of 50 nm. For the visualization of molecular geometries and orbitals VMD 1.9.1 with the internal Tachyon renderer was used[14,15].

3.1 Kohn-Sham Orbitals.

Table S1. *Molecular orbitals for complex **C2** for the S0 geometry from ground state DFT calculations and orbitals for the T1 geometry from TDDFT calculations performed with Gaussian 09 Rev. D.01[5], visualized with VMD 1.9.1[6,7]*

	S_0		T_1	
Orbital	Monomer	Dimer	Monomer	Dimer
LUMO+5	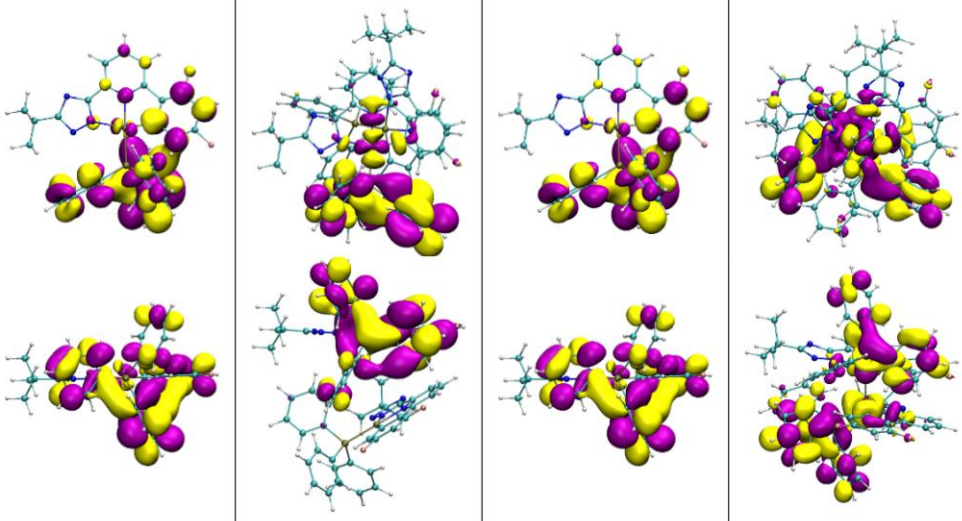 $\varepsilon = -0.593\,\mathrm{eV}$	$\varepsilon = -0.942\,\mathrm{eV}$	$\varepsilon = -0.590\,\mathrm{eV}$	$\varepsilon = -0.904\,\mathrm{eV}$
LUMO+4	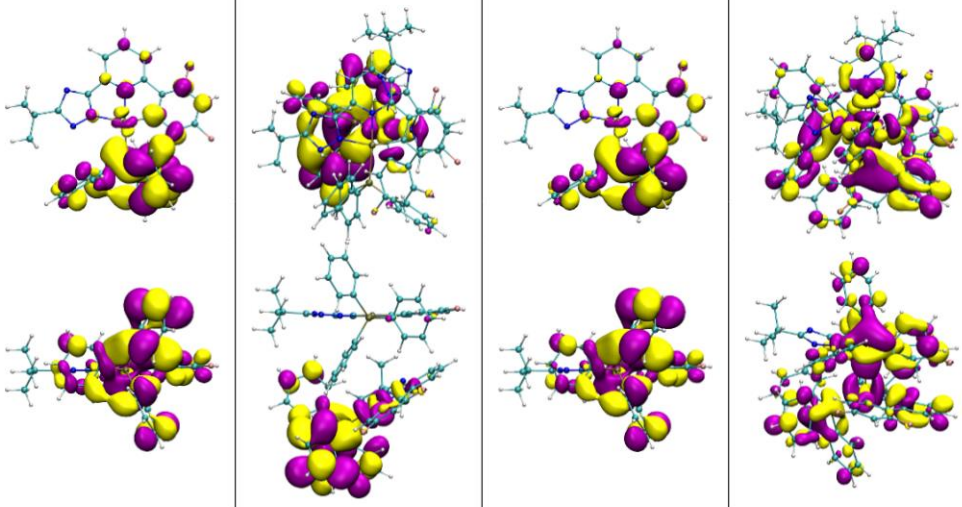 $\varepsilon = -0.696\,\mathrm{eV}$	$\varepsilon = -0.967\,\mathrm{eV}$	$\varepsilon = -0.696\,\mathrm{eV}$	$\varepsilon = -1.109\,\mathrm{eV}$
LUMO+3	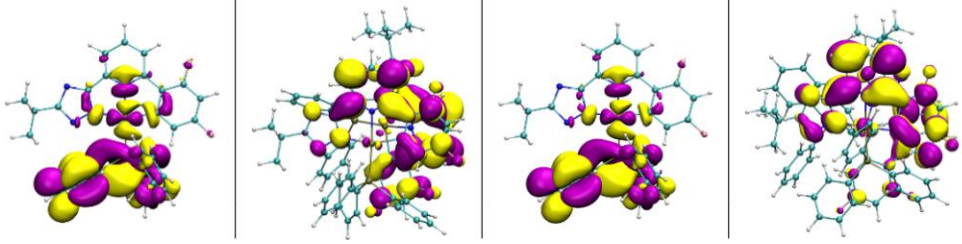			

	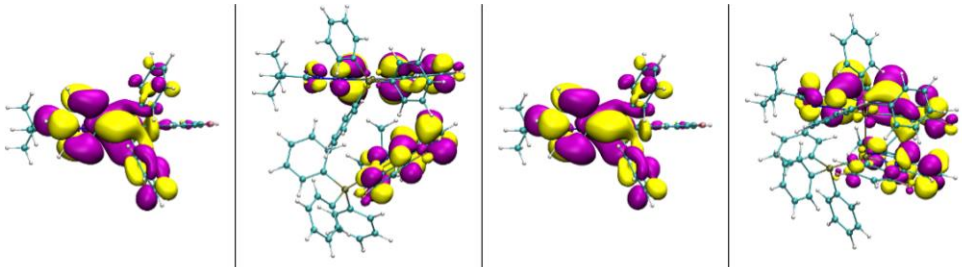 $\varepsilon = -0.900\,\mathrm{eV}$	$\varepsilon = -1.466\,\mathrm{eV}$	$\varepsilon = -0.862\,\mathrm{eV}$	$\varepsilon = -1.413\,\mathrm{eV}$
LUMO+2	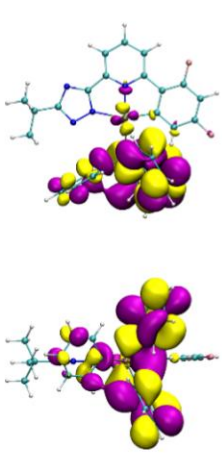 $\varepsilon = -1.013\,\mathrm{eV}$	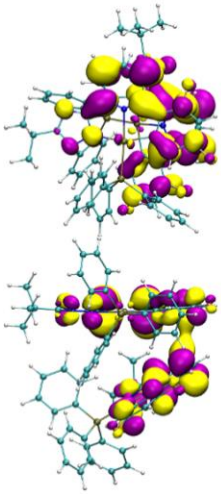 $\varepsilon = -1.535\,\mathrm{eV}$	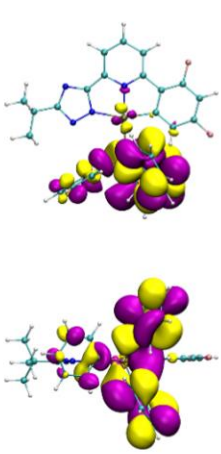 $\varepsilon = -1.013\,\mathrm{eV}$	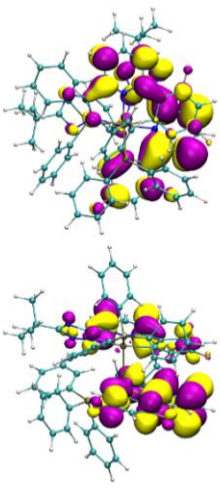 $\varepsilon = -1.488\,\mathrm{eV}$
LUMO+1	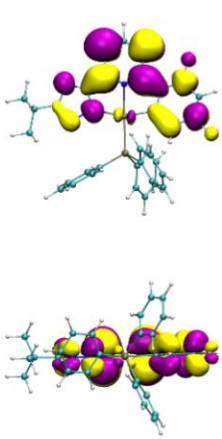 $\varepsilon = -1.542\,\mathrm{eV}$	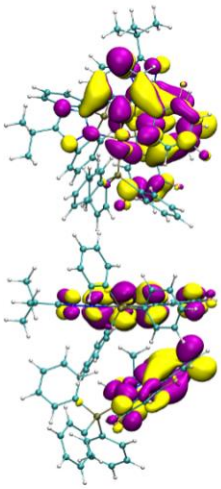 $\varepsilon = -2.133\,\mathrm{eV}$	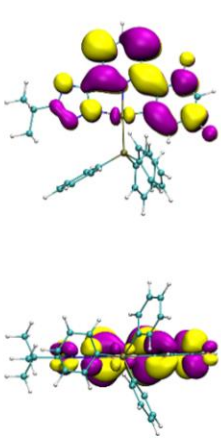 $\varepsilon = -1.608\,\mathrm{eV}$	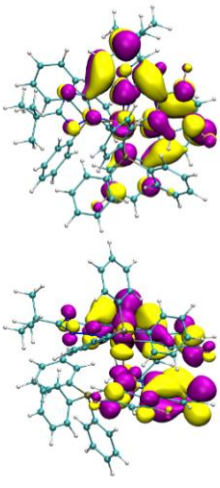 $\varepsilon = -1.800\,\mathrm{eV}$
LUMO	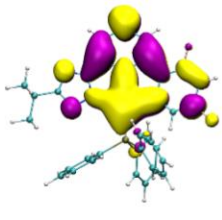	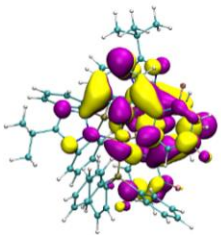	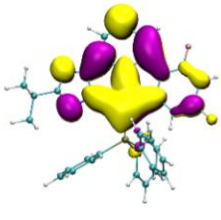	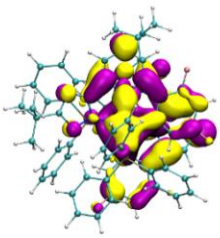

	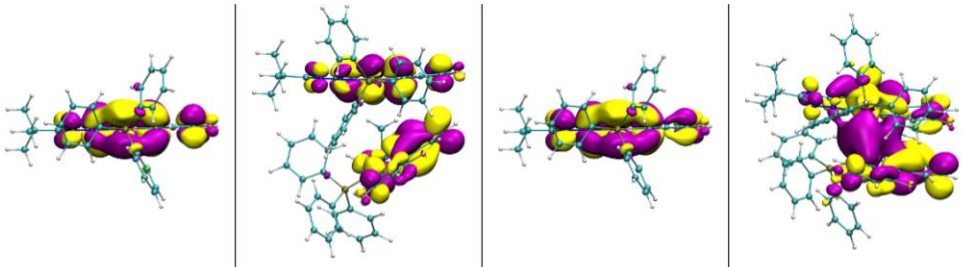 $\varepsilon = -2.190\,\mathrm{eV}$	$\varepsilon = -2.180\,\mathrm{eV}$	$\varepsilon = -2.384\,\mathrm{eV}$	$\varepsilon = -2.419\,\mathrm{eV}$
HOMO	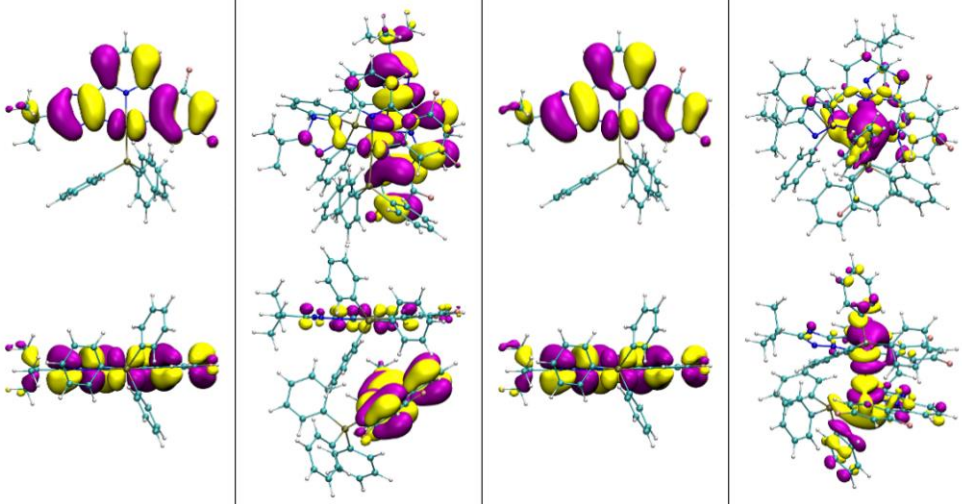 $\varepsilon = -6.262\,\mathrm{eV}$	$\varepsilon = -6.212\,\mathrm{eV}$	$\varepsilon = -6.034\,\mathrm{eV}$	$\varepsilon = -5.666\,\mathrm{eV}$
HOMO-1	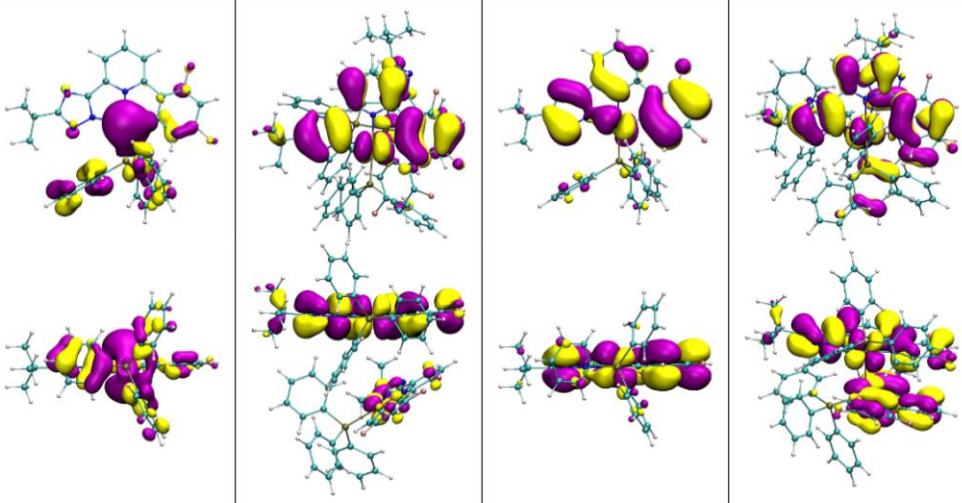 $\varepsilon = -7.040\,\mathrm{eV}$	$\varepsilon = -6.223\,\mathrm{eV}$	$\varepsilon = -7.042\,\mathrm{eV}$	$\varepsilon = -6.103\,\mathrm{eV}$
HOMO-2	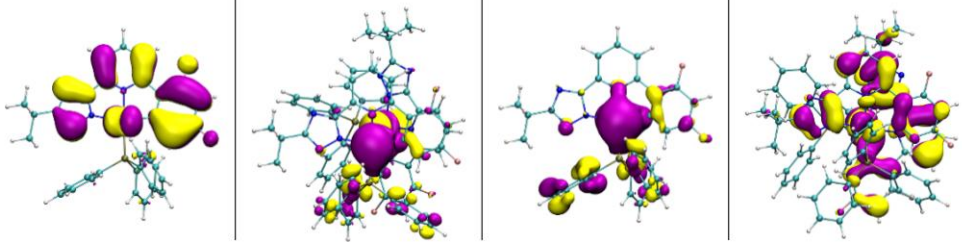			

	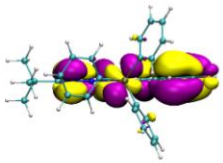 $\varepsilon = -7.107\,\mathrm{eV}$	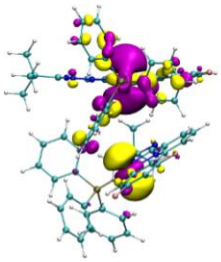 $\varepsilon = -6.984\,\mathrm{eV}$	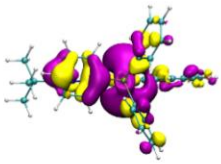 $\varepsilon = -7.080\,\mathrm{eV}$	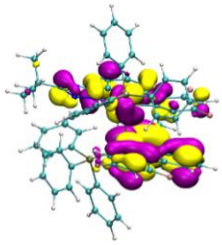 $\varepsilon = -6.222\,\mathrm{eV}$
HOMO-3	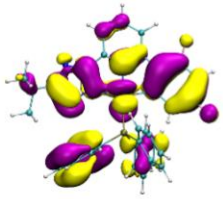 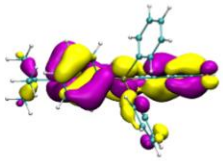 $\varepsilon = -7.217\,\mathrm{eV}$	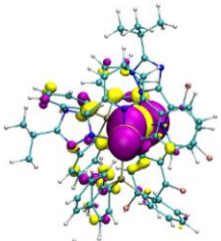 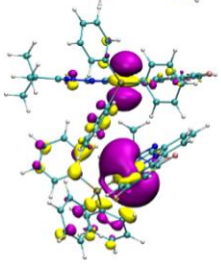 $\varepsilon = -7.012\,\mathrm{eV}$	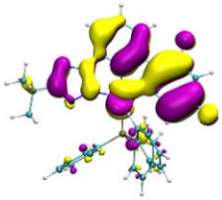 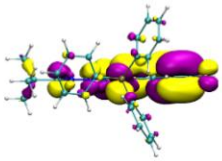 $\varepsilon = -7.167\,\mathrm{eV}$	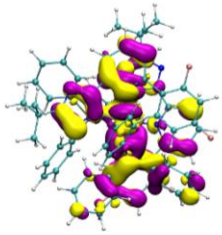 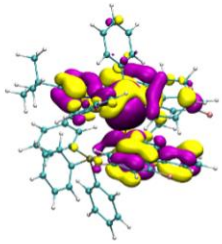 $\varepsilon = -6.531\,\mathrm{eV}$
HOMO-4	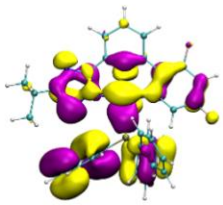 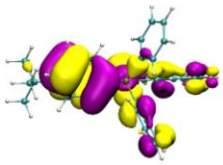 $\varepsilon = -7.248\,\mathrm{eV}$	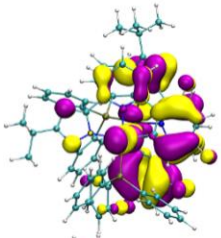 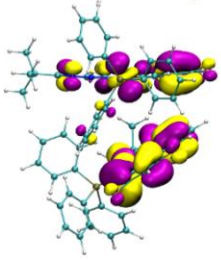 $\varepsilon = -7.032\,\mathrm{eV}$	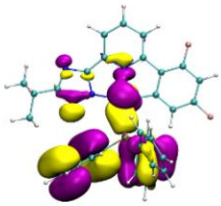 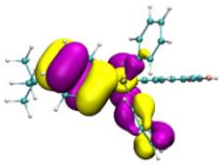 $\varepsilon = -7.254\,\mathrm{eV}$	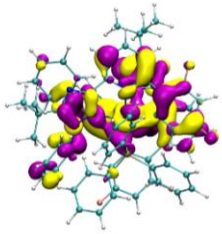 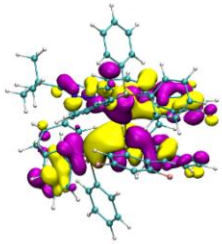 $\varepsilon = -6.624\,\mathrm{eV}$
HOMO-5	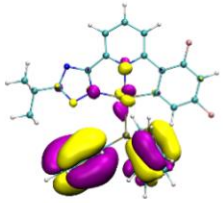	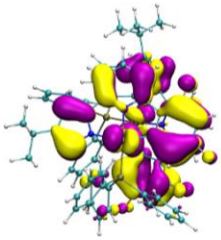	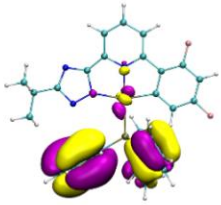	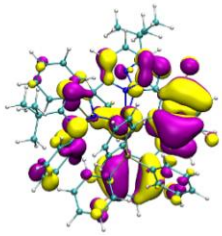

HOMO -5	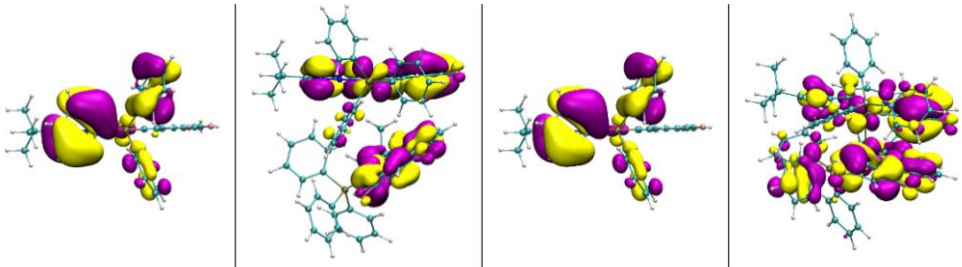			
	$\varepsilon = -7.383\,\mathrm{eV}$	$\varepsilon = -7.093\,\mathrm{eV}$	$\varepsilon = -7.382\,\mathrm{eV}$	$\varepsilon = -6.978\,\mathrm{eV}$

Table S2. *Molecular orbitals for complex **C3** for the S0 geometry from ground state DFT calculations and orbitals for the T1 geometry from TDDFT calculations performed with Gaussian 09 Rev. D.01[5], visualized with VMD 1.9.1[6,7]*

	S_0		T_1	
Orbital	Monomer	Dimer	Monomer	Dimer
LUMO+5	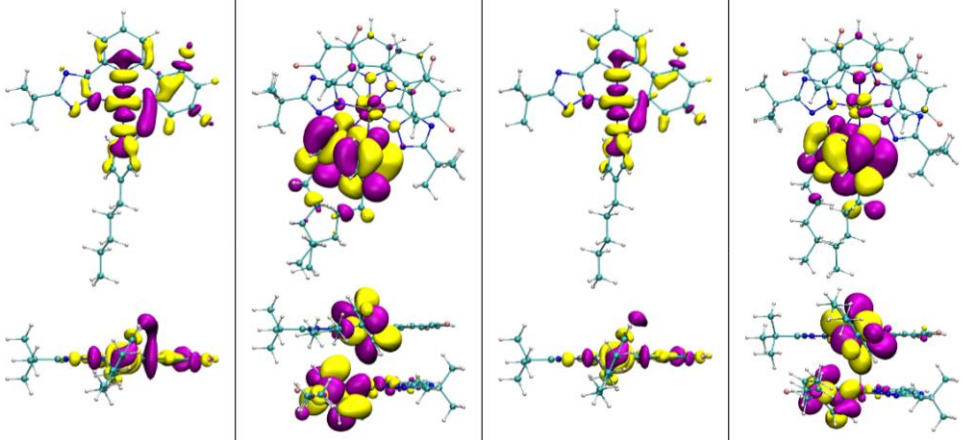			
	$\varepsilon = 0.069\,\mathrm{eV}$	$\varepsilon = -1.262\,\mathrm{eV}$	$\varepsilon = 0.096\,\mathrm{eV}$	$\varepsilon = -1.278\,\mathrm{eV}$
LUMO+4	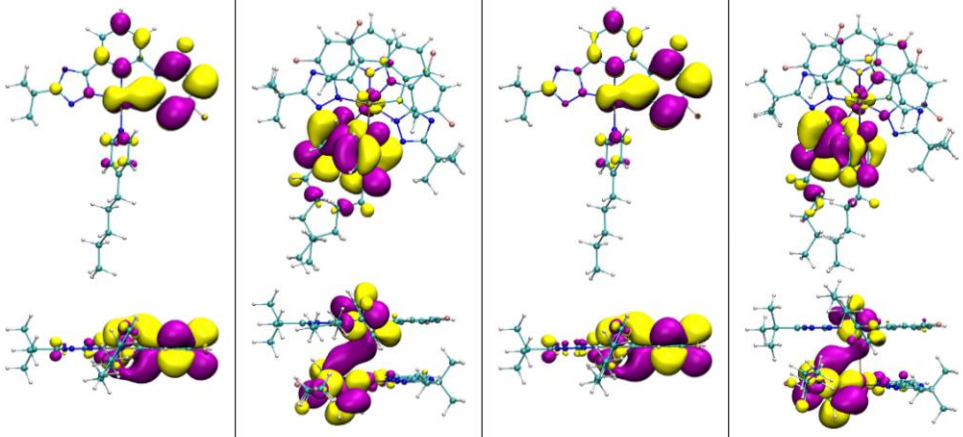			
	$\varepsilon = -0.409\,\mathrm{eV}$	$\varepsilon = -1.343\,\mathrm{eV}$	$\varepsilon = -0.394\,\mathrm{eV}$	$\varepsilon = -1.304\,\mathrm{eV}$

LUMO+3	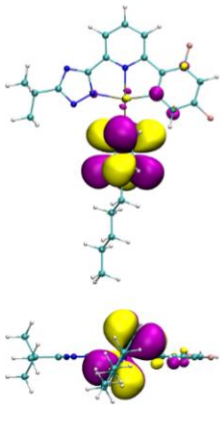 $\varepsilon = -0.738\,\mathrm{eV}$	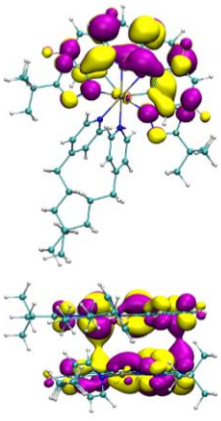 $\varepsilon = -1.429\,\mathrm{eV}$	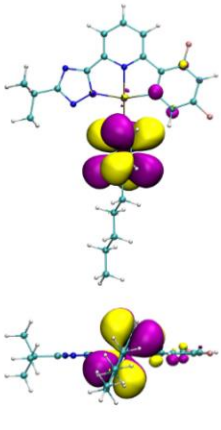 $\varepsilon = -0.740\,\mathrm{eV}$	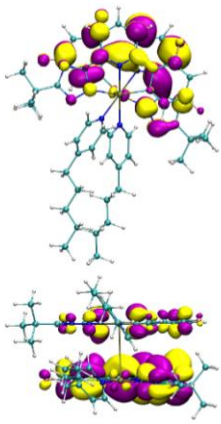 $\varepsilon = -1.455\,\mathrm{eV}$
LUMO+2	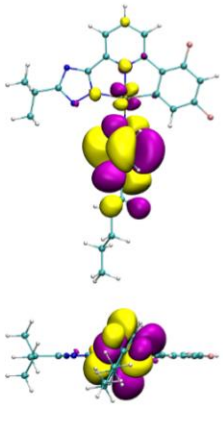 $\varepsilon = -1.327\,\mathrm{eV}$	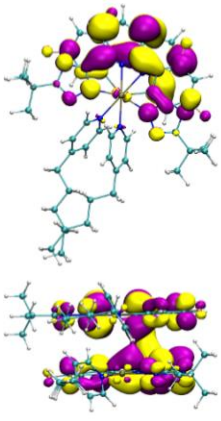 $\varepsilon = -1.534\,\mathrm{eV}$	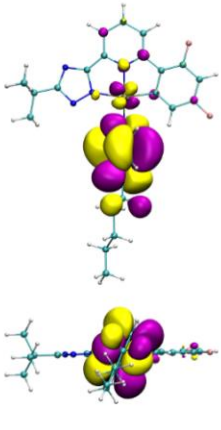 $\varepsilon = -1.327\,\mathrm{eV}$	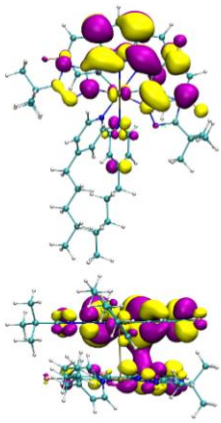 $\varepsilon = -1.567\,\mathrm{eV}$
LUMO+1	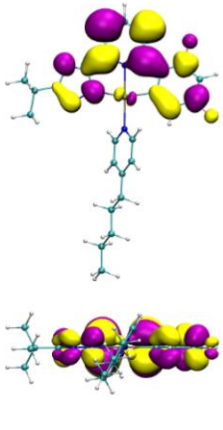 $\varepsilon = -1.534\,\mathrm{eV}$	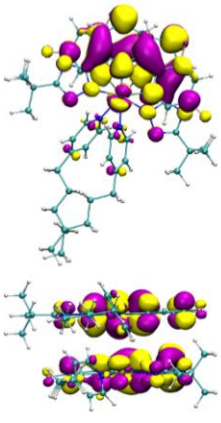 $\varepsilon = -2.035\,\mathrm{eV}$	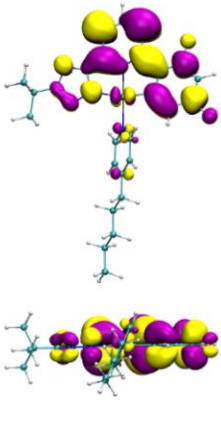 $\varepsilon = -1.607\,\mathrm{eV}$	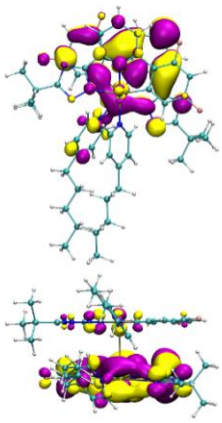 $\varepsilon = -2.072\,\mathrm{eV}$
LUMO	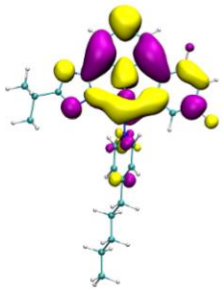	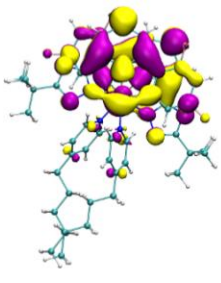	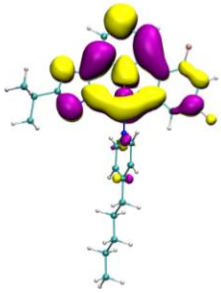	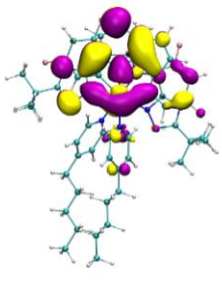

LUMO	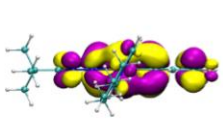 $\varepsilon = -2.143\,\mathrm{eV}$	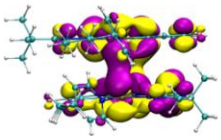 $\varepsilon = -2.140\,\mathrm{eV}$	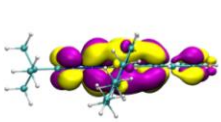 $\varepsilon = -2.330\,\mathrm{eV}$	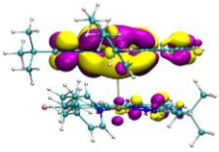 $\varepsilon = -2.287\,\mathrm{eV}$
HOMO	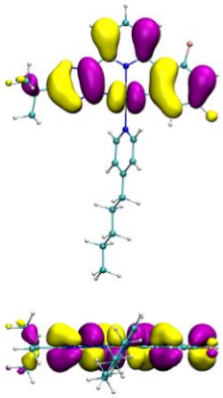 $\varepsilon = -6.220\,\mathrm{eV}$	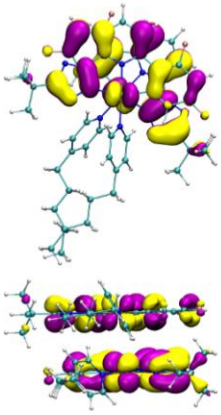 $\varepsilon = -6.153\,\mathrm{eV}$	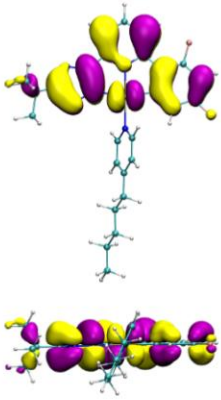 $\varepsilon = -6.010\,\mathrm{eV}$	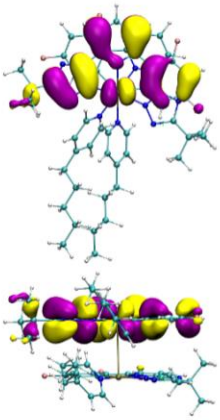 $\varepsilon = -5.940\,\mathrm{eV}$
HOMO-1	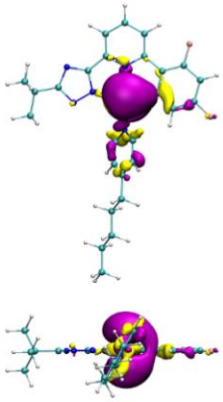 $\varepsilon = -6.972\,\mathrm{eV}$	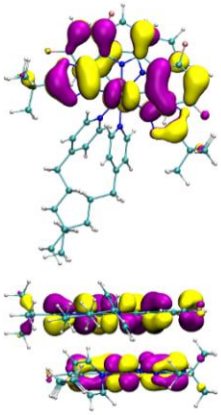 $\varepsilon = -6.161\,\mathrm{eV}$	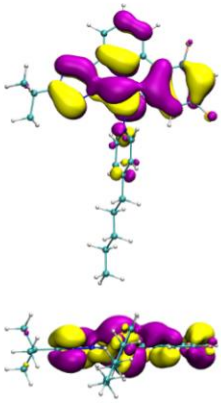 $\varepsilon = -6.975\,\mathrm{eV}$	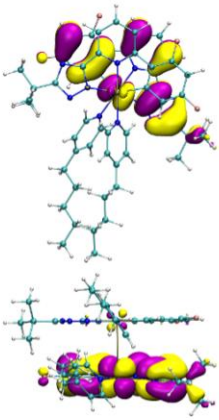 $\varepsilon = -6.157\,\mathrm{eV}$
HOMO-2	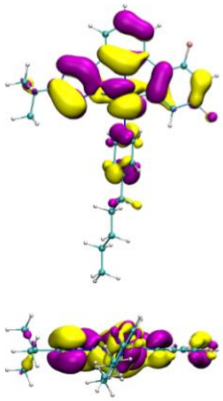 $\varepsilon = -7.091\,\mathrm{eV}$	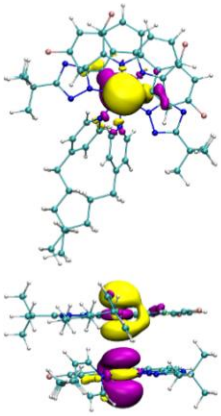 $\varepsilon = -6.509\,\mathrm{eV}$	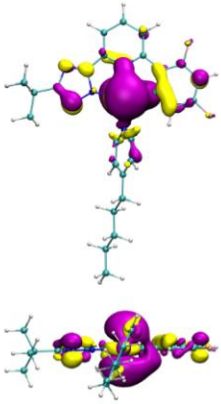 $\varepsilon = -7.017\,\mathrm{eV}$	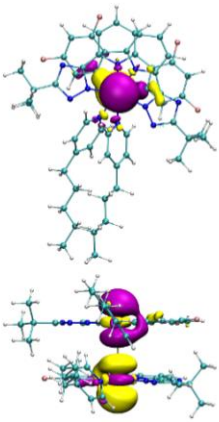 $\varepsilon = -6.491\,\mathrm{eV}$

HOMO-3	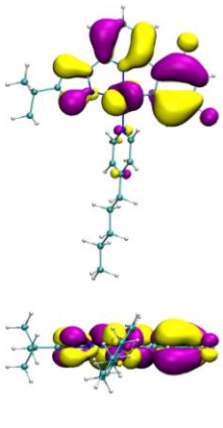 $\varepsilon = -7.124\,\mathrm{eV}$	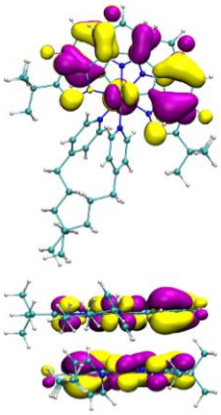 $\varepsilon = -6.966\,\mathrm{eV}$	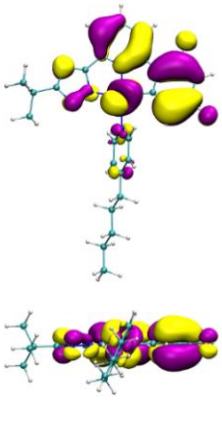 $\varepsilon = -7.138\,\mathrm{eV}$	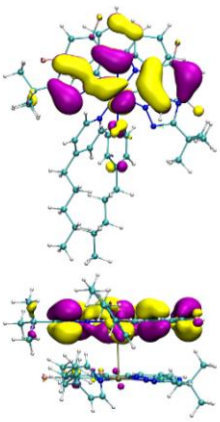 $\varepsilon = -6.878\,\mathrm{eV}$
HOMO-4	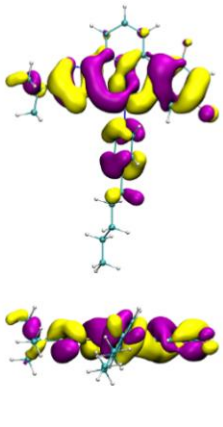 $\varepsilon = -7.361\,\mathrm{eV}$	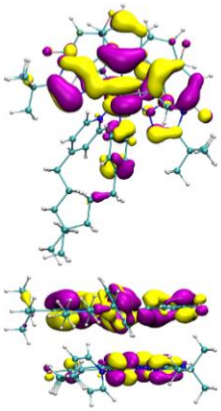 $\varepsilon = -7.027\,\mathrm{eV}$	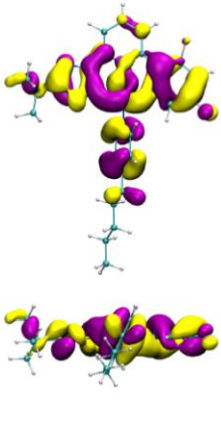 $\varepsilon = -7.368\,\mathrm{eV}$	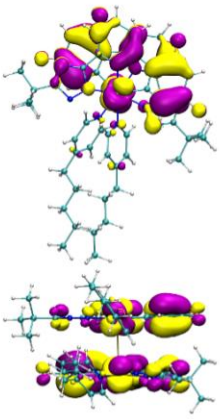 $\varepsilon = -6.977\,\mathrm{eV}$
HOMO-5	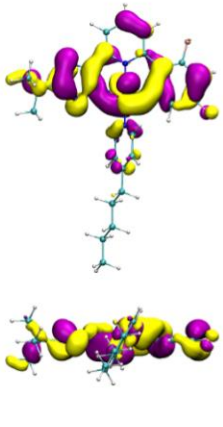 $\varepsilon = -7.592\,\mathrm{eV}$	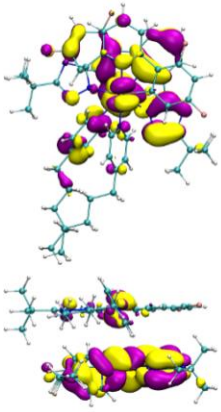 $\varepsilon = -7.030\,\mathrm{eV}$	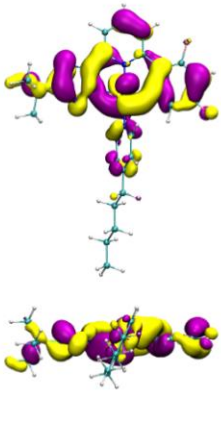 $\varepsilon = -7.592\,\mathrm{eV}$	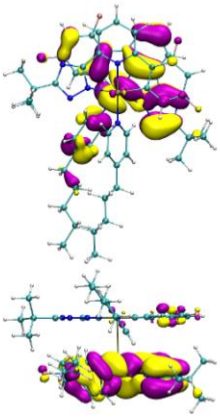 $\varepsilon = -7.016\,\mathrm{eV}$

Table S3. *Molecular orbitals for complex **C4** for the S0 geometry from ground state DFT calculations and orbitals for the T1 geometry from TDDFT calculations performed with Gaussian 09 Rev. D.01[5], visualized with VMD 1.9.1[6,7]*

	S_0		T_1	
Orbital	Monomer	Dimer	Monomer	Dimer
LUMO+5	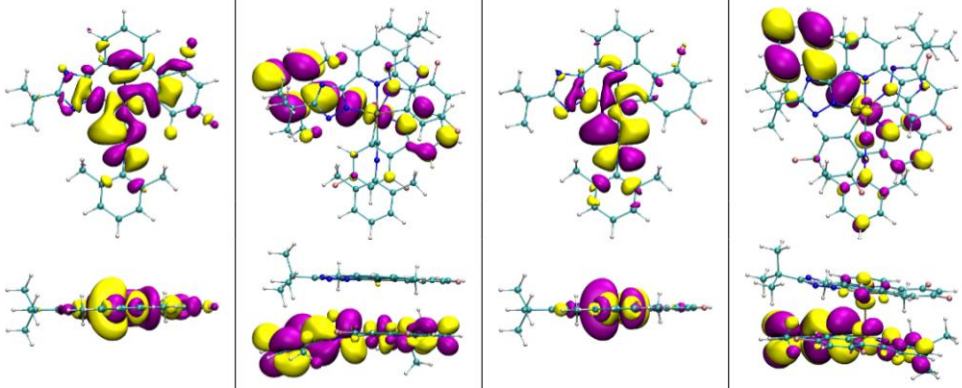 $\varepsilon = -0.147\,\mathrm{eV}$	$\varepsilon = -1.175\,\mathrm{eV}$	$\varepsilon = -0.047\,\mathrm{eV}$	$\varepsilon = -1.186\,\mathrm{eV}$
LUMO+4	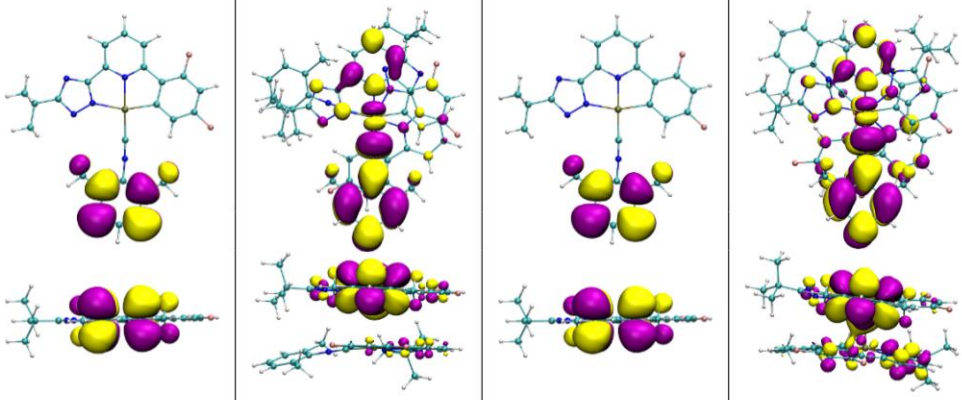 $\varepsilon = -0.235\,\mathrm{eV}$	$\varepsilon = -1.206\,\mathrm{eV}$	$\varepsilon = -0.239\,\mathrm{eV}$	$\varepsilon = -1.238\,\mathrm{eV}$
LUMO+3	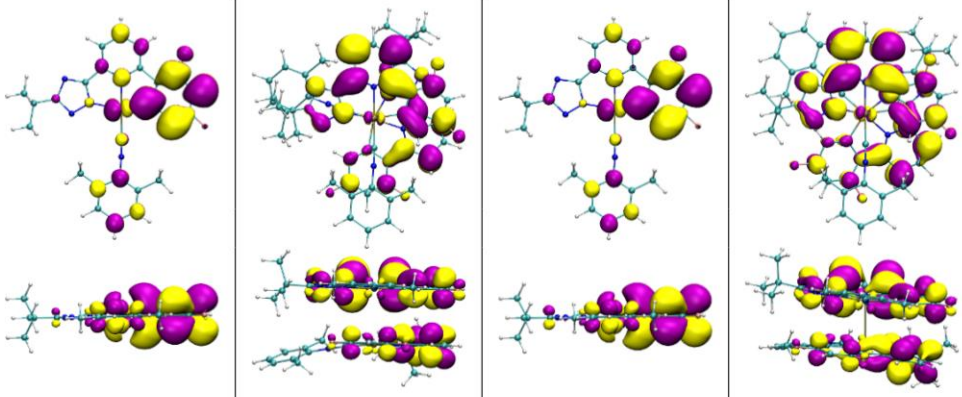 $\varepsilon = -0.499\,\mathrm{eV}$	$\varepsilon = -1.530\,\mathrm{eV}$	$\varepsilon = -0.488\,\mathrm{eV}$	$\varepsilon = -1.517\,\mathrm{eV}$

LUMO+2	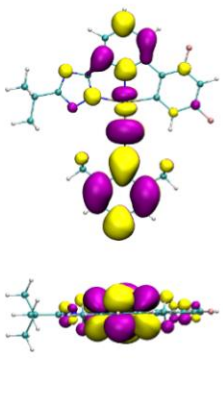 $\varepsilon = -1.248\,\mathrm{eV}$	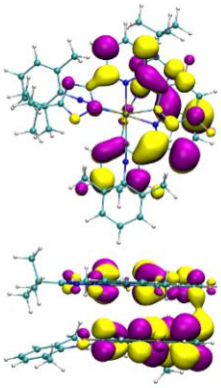 $\varepsilon = -1.628\,\mathrm{eV}$	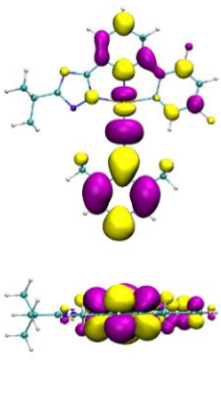 $\varepsilon = -1.264\,\mathrm{eV}$	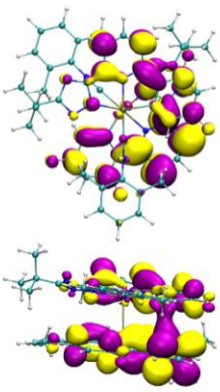 $\varepsilon = -1.644\,\mathrm{eV}$
LUMO+1	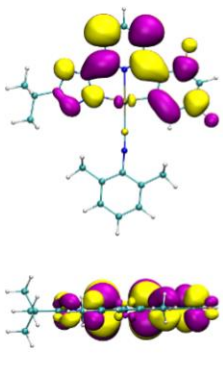 $\varepsilon = -1.632\,\mathrm{eV}$	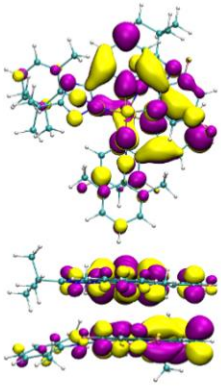 $\varepsilon = -2.216\,\mathrm{eV}$	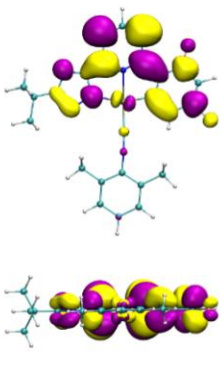 $\varepsilon = -1.703\,\mathrm{eV}$	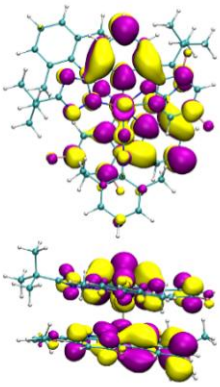 $\varepsilon = -1.998\,\mathrm{eV}$
LUMO	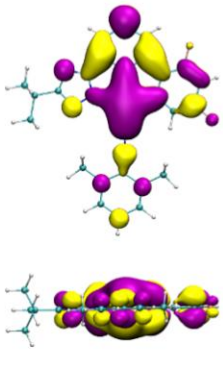 $\varepsilon = -2.452\,\mathrm{eV}$	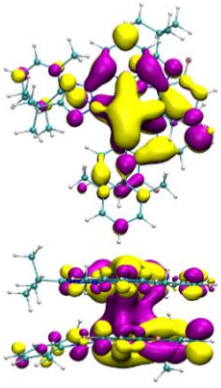 $\varepsilon = -2.530\,\mathrm{eV}$	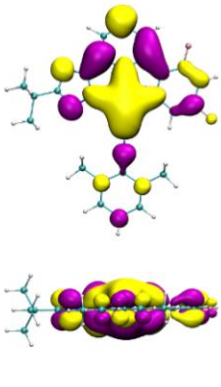 $\varepsilon = -2.622\,\mathrm{eV}$	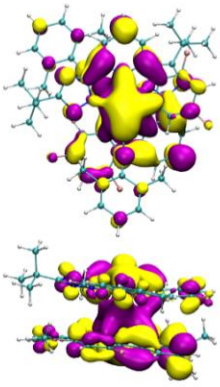 $\varepsilon = -2.766\,\mathrm{eV}$
HOMO	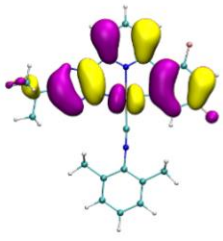	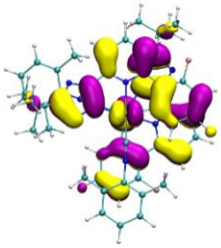	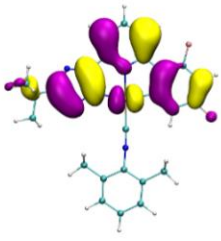	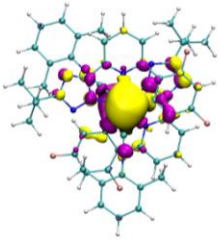

HOMO	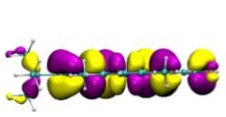 $\varepsilon = -6.441\,\mathrm{eV}$	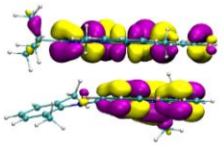 $\varepsilon = -6.326\,\mathrm{eV}$	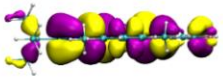 $\varepsilon = -6.187\,\mathrm{eV}$	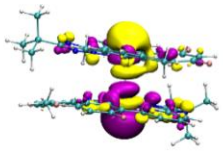 $\varepsilon = -5.914\,\mathrm{eV}$
HOMO-1	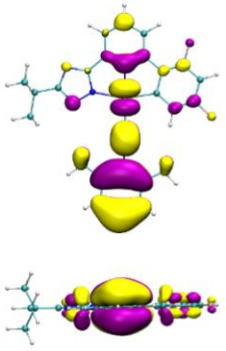 $\varepsilon = -7.049\,\mathrm{eV}$	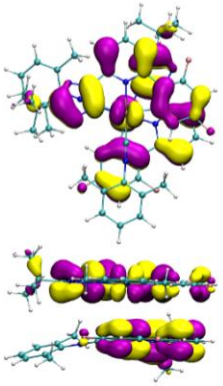 $\varepsilon = -6.420\,\mathrm{eV}$	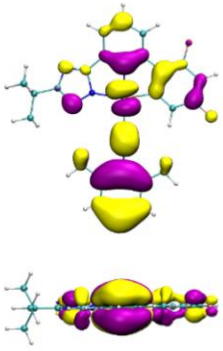 $\varepsilon = -7.026\,\mathrm{eV}$	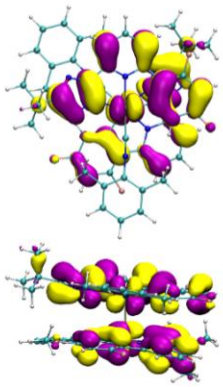 $\varepsilon = -6.264\,\mathrm{eV}$
HOMO-2	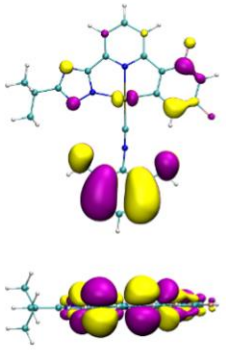 $\varepsilon = -7.231\,\mathrm{eV}$	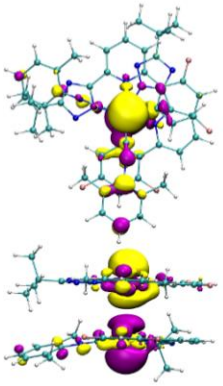 $\varepsilon = -6.813\,\mathrm{eV}$	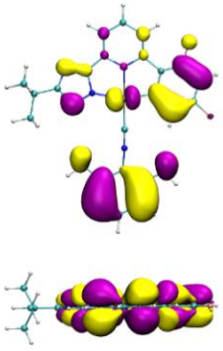 $\varepsilon = -7.230\,\mathrm{eV}$	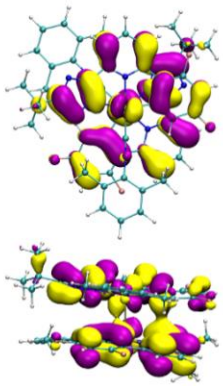 $\varepsilon = -6.438\,\mathrm{eV}$
HOMO-3	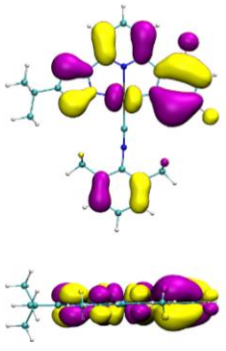 $\varepsilon = -7.279\,\mathrm{eV}$	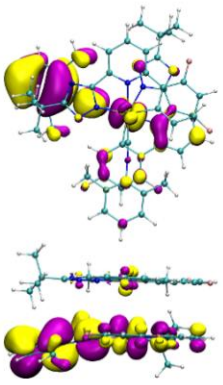 $\varepsilon = -6.979\,\mathrm{eV}$	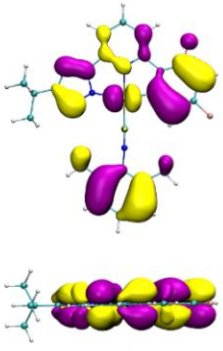 $\varepsilon = -7.256\,\mathrm{eV}$	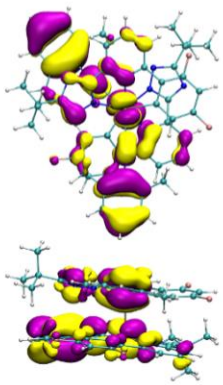 $\varepsilon = -6.900\,\mathrm{eV}$
HOMO-4	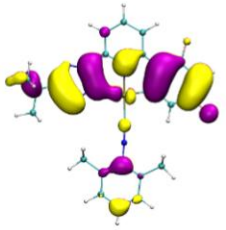	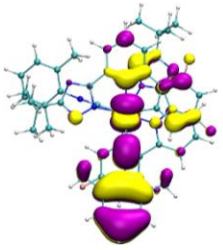	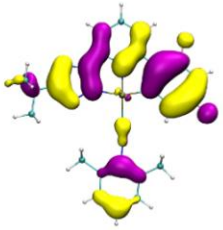	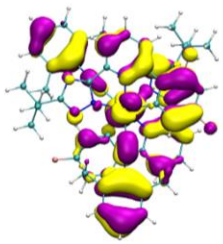

HOMO-4	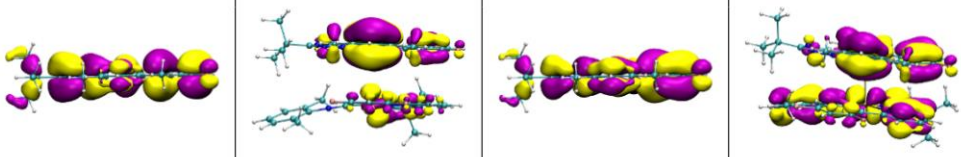 $\varepsilon = -7.433\,\mathrm{eV}$	$\varepsilon = -6.993\,\mathrm{eV}$	$\varepsilon = -7.361\,\mathrm{eV}$	$\varepsilon = -6.956\,\mathrm{eV}$
HOMO-5	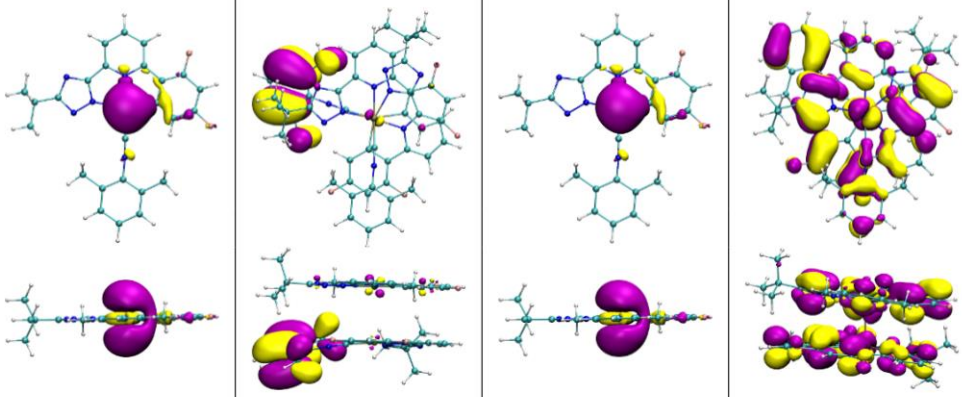 $\varepsilon = -7.491\,\mathrm{eV}$	$\varepsilon = -7.163\,\mathrm{eV}$	$\varepsilon = -7.516\,\mathrm{eV}$	$\varepsilon = -7.126\,\mathrm{eV}$

Table S4. *Molecular orbitals for complex **C5** for the S0 geometry from ground state DFT calculations and orbitals for the T1 geometry from TDDFT calculations performed with Gaussian 09 Rev. D.01[5], visualized with VMD 1.9.1[6,7]*

	S_0		T_1	
Orbital	Monomer	Dimer	Monomer	Dimer
LUMO+5	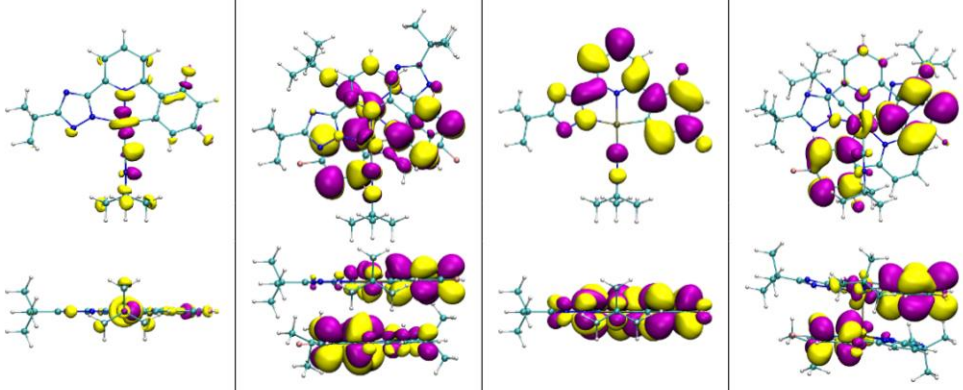 $\varepsilon = 0.171\,\mathrm{eV}$	$\varepsilon = -0.478\,\mathrm{eV}$	$\varepsilon = 0.157\,\mathrm{eV}$	$\varepsilon = -0.282\,\mathrm{eV}$
LUMO+4	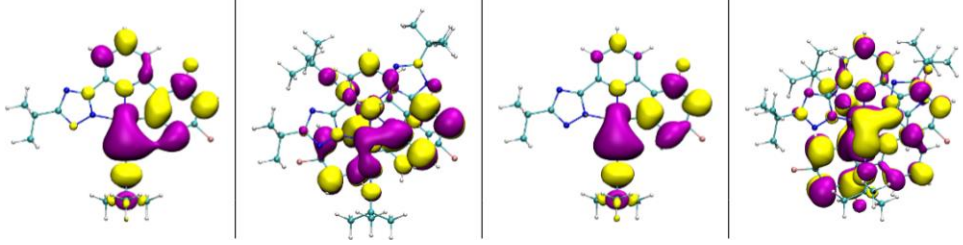			

LUMO+3	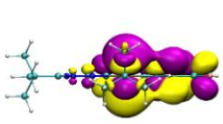 $\varepsilon = 0.014\,\mathrm{eV}$	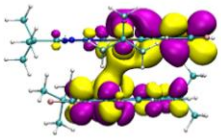 $\varepsilon = -0.556\,\mathrm{eV}$	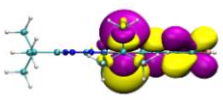 $\varepsilon = 0.033\,\mathrm{eV}$	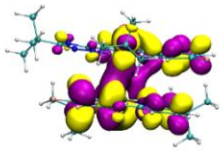 $\varepsilon = -0.631\,\mathrm{eV}$
LUMO+3	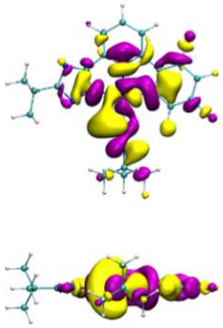 $\varepsilon = -0.067\,\mathrm{eV}$	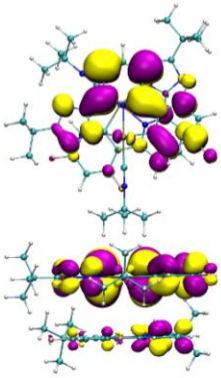 $\varepsilon = -1.537\,\mathrm{eV}$	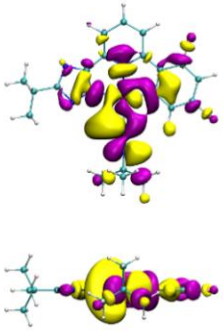 $\varepsilon = 0.012\,\mathrm{eV}$	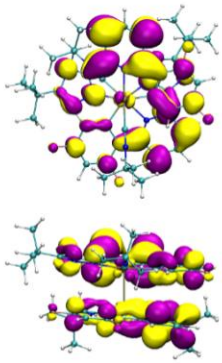 $\varepsilon = -1.492\,\mathrm{eV}$
LUMO+2	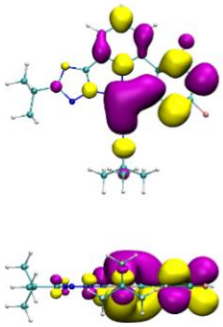 $\varepsilon = -0.596\,\mathrm{eV}$	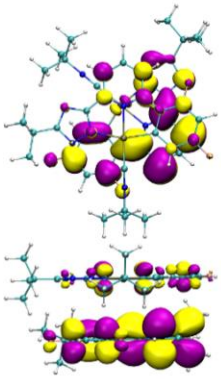 $\varepsilon = -1.561\,\mathrm{eV}$	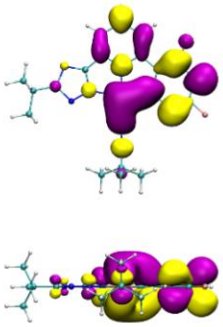 $\varepsilon = -0.573\,\mathrm{eV}$	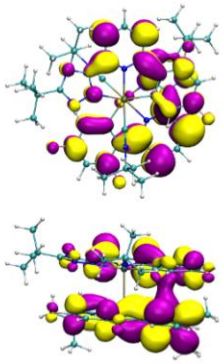 $\varepsilon = -1.610\,\mathrm{eV}$
LUMO+1	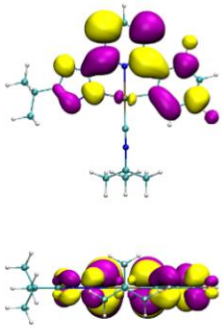 $\varepsilon = -1.611\,\mathrm{eV}$	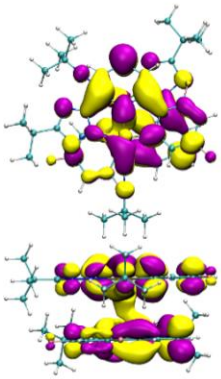 $\varepsilon = -2.233\,\mathrm{eV}$	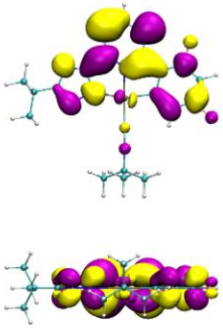 $\varepsilon = -1.673\,\mathrm{eV}$	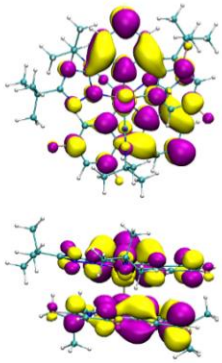 $\varepsilon = -1.949\,\mathrm{eV}$
LUMO	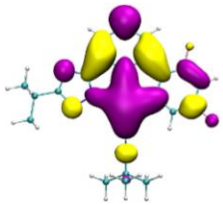	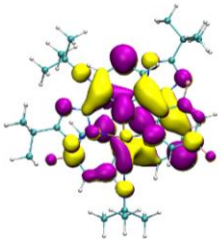	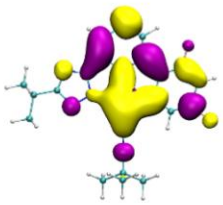	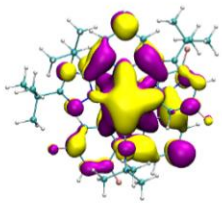

LUMO	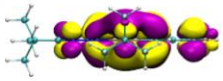 $\varepsilon = -2.352\,\mathrm{eV}$	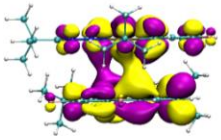 $\varepsilon = -2.322\,\mathrm{eV}$	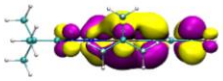 $\varepsilon = -2.564\,\mathrm{eV}$	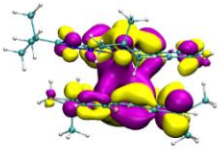 $\varepsilon = -2.651\,\mathrm{eV}$
HOMO	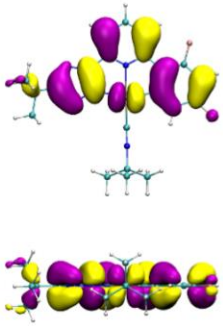 $\varepsilon = -6.403\,\mathrm{eV}$	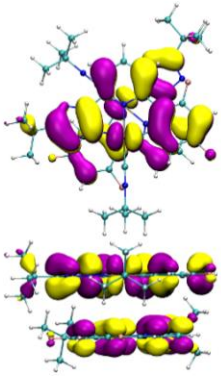 $\varepsilon = -6.329\,\mathrm{eV}$	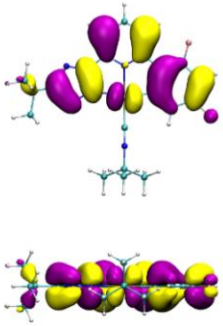 $\varepsilon = -6.251\,\mathrm{eV}$	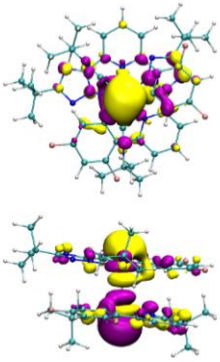 $\varepsilon = -5.834\,\mathrm{eV}$
HOMO-1	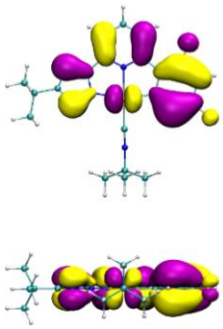 $\varepsilon = -7.247\,\mathrm{eV}$	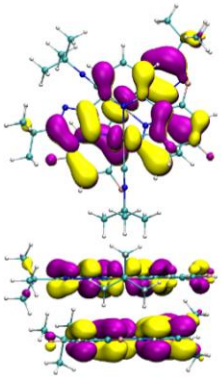 $\varepsilon = -6.341\,\mathrm{eV}$	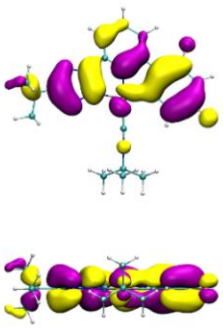 $\varepsilon = -7.165\,\mathrm{eV}$	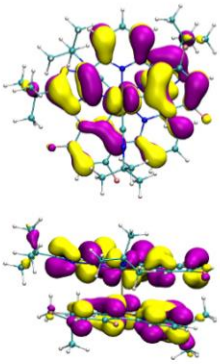 $\varepsilon = -6.221\,\mathrm{eV}$
HOMO-2	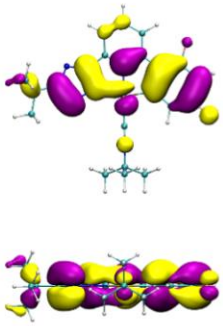 $\varepsilon = -7.357\,\mathrm{eV}$	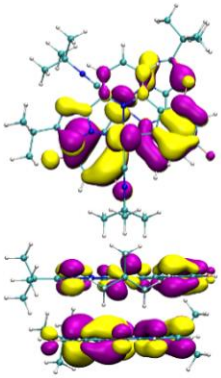 $\varepsilon = -7.167\,\mathrm{eV}$	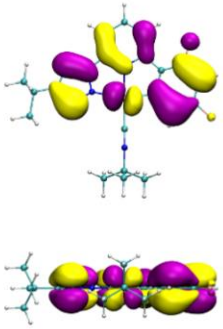 $\varepsilon = -7.309\,\mathrm{eV}$	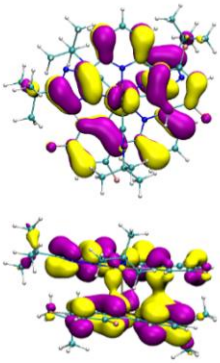 $\varepsilon = -6.409\,\mathrm{eV}$
HOMO-3	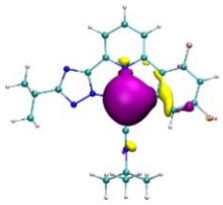	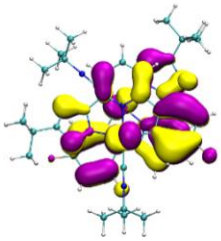	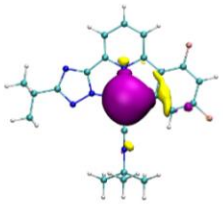	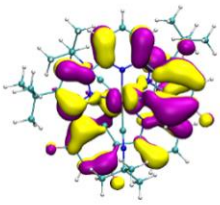

HOMO-3	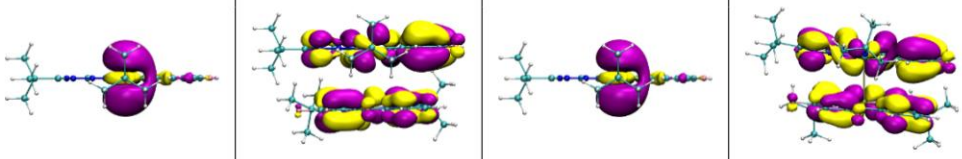 $\varepsilon = -7.412\,\mathrm{eV}$	$\varepsilon = -7.169\,\mathrm{eV}$	$\varepsilon = -7.459\,\mathrm{eV}$	$\varepsilon = -7.010\,\mathrm{eV}$
HOMO-4	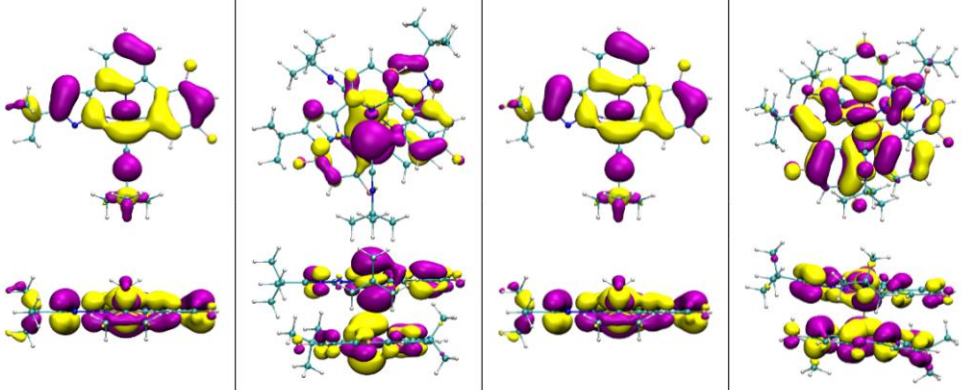 $\varepsilon = -7.770\,\mathrm{eV}$	$\varepsilon = -7.185\,\mathrm{eV}$	$\varepsilon = -7.796\,\mathrm{eV}$	$\varepsilon = -7.175\,\mathrm{eV}$
HOMO-5	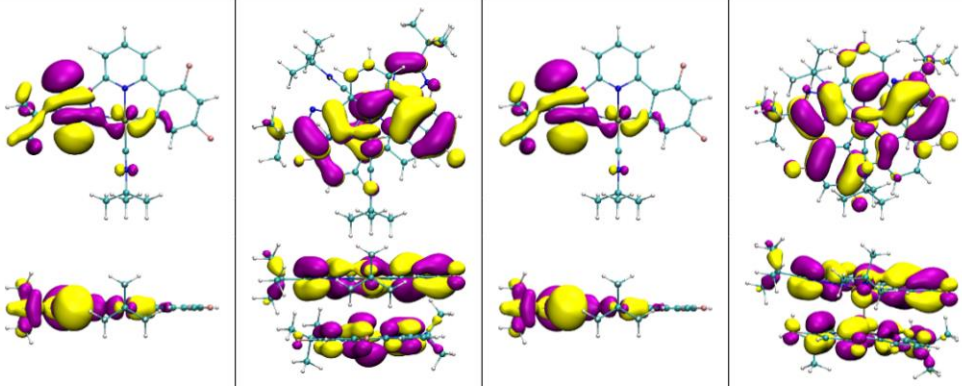 $\varepsilon = -7.790\,\mathrm{eV}$	$\varepsilon = -7.281\,\mathrm{eV}$	$\varepsilon = -7.802\,\mathrm{eV}$	$\varepsilon = -7.218\,\mathrm{eV}$

3.2 CI-Coefficients for the first excited triplet state T1

Table S5. *Coefficients of single excitations to the first triplet state T1 in the CI- expansion, calculated with Gaussian 09 Rev. D.01*[5]

Complex **C2**			
Transition			Coefficient
HOMO-1	→	LUMO	-0.14283
HOMO	→	LUMO	0.63791
HOMO-1	→	LUMO+1	0.21378

Complex **C3**			
Transition			Coefficient
HOMO-1	→	LUMO	0.17364
HOMO	→	LUMO	0.62964
HOMO	→	LUMO+1	0.21643

Complex **C4**			
Transition			Coefficient
HOMO	→	LUMO	-0.63776
HOMO	→	LUMO+1	0.22369

Complex **C5**			
Transition			Coefficient
HOMO-1	→	LUMO	0.25506
HOMO-1	→	LUMO+1	-0.10111
HOMO	→	LUMO	-0.61019
HOMO	→	LUMO+1	0.16907

Complex **C2** - Dimer			
Transition			Coefficient
HOMO	→	LUMO	0.67634
HOMO	→	LUMO+4	0.14386

Complex **C3** - Dimer			
Transition			Coefficient
HOMO-2	→	LUMO	0.18207
HOMO	→	LUMO	0.61050
HOMO	→	LUMO+1	0.12259
HOMO	→	LUMO+2	0.20334
HOMO	→	LUMO+3	-0.10689

Complex **C4** - Dimer			
Transition			Coefficient
HOMO	→	LUMO	0.69973

Complex **C5** - Dimer			
Transition			Coefficient
HOMO	→	LUMO	0.70009

3.3 Pt-Pt distances and binding energies for the dimers

Table S6. *Distances between the Platinum-atoms in the optimized dimer-structures and corresponding binding energies.*

Complex	Distance [Å]		Binding Energy [eV]	
	S_0	T_1	S_0	T_1
C2	5.9523	2.8674	-0.1407	0.5129
C3	3.9265	3.8491	-0.3584	-0.3523
C4	3.6245	2.8224	-0.2554	-0.2119
C5	4.4919	2.8184	-0.2362	-0.1670

[5] M. J. Frisch, G. W. Trucks, H. B. Schlegel, G. E. Scuseria, M. A. Robb, J.R. Cheeseman, G. Scalmani, V. Barone, B. Mennucci, G. A. Petersson, H. Nakatsuji, M. Caricato, X. Li, H. P. Hratchian, A. F. Izmaylov, J. Bloino, G. Zheng, J. L. Sonnenberg, M. Hada, M. Ehara, K. Toyota, R. Fukuda, J. Hasegawa, M. Ishida, T. Nakajima, Y. Honda, O. Kitao, H. Nakai, T. Vreven, J. A. Montgomery Jr., J. E. Peralta, F. Ogliaro, M. Bearpark, J. J. Heyd, E. Brothers, K. N. Kudin, V. N. Staroverov, R. Kobayashi, J. Normand, K. Raghavachari, A. Rendell, J. C. Burant, S. S. Iyengar, J. Tomasi, M. Cossi, N. Rega, J. M. Millam, M. Klene, J. E. Knox, J. B. Cross, V. Bakken, C. Adamo, J. Jaramillo, R. Gomperts, R. E. Stratmann, O. Yazyev, A. J. Austin, R. Cammi, C. Pomelli, J. W. Ochterski, R. L. Martin, K. Morokuma, V. G. Zakrzewski, G. A. Voth, P. Salvador, J. J. Dannenberg, S. Dapprich, A. D. Daniels, . Farkas, J. B. Foresman, J. V. Ortiz, J. Cioslowski, and D. J. Fox. Gaussian 09 Revision D.01. Gaussian Inc.Wallingford CT 2009 (cit. on pp. 1, 5, 9, 12, 16).

[6] C. Adamo, V. Barone, *J. Chem. Phys.* **2015**, *110*, 6158

[7] T. H. Dunning Jr., P. J. Hay, *Modern Theoretical Chemistry*, Vol. 3, edited by H. F. Schaefer III, pp.1-28

[8] D. Andrae, U. Huermann, M. Dolg, H. Stoll, H. Preu, *Theor. Chim. Acta*, **1990**, *77*, 123

[9] S. Miertus, E. Scrocco, J. Tomasi, *Chem. Phys.* **1981**, *55*, 117

[10] R. Improta, V. Barone, G. Scalmani, M. J. Frisch, *J. Chem. Phys.* **2006**, *125*, 054103

[11] A. Bondi *J. Chem. Phys.* **1964**, *68*, 441

[12] V. Barone, J. Bloino, M. Biczysko, F. Santoro, *J. Chem. Theory Comput.* **2009**, *5*, 540

[13] W. Humphrey, A. Dalke, and K. Schulten. "VMD – Visual Molecular Dynamics". In: *Journal of Molecular Graphics 14*, **1996**, pp. 33–38 (cit. on pp. 1, 5, 9, 12).

[14] J. Stone. “An Efficient Library for Parallel Ray Tracing and Animation”. MA thesis. Computer Science Department, University of Missouri-Rolla, 1998 (cit. on pp. 1, 5, 9, 12).

4 Photophysics

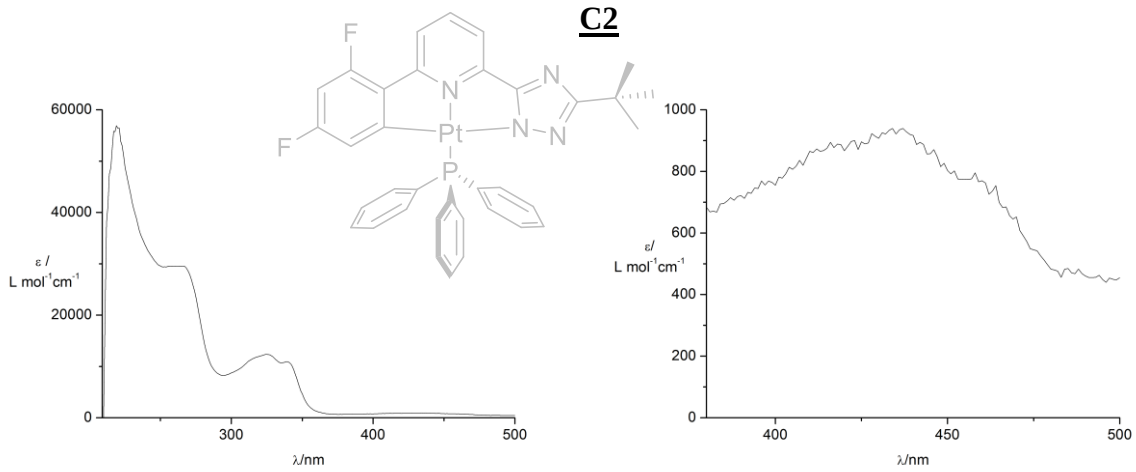

Absorption spectrum of **C2** at room temperature in THF, 10^{-5} M (the spectral region between 375 nm and 500 nm is displayed on a smaller scale for clarity).

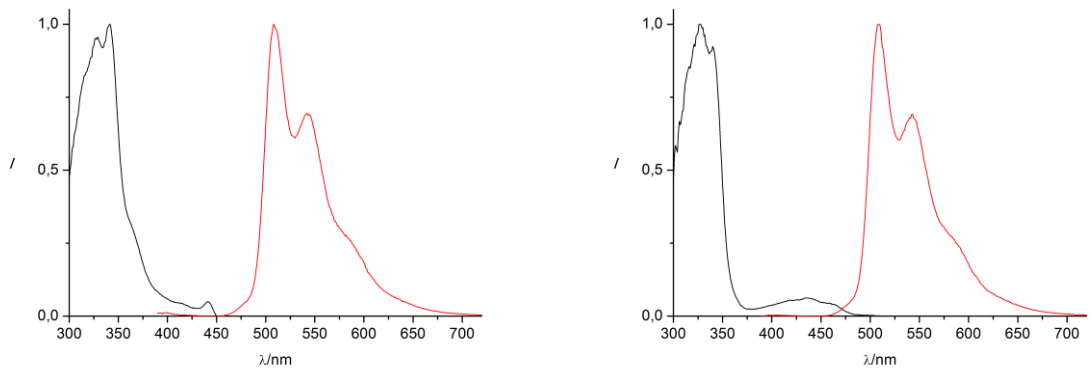

Excitation (black) and *emission* (red) spectra of **C2** in *aerated* (left) and *deaerated* (right) THF, 10^{-5} M (λ_{exc} = 340 nm; λ_{em} = 570 nm).

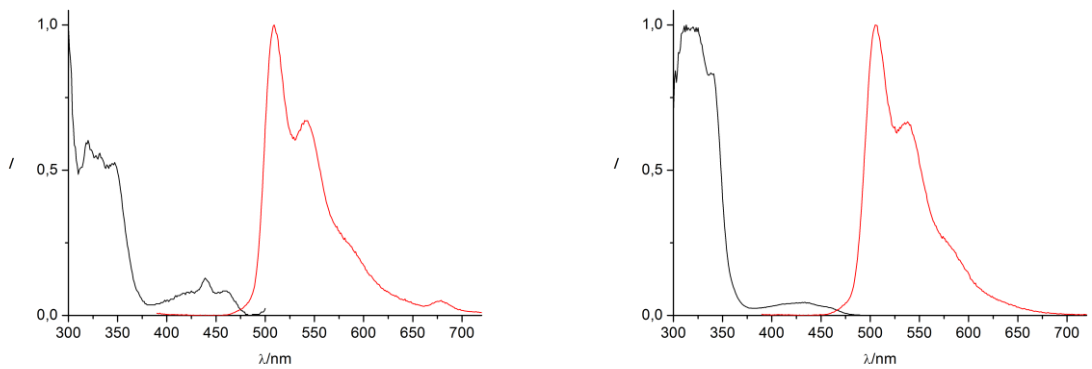

Excitation (black) and *emission* (red) spectra of **C2** in *neat* (left) and *10%* doped into *PMMA* (right) *films* (λ_{exc} = 340 nm; λ_{em} = 570 nm).

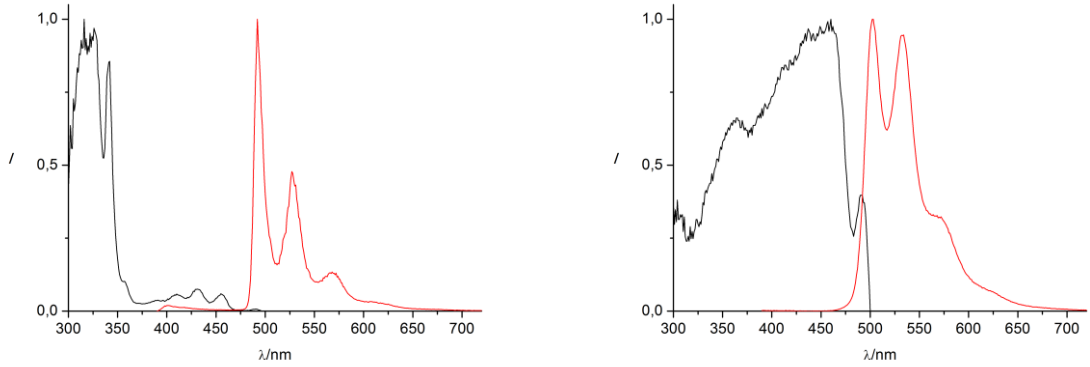

Excitation (black) and *emission* (red) spectra of **C2** in a *frozen glassy matrix at 77 K* (left, 2-MeTHF, λ_{exc} = 340 nm; λ_{em} = 570 nm) and in the *solid state at room temperature* (right, λ_{exc} = 340 nm; λ_{em} = 570 nm)

	λ_{exc} (nm)	λ_{em} (nm)	Φ_{ph}	$\tau^{a)}$ (µs)	k_r ($10^5 s^{-1}$)	k_{nr} ($10^5 s^{-1}$)
aerated	341	508	0,007	0,17	0,41	58,68
deaerated	327	508	0,708	15,15	0,47	0,19
neat	300	509	0,049	1,65	0,30	5,78
PMMA	313	505	0,732	14,83	0,49	0,18
77K	316	492	1	15,24	0,66	-
solid	460	503	0,838	15,42	0,54	0,11

Summary of photophysical data for complex **C2**. [a]The excitation and emission maxima with the shortest wavelengths are indicated. [b] Amplitude-weighted average lifetimes.

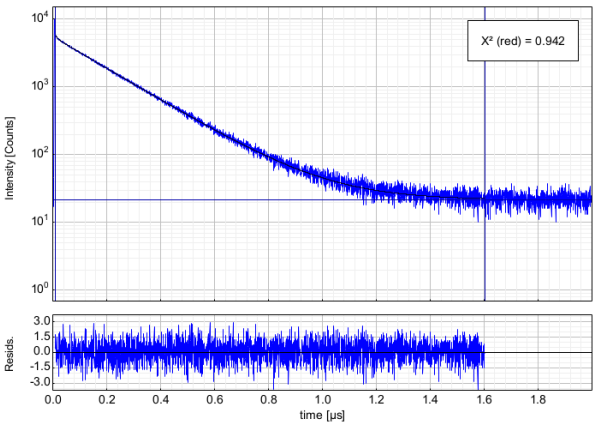

Parameter	Value	Conf. Lower	Conf. Upper
A_1 [Cnts]	5221.6	-33.0	+33.0
τ_1 [µs]	0.184014	-0.000878	+0.000878
A_2 [Cnts]	480	-216	+216
τ_2 [µs]	0.00821	-0.00518	+0.00518
Bkgr. Dec [Cnts]	21.63	-1.21	+1.21

Left: Time-resolved luminescence decay of **C2** in *aerated THF* including the residuals (left, λ_{exc} =376.7 nm). Right: Fitting parameters including pre-exponential factors and confidence limits.

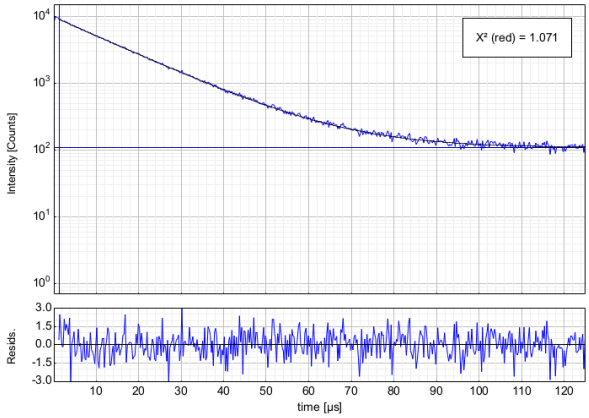

Parameter	Value	Conf. Lower	Conf. Upper
A_1 [Cnts]	8969.8	-45.2	+45.2
τ_1 [µs]	15.1498	-0.0615	+0.0615
Bkgr. Dec [Cnts]	108.53	-2.52	+2.52

Left: Time-resolved luminescence decay of **C2** in *deaerated THF* including the residuals (left, λ_{exc} =376.7 nm). Right: Fitting parameters including pre-exponential factors and confidence limits.

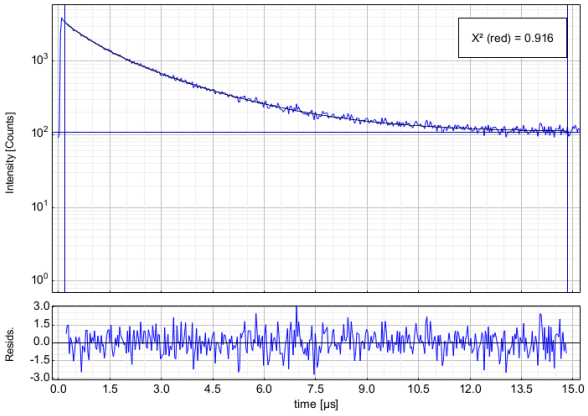

Parameter	Value	Conf. Lower	Conf. Upper
A_1 [Cnts]	1659.1	-18.5	+18.5
τ_1 [µs]	2.4200	-0.0229	+0.0229
A_2 [Cnts]	1460.4	-44.4	+44.4
τ_2 [µs]	0.7676	-0.0259	+0.0259
Bkgr. Dec [Cnts]	107.22	-2.14	+2.14

Left: Time-resolved luminescence decay of **C2** *in a neat film* including the residuals (left, λ_{exc} =376.7 nm). Right: Fitting parameters including pre-exponential factors and confidence limits.

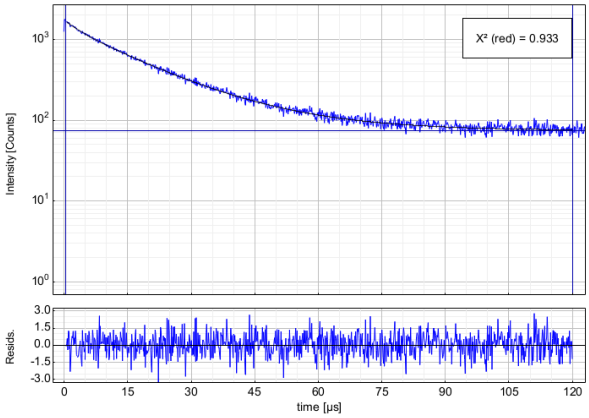

Parameter	Value	Conf. Lower	Conf. Upper
A_1 [Cnts]	1233.1	-17.3	+17.3
τ_1 [µs]	15.866	-0.203	+0.203
A_2 [Cnts]	117.5	-10.7	+10.7
τ_2 [µs]	27.29	-2.08	+2.08
A_3 [Cnts]	237.4	-48.0	+48.0
τ_3 [µs]	3.337	-0.855	+0.855
Bkgr. Dec [Cnts]	73.93	-1.75	+1.75

Left: Time-resolved luminescence decay of *10%* **C2** *in a PMMA film* including the residuals (left, λ_{exc} =376.7 nm). Right: Fitting parameters including pre-exponential factors and confidence limits.

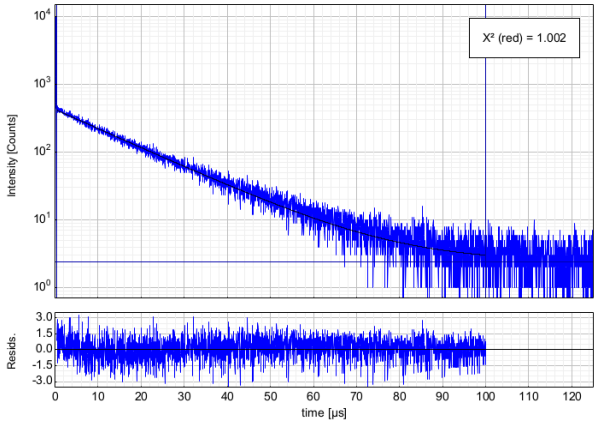

Parameter	Value	Conf. Lower	Conf. Upper
A_1 [Cnts]	411.26	-8.41	+8.41
τ_1 [µs]	15.243	-0.250	+0.250
Bkgr. Dec [Cnts]	2.420	-0.563	+0.563

Left: Time-resolved luminescence decay of **C2** *in a frozen 2-MeTHF glassy matrix* at *77K* including the residuals (left, λ_{exc} =376.7 nm). Right: Fitting parameters including pre-exponential factors and confidence limits.

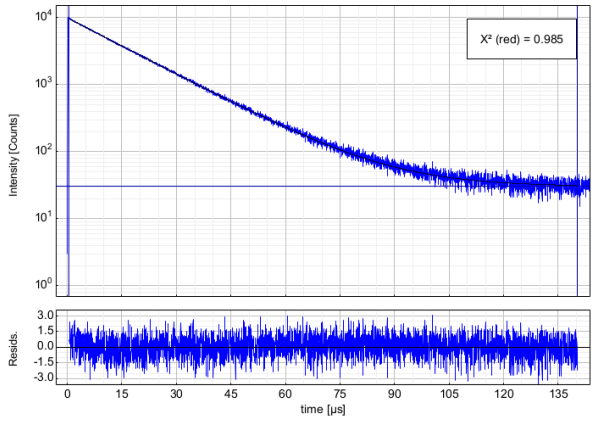

Parameter	Value	Conf. Lower	Conf. Upper
A_1 [Cnts]	9556.0	-46.6	+46.6
τ_1 [µs]	15.4198	-0.0563	+0.0563
Bkgr. Dec [Cnts]	30.32	-1.45	+1.45

Left: Time-resolved luminescence decay of **C2** *in the solid state* including the residuals (left, λ_{exc} =376.7 nm). Right: Fitting parameters including pre-exponential factors and confidence limits.

C3

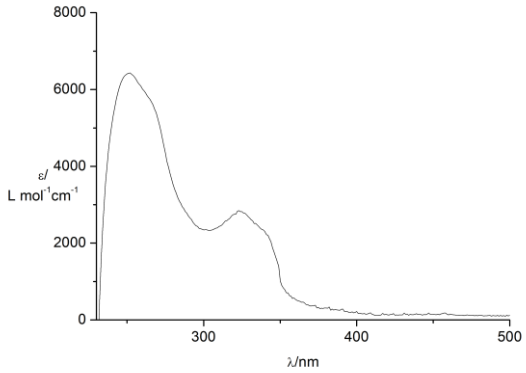

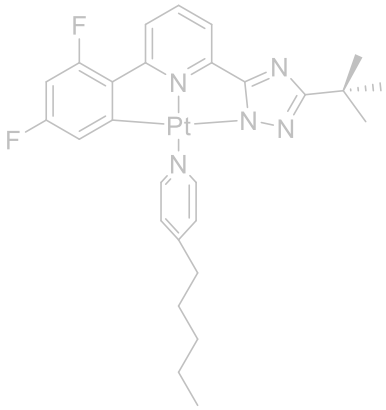

Absorption spectrum of **C3** at room temperature in CH_2Cl_2, 10^{-5}M.

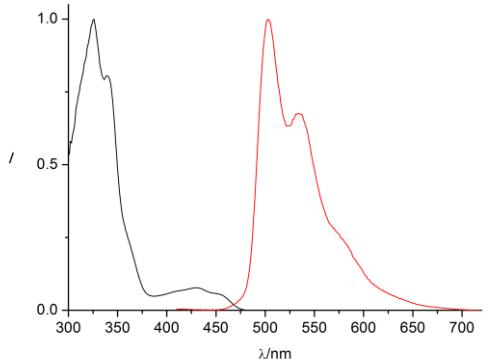

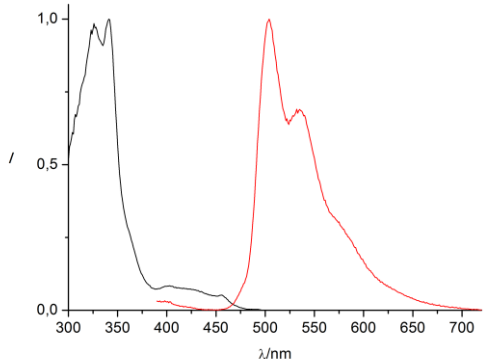

Excitation (black) and *emission* (red) spectra of **C3** in *aerated* (left) and *deaerated* (right) CH_2Cl_2, 10^{-5} M (λ_{exc} = 320 nm; λ_{em} = 570 nm).

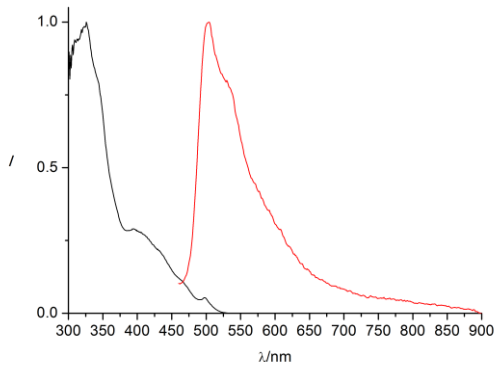

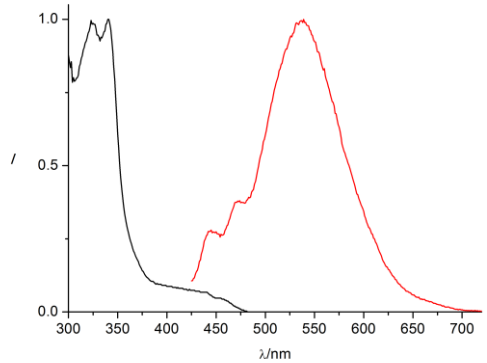

Excitation (black) and *emission* (red) spectra of **C3** in *neat* (left) and *10%* doped into *PMMA* (right) *films* (λ_{exc} = 320 nm; λ_{em} = 570 nm).

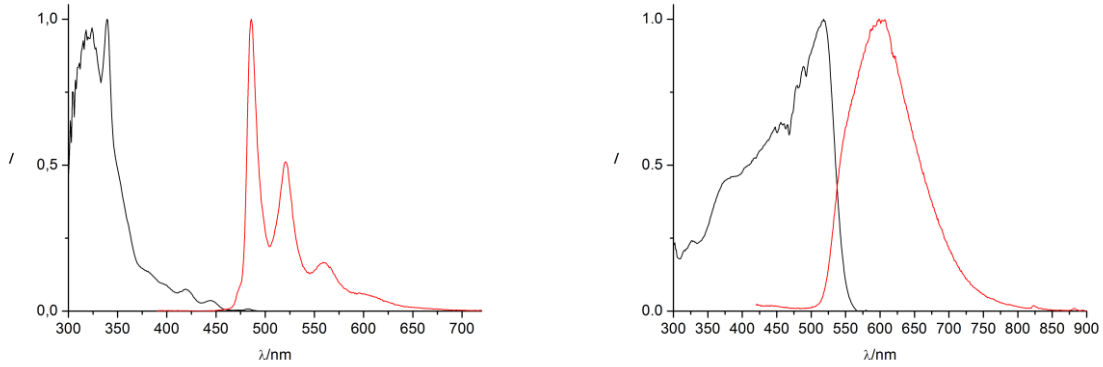

Excitation (black) and *emission* (red) spectra of **C3** in a *frozen glassy matrix at 77 K* (left, CH_2Cl_2/MeOH 1:1, λ_{exc} = 320 nm; λ_{em} = 570 nm) and in the *solid state at room temperature* (right, λ_{exc} = 320 nm; λ_{em} = 570 nm)

	λ_{exc} (nm)	λ_{em} (nm)	Φ_{ph}	$\tau^{a)}$ (µs)	k_r ($10^5 s^{-1}$)	k_{nr} ($10^5 s^{-1}$)
aerated	326	503	0,024	0,12	2,02	81,99
deaerated	341	504	0,082	2,02	0,41	4,55
neat	326	504	0,078	0,84	0,92	10,92
PMMA	340	539	0,422	7,91	0,53	0,73
77K	339	486	1	12,23	0,82	-
solid	518	599	0,100	1,40	0,71	6,43

Summary of photophysical data for complex **C3**. [a]The excitation and emission maxima with the shortest wavelengths are indicated. [b] Amplitude-weighted average lifetimes.

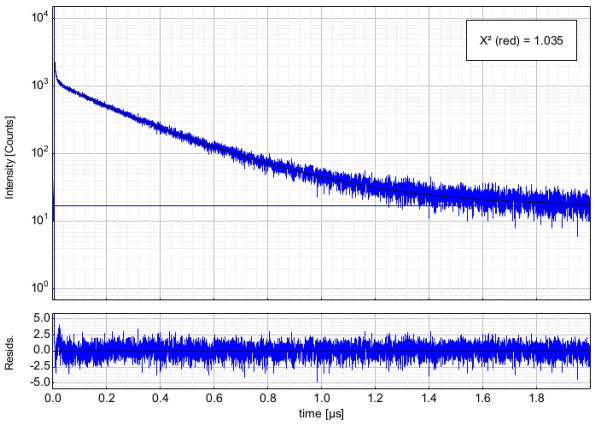

Parameter	Value	Conf. Lower	Conf. Upper
A_1 [Cnts]	718.8	-13.1	+13.1
τ_1 [µs]	0.30696	-0.00429	+0.00429
A_2 [Cnts]	1254	-212	+212
τ_2 [µs]	0.004274	-0.000904	+0.000904
A_3 [Cnts]	436.9	-25.2	+25.2
τ_3 [µs]	0.13916	-0.00829	+0.00829
Bkgr. Dec [Cnts]	17.06	-1.06	+1.06

Left: Time-resolved luminescence decay of **C3** in *aerated* CH_2Cl_2 including the residuals (left, λ_{exc} =376.7 nm). Right: Fitting parameters including pre-exponential factors and confidence limits.

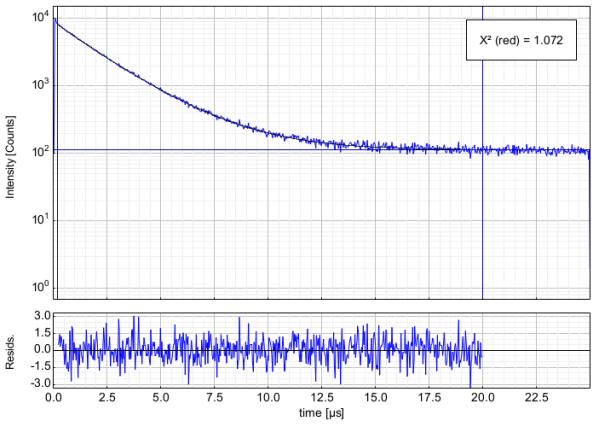

Parameter	Value	Conf. Lower	Conf. Upper
A_1 [Cnts]	4104.8	-58.1	+58.1
τ_1 [µs]	1.5327	-0.0202	+0.0202
A_2 [Cnts]	3795.9	-37.3	+37.3
τ_2 [µs]	2.5445	-0.0189	+0.0189
Bkgr. Dec [Cnts]	112.70	-2.40	+2.40

Left: Time-resolved luminescence decay of **C3** in *deaerated* CH_2Cl_2 including the residuals (left, λ_{exc} =376.7 nm). Right: Fitting parameters including pre-exponential factors and confidence limits.

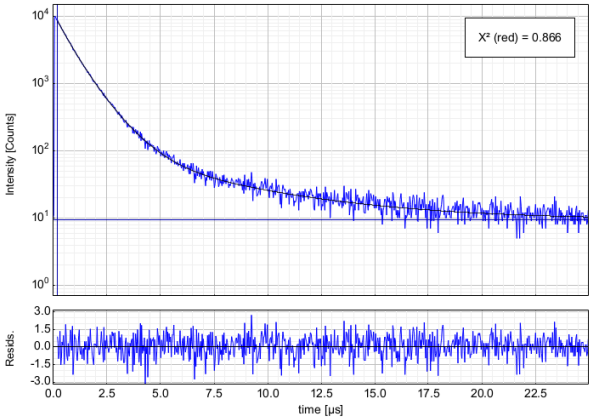

Parameter	Value	Conf. Lower	Conf. Upper
A_1 [Cnts]	3818.2	-57.6	+57.6
τ_1 [µs]	1.0534	-0.0113	+0.0113
A_2 [Cnts]	4681.0	-98.4	+98.4
τ_2 [µs]	0.5752	-0.0115	+0.0115
A_3 [Cnts]	108.59	-6.41	+6.41
τ_3 [µs]	5.111	-0.194	+0.194
Bkgr. Dec [Cnts]	9.565	-0.703	+0.703

Left: Time-resolved luminescence decay of **C3** *in a neat film* including the residuals (left, λ_{exc} =376.7 nm). Right: Fitting parameters including pre-exponential factors and confidence limits.

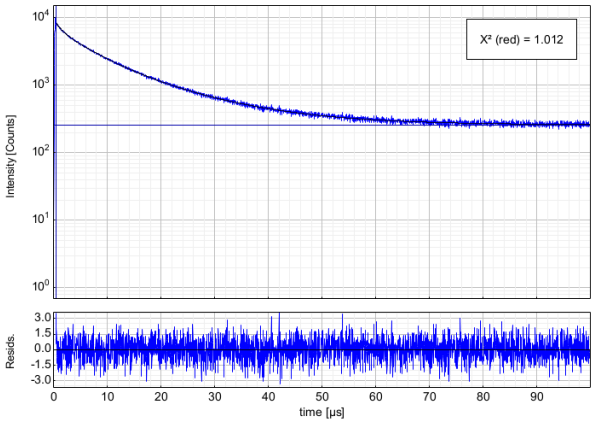

Parameter	Value	Conf. Lower	Conf. Upper
A_1 [Cnts]	3648.2	-64.4	+64.4
τ_1 [µs]	5.900	-0.105	+0.105
A_2 [Cnts]	1707	-179	+179
τ_2 [µs]	1.137	-0.153	+0.153
A_3 [Cnts]	2874.7	-30.6	+30.6
τ_3 [µs]	14.478	-0.128	+0.128
Bkgr. Dec [Cnts]	259.67	-3.24	+3.24

Left: Time-resolved luminescence decay of *10%* **C3** *in a PMMA film* including the residuals (left, λ_{exc} =376.7 nm). Right: Fitting parameters including pre-exponential factors and confidence limits.

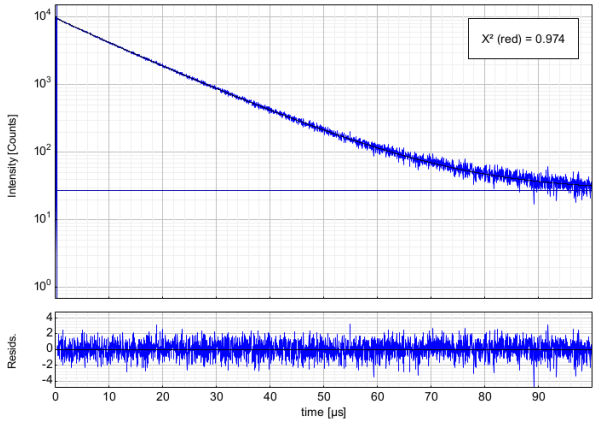

Parameter	Value	Conf. Lower	Conf. Upper
A_1 [Cnts]	5842.8	-37.8	+37.8
τ_1 [µs]	14.0664	-0.0634	+0.0634
A_2 [Cnts]	3551.2	-55.4	+55.4
τ_2 [µs]	9.206	-0.130	+0.130
Bkgr. Dec [Cnts]	26.93	-1.63	+1.63

Left: Time-resolved luminescence decay of **C3** *in a frozen CH_2Cl_2/MeOH 1:1 glassy matrix* at *77K* including the residuals (left, λ_{exc} =376.7 nm). Right: Fitting parameters including pre-exponential factors and confidence limits.

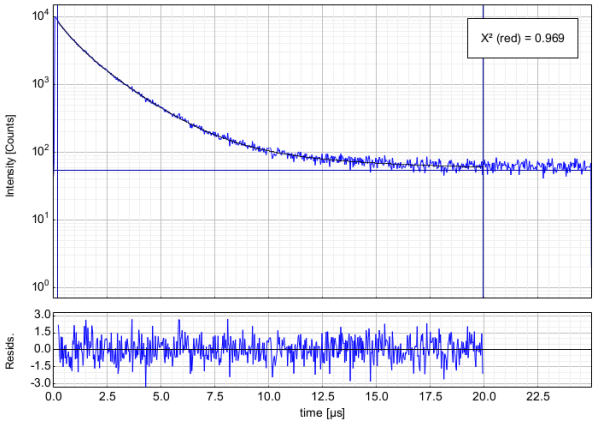

Parameter	Value	Conf. Lower	Conf. Upper
A_1 [Cnts]	4759.5	-41.5	+41.5
τ_1 [µs]	1.7829	-0.0120	+0.0120
A_2 [Cnts]	3353.4	-92.4	+92.4
τ_2 [µs]	0.6429	-0.0194	+0.0194
A_3 [Cnts]	148.19	-9.11	+9.11
τ_3 [µs]	6.179	-0.291	+0.291
Bkgr. Dec [Cnts]	54.52	-1.68	+1.68

Left: Time-resolved luminescence decay of **C3** *in the solid state* including the residuals (left, λ_{exc} =376.7 nm). Right: Fitting parameters including pre-exponential factors and confidence limits.

C4

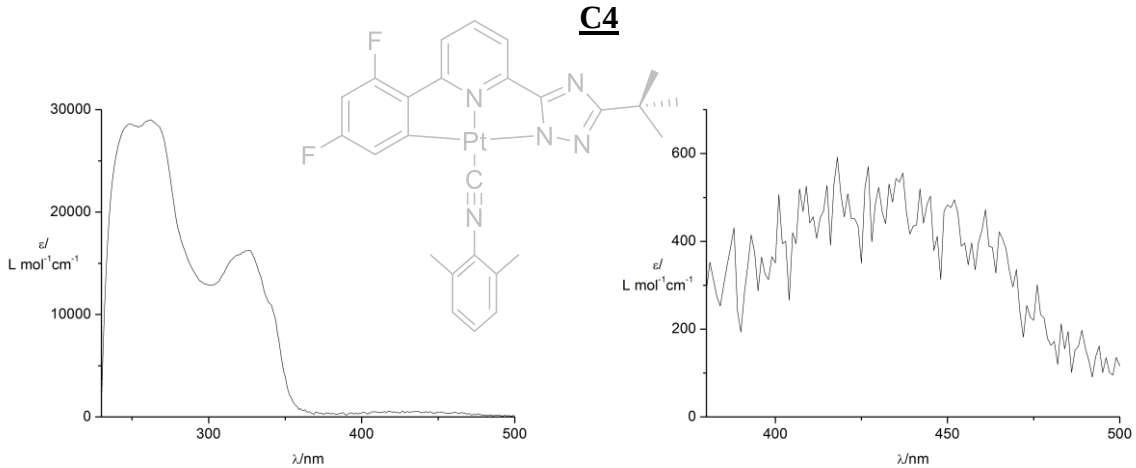

Absorption spectrum of **C4** at room temperature in CH_2Cl_2, 10^{-5} M (the spectral region between 375 nm and 500 nm is displayed on a smaller scale for clarity).

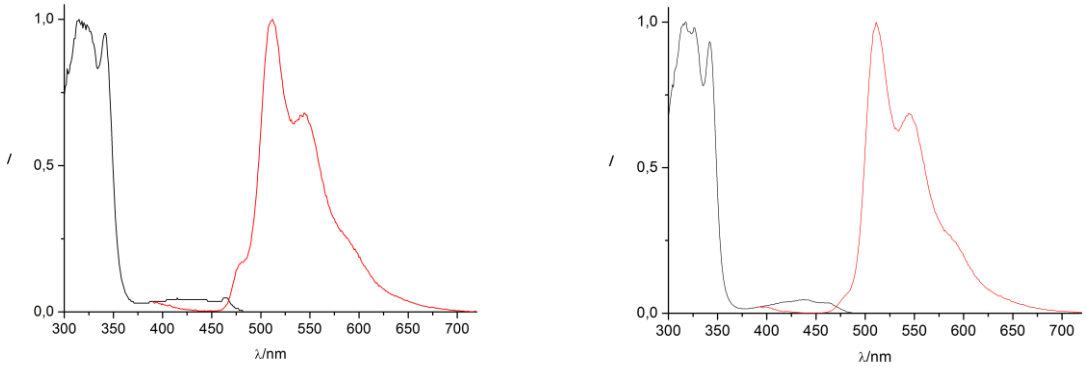

Excitation (black) and *emission* (red) spectra of **C4** in *aerated* (left) and *deaerated* (right) CH_2Cl_2, 10^{-5} M (λ_{exc} = 320 nm; λ_{em} = 540 nm).

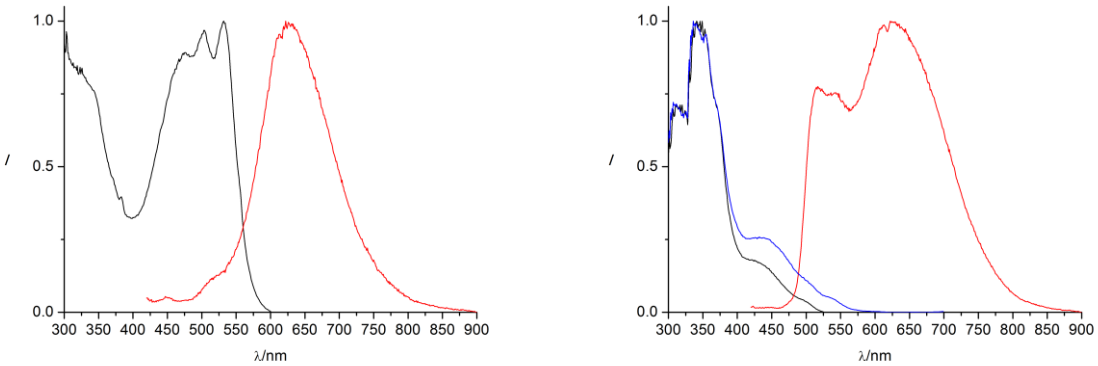

Excitation (black) and *emission* (red) spectra of **C4** in *neat* (left) (λ_{exc} = 320 nm; λ_{em} = 540 nm) and *10%* doped into *PMMA* (right) *films* (λ_{exc} = 320 nm; λ_{em} = 520 nm (black), λ_{em} = 700 nm (blue)).

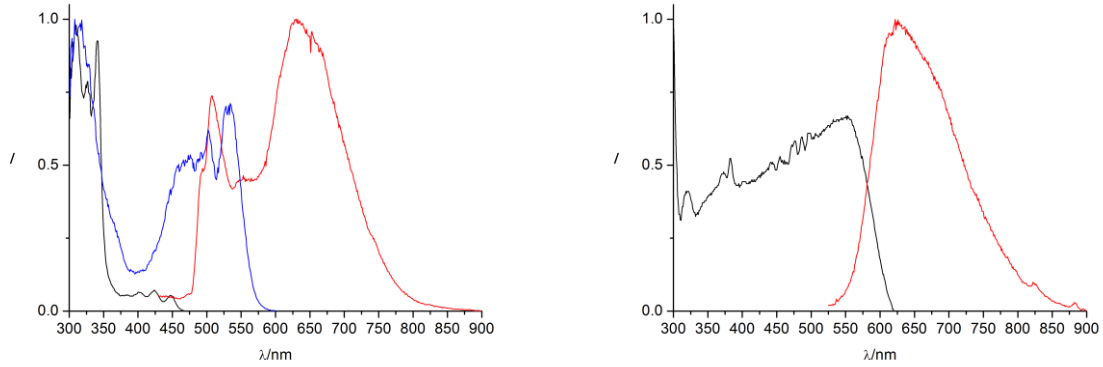

Excitation (black) and *emission* (red) spectra of **C4** in a *frozen glassy matrix at 77 K* (left, CH_2Cl_2/MeOH 1:1, λ_{exc} = 320 nm; λ_{em} = 520 nm (black); λ_{em} = 700 nm (blue)) and in the *solid state at room temperature* (right, λ_{exc} = 320 nm; λ_{em} = 540 nm)

	λ_{exc} (nm)	λ_{em} (nm)	Φ_{ph}	$\tau^{a)}$ (µs)	k_r ($10^5 s^{-1}$)	k_{nr} ($10^5 s^{-1}$)
aerated	315	512	0,05	1,15	0,41	8,30
deaerated	318	511	0,71	13,40	0,53	0,22
neat	532	622	0,20	1,48	1,35	5,40
PMMA	341 336	622	0,51	1,65 2,79	3,09 1,83	2,97 1,76
77K	308 308	630	1	10,61 3,34	0,94 3,00	-
solid	300	622	0,14	0,13	10,97	67,40

Summary of photophysical data for complex **C4** (written in blue are the data for 700 nm emission). [a]The excitation and emission maxima with the shortest wavelengths are indicated. [b] Amplitude-weighted average lifetimes.

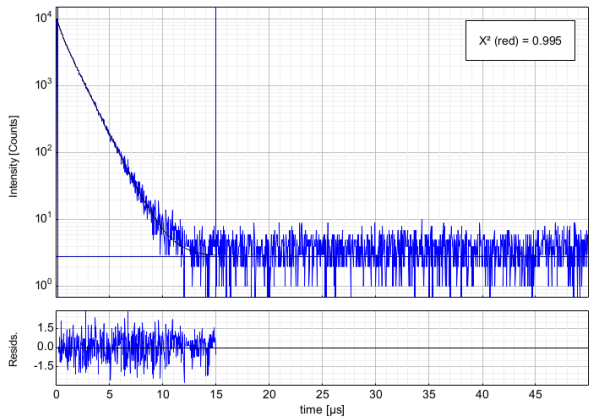

Parameter	Value	Conf. Lower	Conf. Upper
A_1 [Cnts]	6856.0	-44.4	+44.4
τ_1 [µs]	1.33383	-0.00613	+0.00613
A_2 [Cnts]	1618	-113	+113
τ_2 [µs]	0.3639	-0.0311	+0.0311
Bkgr. Dec [Cnts]	2.832	-0.570	+0.570

Left: Time-resolved luminescence decay of **C4** in *aerated* CH_2Cl_2 including the residuals (left, λ_{exc} =376.7 nm). Right: Fitting parameters including pre-exponential factors and confidence limits.

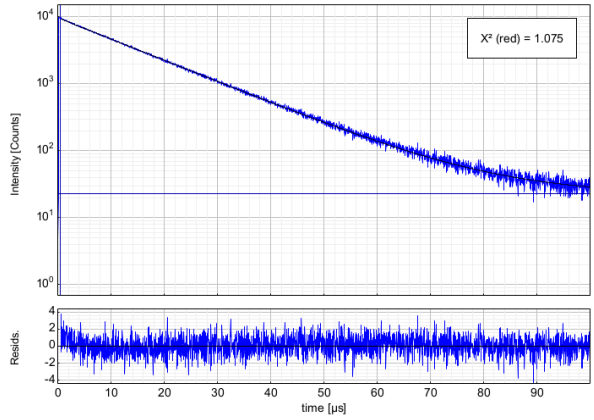

Parameter	Value	Conf. Lower	Conf. Upper
A_1 [Cnts]	9302.4	-43.1	+43.1
τ_1 [µs]	13.5718	-0.0471	+0.0471
Bkgr. Dec [Cnts]	22.77	-1.73	+1.73

Left: Time-resolved luminescence decay of **C4** in *deaerated* CH_2Cl_2 including the residuals (left, λ_{exc} =376.7 nm). Right: Fitting parameters including pre-exponential factors and confidence limits.

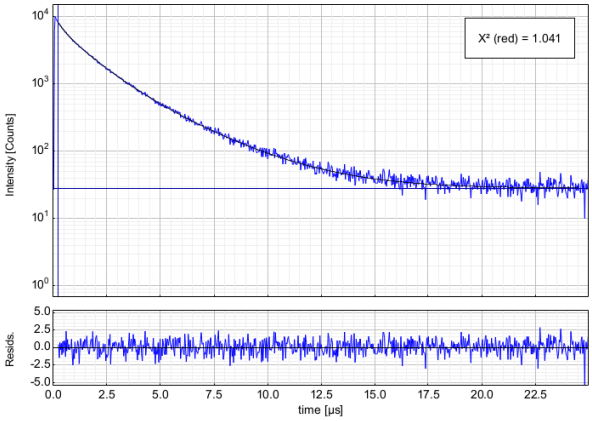

Parameter	Value	Conf. Lower	Conf. Upper
A_1 [Cnts]	4568.3	-65.9	+65.9
τ_1 [µs]	1.2479	-0.0165	+0.0165
A_2 [Cnts]	1400	-162	+162
τ_2 [µs]	0.3049	-0.0453	+0.0453
A_3 [Cnts]	2019.4	-29.7	+29.7
τ_3 [µs]	2.8253	-0.0273	+0.0273
Bkgr. Dec [Cnts]	28.06	-1.23	+1.23

Left: Time-resolved luminescence decay of **C4** *in a neat film* including the residuals (left, λ_{exc} =376.7 nm). Right: Fitting parameters including pre-exponential factors and confidence limits.

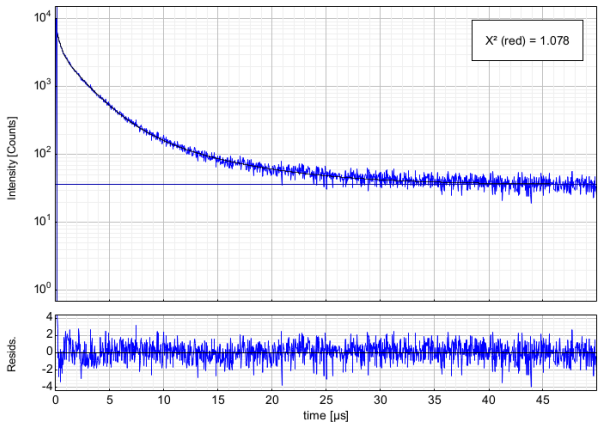

Parameter	Value	Conf. Lower	Conf. Upper
A_1 [Cnts]	2927.1	-51.7	+51.7
τ_1 [µs]	2.1417	-0.0325	+0.0325
A_2 [Cnts]	2709	-182	+182
τ_2 [µs]	0.3557	-0.0291	+0.0291
A_3 [Cnts]	355.0	-13.8	+13.8
τ_3 [µs]	7.427	-0.204	+0.204
Bkgr. Dec [Cnts]	36.18	-1.27	+1.27

Left: Time-resolved luminescence decay of *10%* **C4** *in a PMMA film* including the residuals (left, λ_{exc} =376.7 nm, λ_{em} = 520 nm). Right: Fitting parameters including pre-exponential factors and confidence limits.

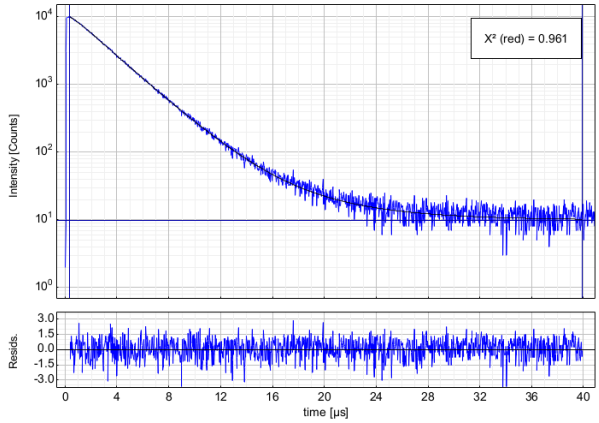

Parameter	Value	Conf. Lower	Conf. Upper
A_1 [Cnts]	212.3	-19.1	+19.1
τ_1 [µs]	6.055	-0.261	+0.261
A_2 [Cnts]	10781.0	-64.4	+64.4
τ_2 [µs]	2.5067	-0.0115	+0.0115
A_3 [Cnts]	-1048	-178	+178
τ_3 [µs]	0.520	-0.117	+0.117
Bkgr. Dec [Cnts]	9.919	-0.774	+0.774

Left: Time-resolved luminescence decay of *10%* **C4** *in a PMMA film* including the residuals (left, λ_{exc} =376.7 nm, λ_{em} = 700 nm). Right: Fitting parameters including pre-exponential factors and confidence limits.

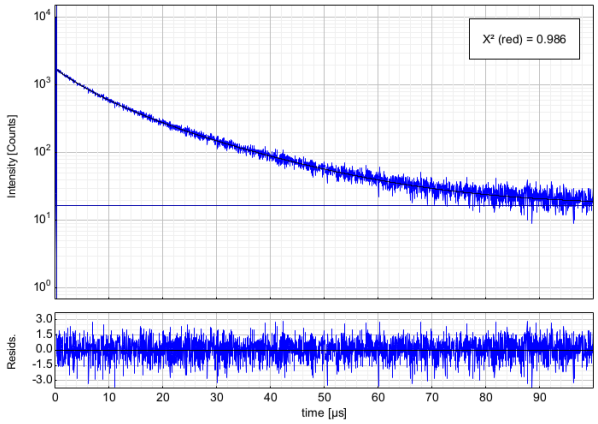

Parameter	Value	Conf. Lower	Conf. Upper
A_1 [Cnts]	665.8	-12.1	+12.1
τ_1 [µs]	17.721	-0.241	+0.241
A_2 [Cnts]	182.0	-46.8	+46.8
τ_2 [µs]	3.006	-0.889	+0.889
A_3 [Cnts]	838.3	-28.3	+28.3
τ_3 [µs]	6.613	-0.226	+0.226
Bkgr. Dec [Cnts]	16.75	-1.11	+1.11

Left: Time-resolved luminescence decay of **C4** *in a frozen CH_2Cl_2/MeOH 1:1 glassy matrix* at *77K* including the residuals (left, λ_{exc} =376.7 nm, λ_{em} = 500 nm). Right: Fitting parameters including pre-exponential factors and confidence limits.

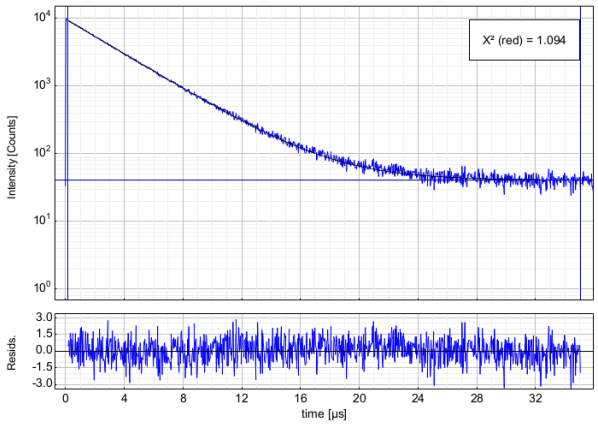

Parameter	Value	Conf. Lower	Conf. Upper
A_1 [Cnts]	9218.1	-51.7	+51.7
τ_1 [µs]	3.3429	-0.0144	+0.0144
Bkgr. Dec [Cnts]	40.91	-1.55	+1.55

Left: Time-resolved luminescence decay of **C4** *in a frozen CH_2Cl_2/MeOH 1:1 glassy matrix* at *77K* including the residuals (left, λ_{exc} =376.7 nm, λ_{em} = 700 nm). Right: Fitting parameters including pre-exponential factors and confidence limits.

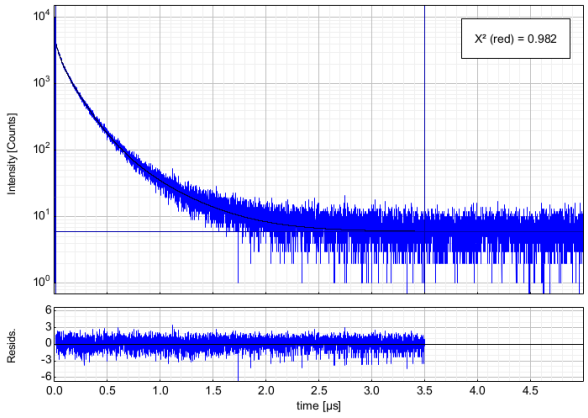

Parameter	Value	Conf. Lower	Conf. Upper
A_1 [Cnts]	270.6	-12.9	+12.9
τ_1 [µs]	0.4221	-0.0116	+0.0116
A_2 [Cnts]	1487	-115	+115
τ_2 [µs]	0.04052	-0.00361	+0.00361
A_3 [Cnts]	2325.6	-43.9	+43.9
τ_3 [µs]	0.14896	-0.00228	+0.00228
Bkgr. Dec [Cnts]	5.985	-0.588	+0.588

Left: Time-resolved luminescence decay of **C4** *in the solid state* including the residuals (left, λ_{exc} =376.7 nm). Right: Fitting parameters including pre-exponential factors and confidence limits.

C5

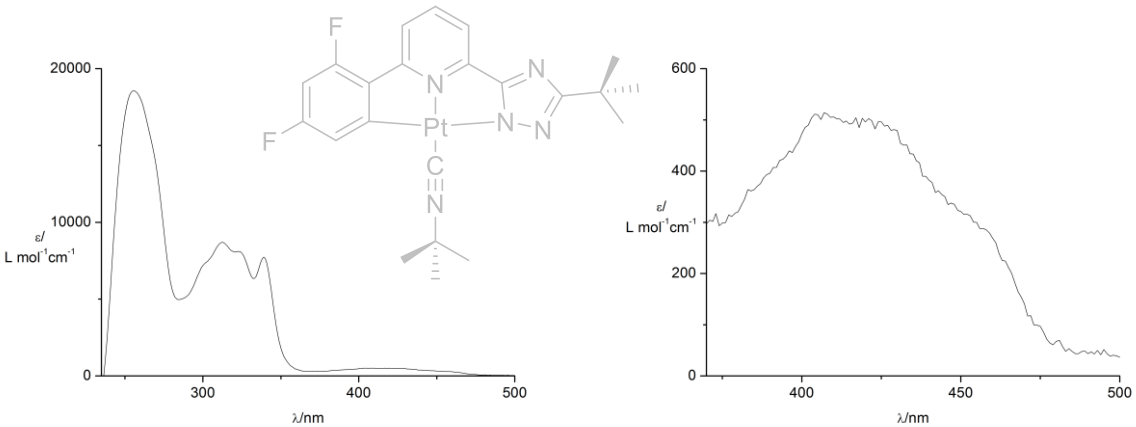

Absorption spectrum of **C5** at room temperature in CH_2Cl_2, 10^{-5} M (the spectral region between 375 nm and 500 nm is displayed on a smaller scale for clarity).

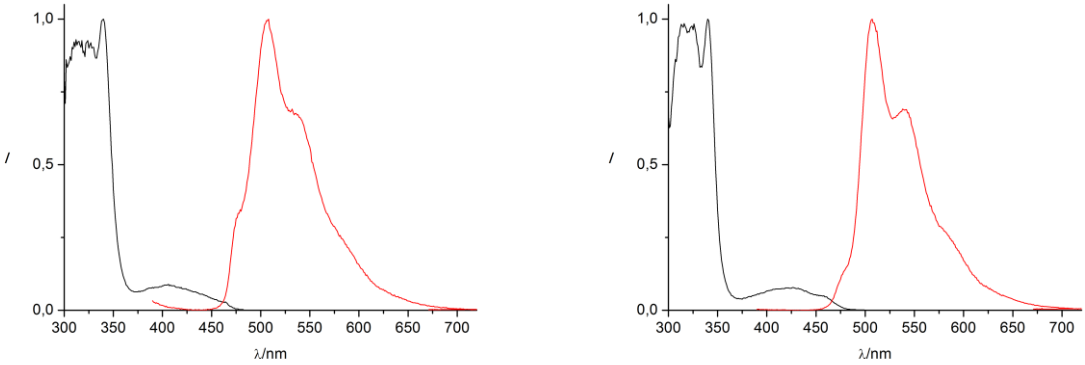

Excitation (black) and *emission* (red) spectra of **C5** in *aerated* (left) and *deaerated* (right) CH_2Cl_2, 10^{-5} M (λ_{exc} = 320 nm; λ_{em} = 540 nm).

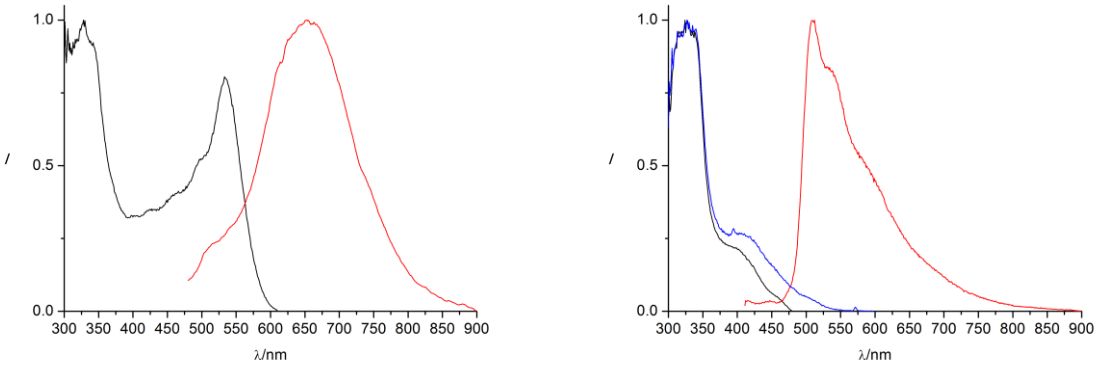

Excitation (black) and *emission* (red) spectra of **C5** in *neat* (left) and *10%* doped into *PMMA* (right) *films* (λ_{exc} = 320 nm; λ_{em} = 540 nm (black); λ_{em} = 700 nm (blue)).

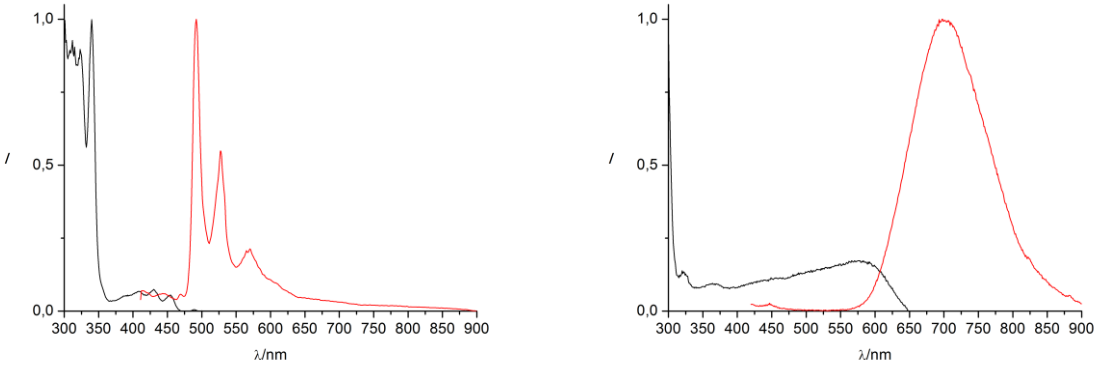

Excitation (black) and *emission* (red) spectra of **C5** in a *frozen glassy matrix at 77 K* (left, CH_2Cl_2/MeOH 1:1, λ_{exc} = 320 nm; λ_{em} = 540 nm) and in the *solid state at room temperature* (right, λ_{exc} = 320 nm; λ_{em} = 540 nm)

	λ_{exc} (nm)	λ_{em} (nm)	Φ_{ph}	$\tau^{a)}$ (µs)	k_r ($10^5 s^{-1}$)	k_{nr} ($10^5 s^{-1}$)
aerated	340	508	0,02	1,10	0,21	8,90
deaerated	340	507	0,73	16,46	0,44	0,17
neat	328	653	0,10	0,70	1,43	12,86
PMMA	324 327	512	0,56	3,30 4,66	1,70 1,20	1,33 0,94
77K	300	492	1	13,50	0,74	-
solid	300	698	0,31	0,65	4,81	10,66

Summary of photophysical data for complex **C5** (written in blue are the data for 700 nm emission). [a]The excitation and emission maxima with the shortest wavelengths are indicated. [b] Amplitude-weighted average lifetimes.

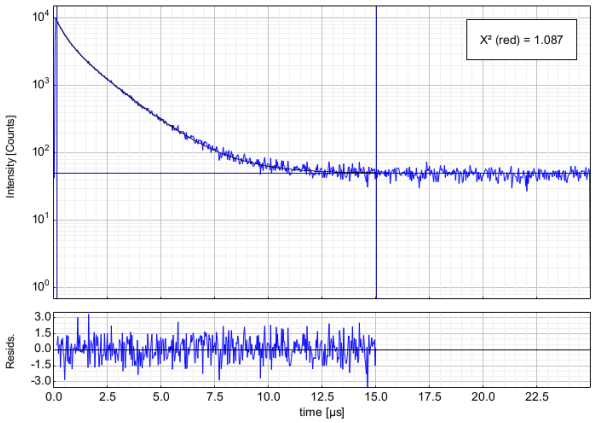

Parameter	Value	Conf. Lower	Conf. Upper
A_1 [Cnts]	4721.3	-37.4	+37.4
τ_1 [µs]	1.67627	-0.00982	+0.00982
A_2 [Cnts]	4110	-107	+107
τ_2 [µs]	0.4331	-0.0129	+0.0129
Bkgr. Dec [Cnts]	50.25	-1.69	+1.69

Left: Time-resolved luminescence decay of **C5** in *aerated* CH_2Cl_2 including the residuals (left, λ_{exc} =376.7 nm). Right: Fitting parameters including pre-exponential factors and confidence limits.

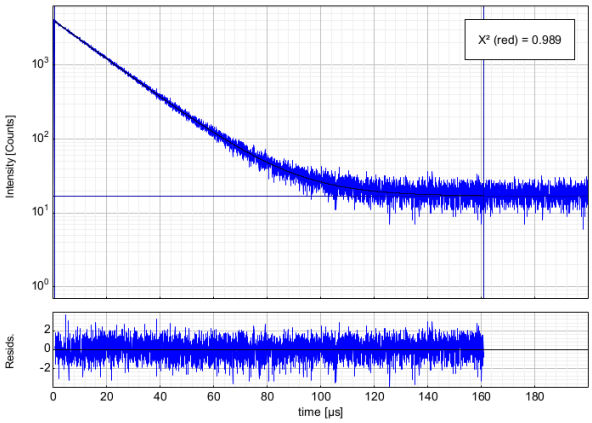

Parameter	Value	Conf. Lower	Conf. Upper
A_1 [Cnts]	3901.8	-31.0	+31.0
τ_1 [µs]	16.456	-0.100	+0.100
Bkgr. Dec [Cnts]	16.94	-1.02	+1.02

Left: Time-resolved luminescence decay of **C5** in *deaerated* CH_2Cl_2 including the residuals (left, λ_{exc} =376.7 nm). Right: Fitting parameters including pre-exponential factors and confidence limits.

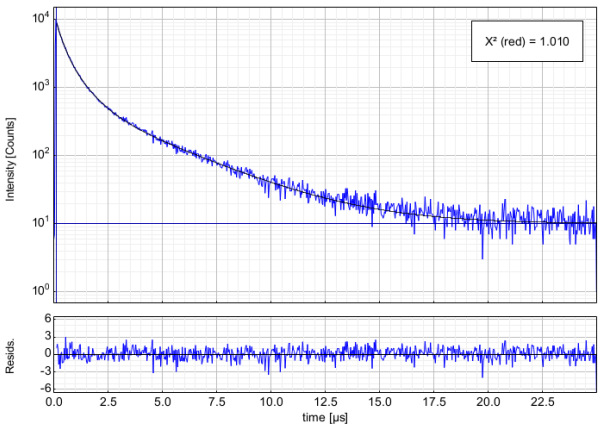

Parameter	Value	Conf. Lower	Conf. Upper
A_1 [Cnts]	4556	-161	+161
τ_1 [µs]	0.2747	-0.0107	+0.0107
A_2 [Cnts]	3494.9	-75.6	+75.6
τ_2 [µs]	0.7473	-0.0137	+0.0137
A_3 [Cnts]	710.6	-15.9	+15.9
τ_3 [µs]	3.1448	-0.0458	+0.0458
Bkgr. Dec [Cnts]	10.023	-0.788	+0.788

Left: Time-resolved luminescence decay of **C5** *in a neat film* including the residuals (left, λ_{exc} =376.7 nm, λ_{em} = 700 nm). Right: Fitting parameters including pre-exponential factors and confidence limits.

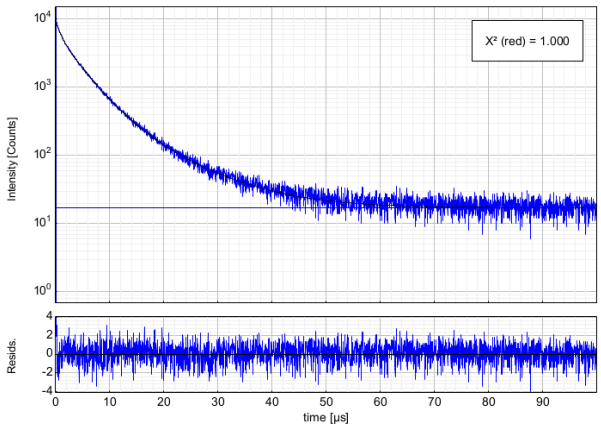

Parameter	Value	Conf. Lower	Conf. Upper
A_1 [Cnts]	6131.1	-70.7	+70.7
τ_1 [µs]	1.4346	-0.0143	+0.0143
A_2 [Cnts]	1552	-166	+166
τ_2 [µs]	0.4020	-0.0533	+0.0533
A_3 [Cnts]	1498.7	-30.7	+30.7
τ_3 [µs]	3.1808	-0.0408	+0.0408
Bkgr. Dec [Cnts]	33.54	-1.22	+1.22

Left: Time-resolved luminescence decay of *10%* **C5** *in a PMMA film* including the residuals (left, λ_{exc} =376.7 nm, λ_{em} = 520 nm). Right: Fitting parameters including pre-exponential factors and confidence limits.

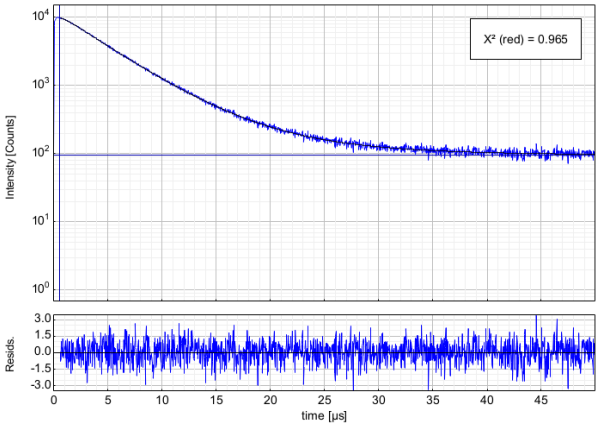

Parameter	Value	Conf. Lower	Conf. Upper
A_1 [Cnts]	-964	-199	+199
τ_1 [µs]	0.536	-0.153	+0.153
A_2 [Cnts]	703.6	-24.8	+24.8
τ_2 [µs]	8.744	-0.198	+0.198
A_3 [Cnts]	9942.2	-58.5	+58.5
τ_3 [µs]	3.9671	-0.0196	+0.0196
Bkgr. Dec [Cnts]	95.62	-2.09	+2.09

Left: Time-resolved luminescence decay of *10%* **C5** *in a PMMA film* including the residuals (left, λ_{exc} =376.7 nm, λ_{em} = 700 nm). Right: Fitting parameters including pre-exponential factors and confidence limits.

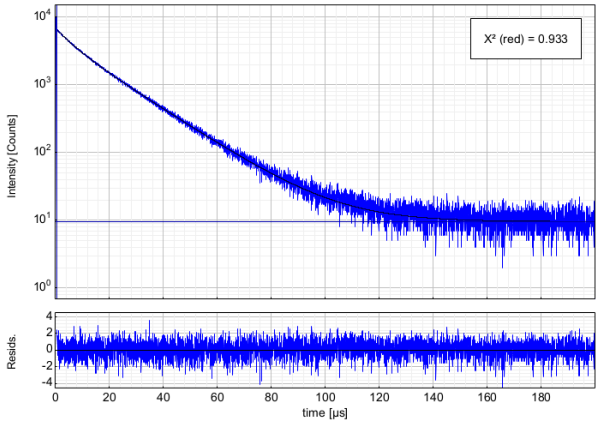

Parameter	Value	Conf. Lower	Conf. Upper
A_1 [Cnts]	4489.1	-37.9	+37.9
τ_1 [µs]	16.803	-0.101	+0.101
A_2 [Cnts]	1947.2	-87.3	+87.3
τ_2 [µs]	5.883	-0.289	+0.289
Bkgr. Dec [Cnts]	9.593	-0.735	+0.735

Left: Time-resolved luminescence decay of **C5** *in a frozen CH_2Cl_2/MeOH 1:1 glassy matrix* at *77K* including the residuals (left, λ_{exc} =376.7 nm). Right: Fitting parameters including pre-exponential factors and confidence limits.

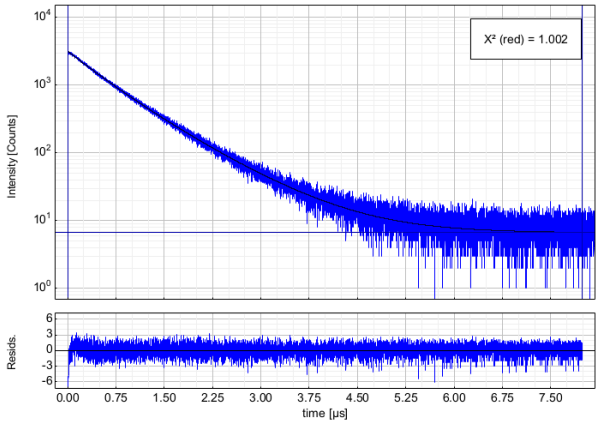

Parameter	Value	Conf. Lower	Conf. Upper
A_1 [Cnts]	1311.0	-23.2	+23.2
τ_1 [µs]	0.85281	-0.00958	+0.00958
A_2 [Cnts]	1974.2	-39.4	+39.4
τ_2 [µs]	0.48749	-0.00881	+0.00881
A_3 [Cnts]	-170.6	-36.0	+36.0
τ_3 [µs]	0.5449	-0.0964	+0.0964
Bkgr. Dec [Cnts]	6.634	-0.685	+0.685

Left: Time-resolved luminescence decay of **C5** *in the solid state* including the residuals (left, λ_{exc} =376.7 nm). Right: Fitting parameters including pre-exponential factors and confidence limits.

5 OLED fabrication

5.1 Frontier Orbitals. The electrochemical behaviour of complex **C2** was investigated by cyclic voltammetry. The characterisation was performed on a Princeton Applied Research potentiostat/galvanostat model 283 voltammetric analyser in methylene chloride solutions at a scan rate of 100 mV/s with tetrabutylammonium hexafluorophosphate (TBAH, 0.1 M) as supporting electrolyte. The concentration of the complex was 0.5 mM. A platinum plate was employed as working electrode, a silver wire as the reference electrode and a platinum wire as the counter electrode. The reference electrode was calibrated at the end of each experiment against the ferrocene/ferricenium couple.

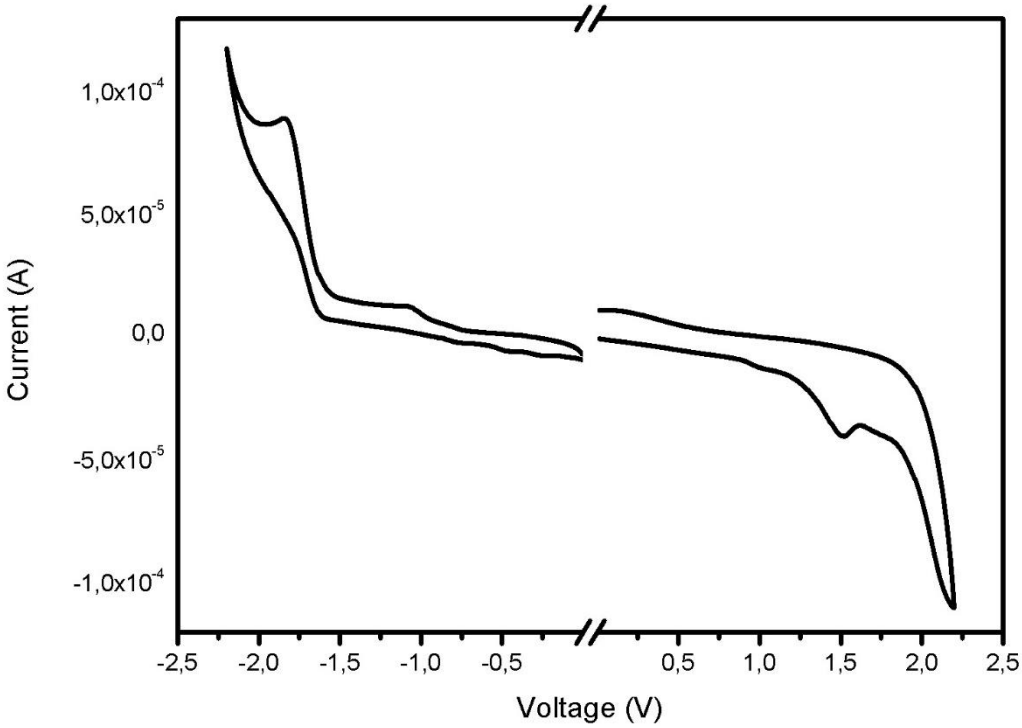

Figure S6. *Cyclic voltammogram of complex **C2**.*

UV Photoelectron Spectroscopy (UPS) was measured on a Riken Keiki AC-2 system using low-energy electron counter method with a deuterium lamp as the light source and a grating type monochromator as the spectrometer.

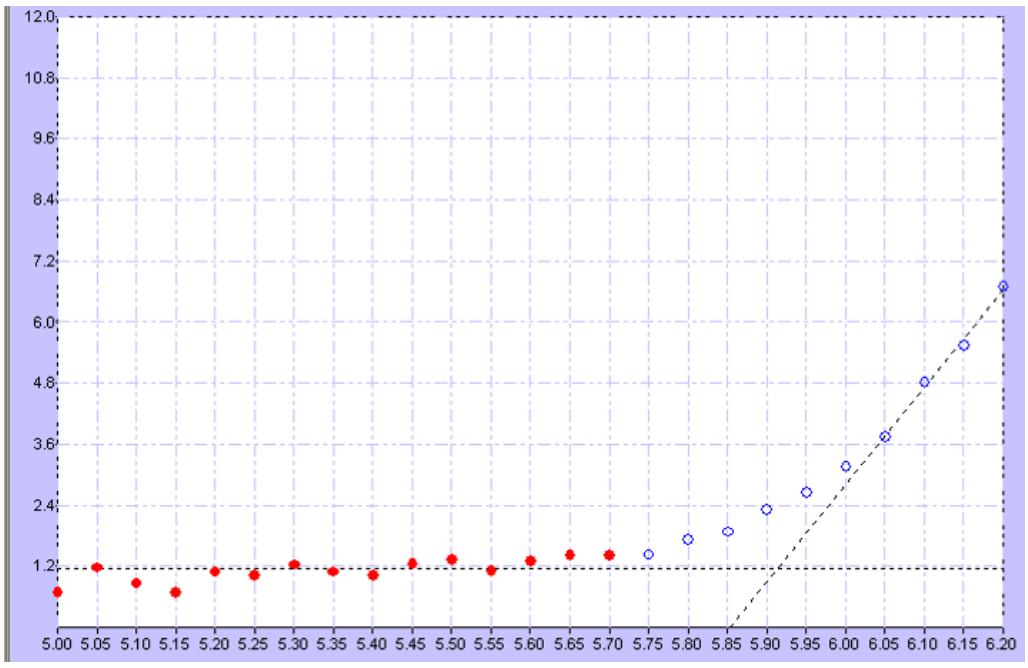

Figure S7. *UPS spectra for complex **C2**.*

E_{ox}(HOMO)[a]	E_{red}(LUMO)[a]	$\Delta E_{HOMO-LUMO}$
1.27 V	-1.62 V	2.89 eV
(-5.57 eV)	(-2.68 eV)	
HOMO[b]	LUMO[c]	$\Delta E_{HOMO-LUMO}$
-5.91 eV	-2.44 eV	3.47 eV

Table S7. *[a]Solution of 0.5 mM Complex **C2** in DCM/0.1 M TBAF were investigated. [b]The HOMO levels of dropcasted films were measured by UPS. [c]Calculated by HOMO(UPS) - Absorption(onset)*

5.2 Film and device Fabrication.

Films**:** For the synthesis of the host material, poly(N-vinylcarbazole) (PVK, 120 mg) and 1,3-bis[5-(4-*tert*-butylphenyl)-1,3,4-oxadiazol-2-yl]benzene (OXD-7, 60 mg) were combined in 20 mL dichloroethane and stirred overnight at roomtemperature. Films, neat and doped with 10 wt-% of complex **C2**, were made on quartz substrates using drop casting methods and were recorded with a UV-vis spectrophometer (Agilent 8453). Steady state emission spectra were recorded with an Edingburgh Instruments spectrofluorimeter (FLSP920).

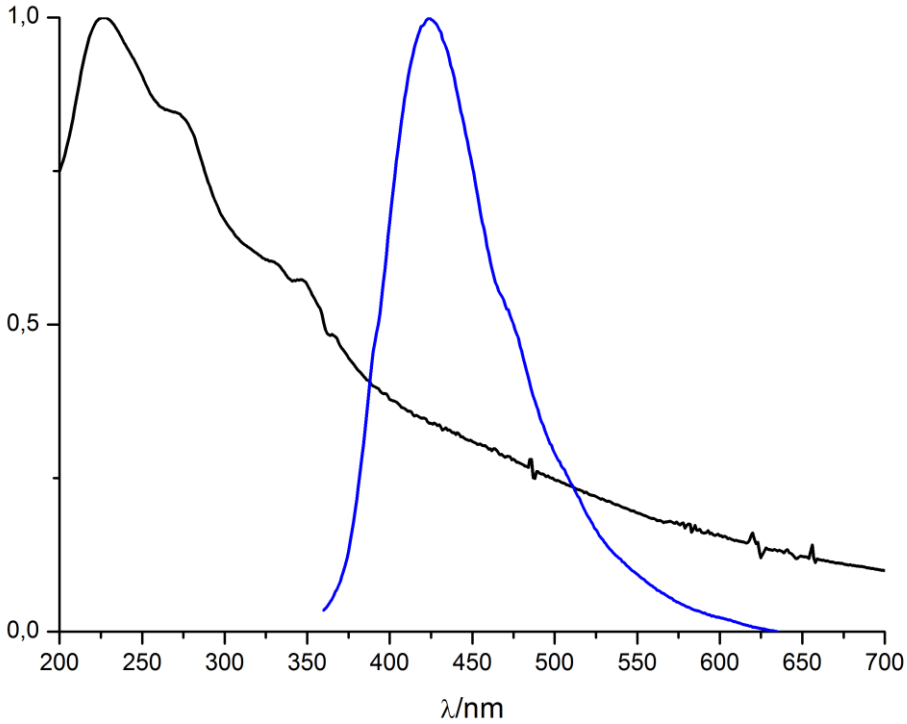

Figure S8. *Absorption spectrum of **C2** (black) and emission spectrum of the host material PVK : OXD-7 (blue) in neat films.*

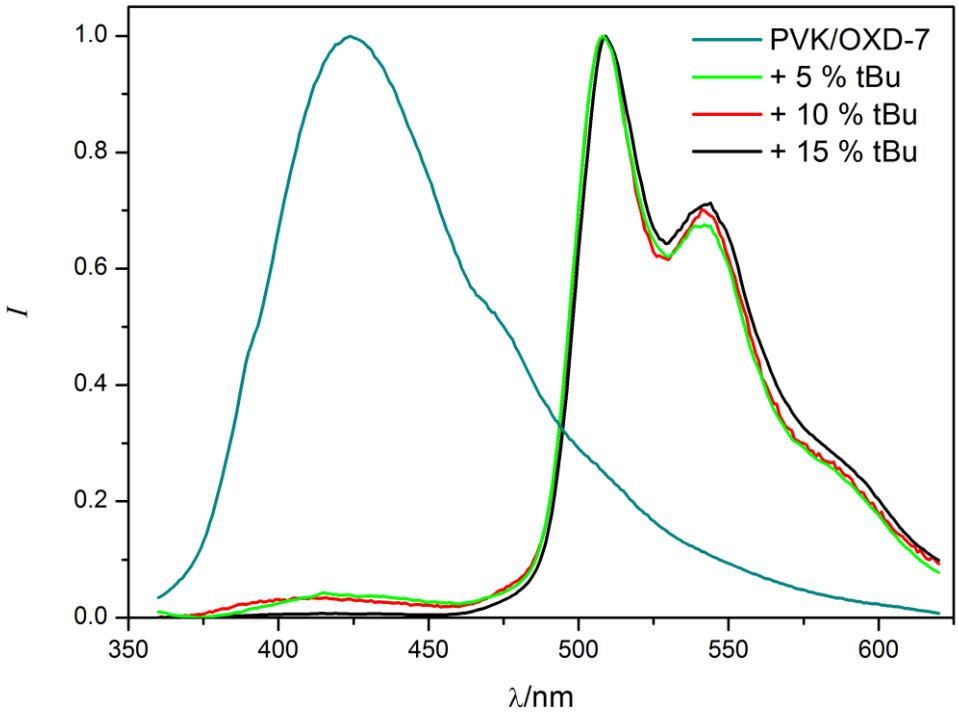

Figure S9. *Photoluminescence spectra of the neat host material PVK : OXD-7 (blue) and host material doped with 10% of complex **C2**.*

OLEDs: Indium-tin oxide (ITO) substrates with a sheet resistance of 15 Ω/sq were thoroughly cleaned using chemical and UV-ozone methods before the organic layers were deposited. For optimisation purposes a simple spin coated device structure was chosen (ITO / (PEDOT:PSS) / PVK:OXD-7:x% **C2** / Cs_2CO_3 / Al), where the conducting polymer PEDOT:PSS was used as the hole-injection layer, OXD-7 was mixed into the host material as electron-transporting layer and Cs_2CO_3 was used as the electron injection layer. First, the doping level of the platinum phosphor was varied at four different weight concentrations (x% = 2.5%, 5%, 10%, and 15%). The best performances of the devices are achieved at the doping level of 5 wt % dopant concentration. The Comission International de L´Eclairage (CIE) colour coordinate for the devices with 10 wt-% is (0.30, 0.60) and the turn on voltage is 7.3 V. The maximum current efficiency for this setup is around 4.85 cd/A and the EQE are around 1.9 %. To improve the device characteristics, spin coated devices with an additional ETL/HBL layer (TPBi) were build (ITO / (PEDOT:PSS) / PVK:OXD-7:5 wt % **C2** / TPBi / Cs_2CO_3 / Al)

showing increased EQE up to 6.9 %, lower turn on voltages of 6.3 V and higher maximum current efficiencies around 21.8 cd/A. First, a poly(3,4-ethylenedioxythiophene:polystyrene sulfonate) (PEDOT:PSS, Heraeus, CLEVIOS™ P VP CH 8000) solution was spin-coated onto the ITO substrate in air and baked at 200 °C for 10 min (60 nm). After transferring the substrate in a nitrogen-atmosphere glovebox, a solution of PVK / OXD-7 and *x* wt-% complex **C2** (*x* = 5,10, 15) in 1,2-dichloroethane was spin-coated onto the PEDOT/PSS-coated substrate as the light-emitting layer and baked at 80 °C for 30 min (85 nm). Afterwards the substrate was transferred into an evaporation chamber, where 1,3,5-tris(*N*-phenylbenzimidazole)benzene (TPBI) was evaporated at an evaporation rate of 1-2 Å s^{-1} under a pressure of 4 x 10^{-4} Pa and the Cs_2CO_3 (2 nm) / Al (150 nm) bilayer cathode was evaporated at evaporation rates of 0.2 and 8-10 Å s^{-1} for Cs_2CO_3 and Al, respectively, under a pressure of 1 x 10^{-3} Pa.

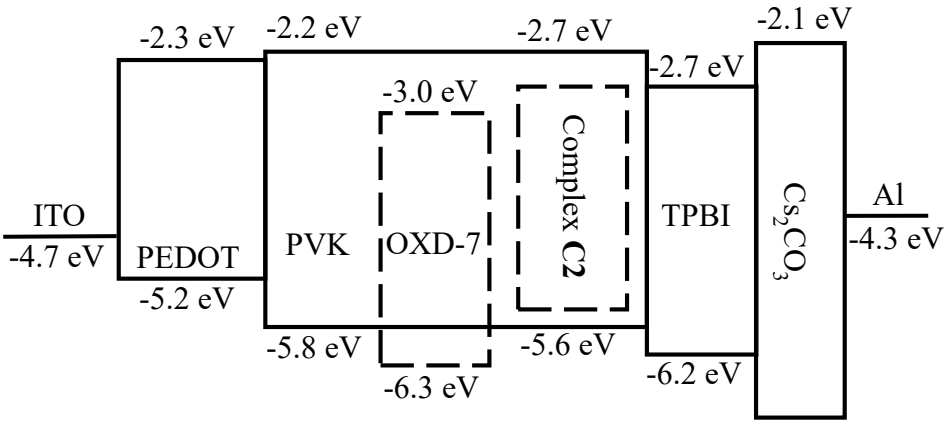

Figure S10. *Device structure and energy level diagram of the materials used for spin coated processed devices*

The device structure of the thermal evaporation processed OLEDs was ITO/HATCN (5 nm)/NPB (35 nm)/TCTA (5 nm)/26DCzPPy (11 nm): 5 or 10 wt-% complex **C2** / Bphen (30 nm)/LiF (2 nm)/Al (150 nm). The OLEDs were fabricated by thermal evaporation under high vacuum (~7×10^{-4} Pa) where HATCN was used as a hole injection layer, NPB used as a hole transport layer, TCTA as an electron blocking layer, BPHEN as an electron transport layer/hole blocking layer and LiF as electron injection layer. The best performances were achieved with 10 wt-% of the complex **C2**. With turn on voltages of 5.7 V, maximum current efficiencies of 10.4 cd/A and EQE around 3.3 % the devices proof the concept for the stability of the compound **C2**, nevertheless the device setup is not optimized, which explains the rather low performances. However the CIE colour coordinates, as well as the EL spectra of the thermal evaporation processed device coincide with the spin coated processed ones. Also there is no

host emission in the EL spectra recognizable, indicating an efficient energy transfer from the host to the dopant.

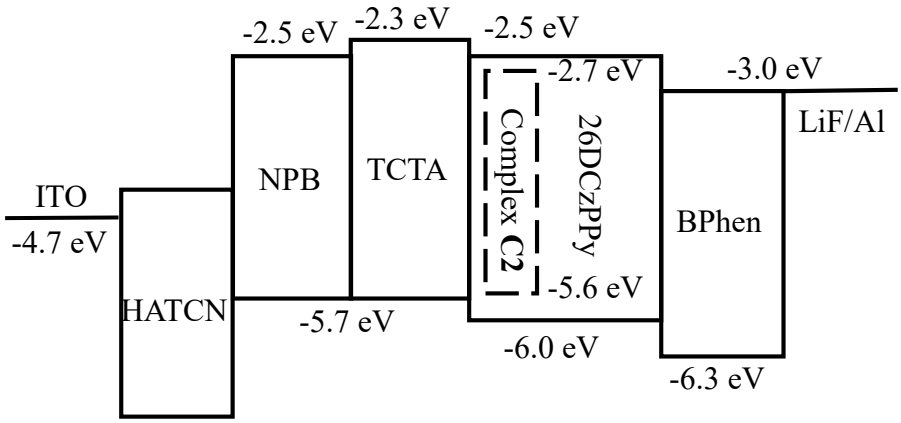

Figure S11. *Device structure and energy level diagram of the materials used for sublimation processed devices*

5.3 Device Characterization. The current-voltage-brightness characteristics of the devices were recorded with a Keithley 4200 semiconductor characterization system whereas the EL spectra were collected with a Photo Research PR705 spectrophotometer. All measurements of the devices were carried out in an ambient atmosphere without further encapsulation.

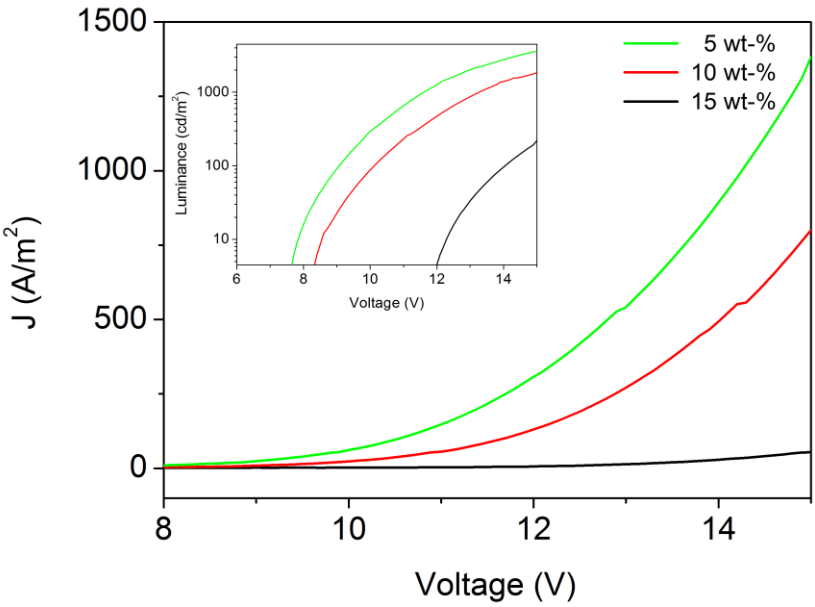

Figure S12. *Current density-voltage characteristics of spin coated processed OLEDs with different doping concentrations of complex* ***C2****. The inset shows the corresponding brightness-voltage curves of the devices.*

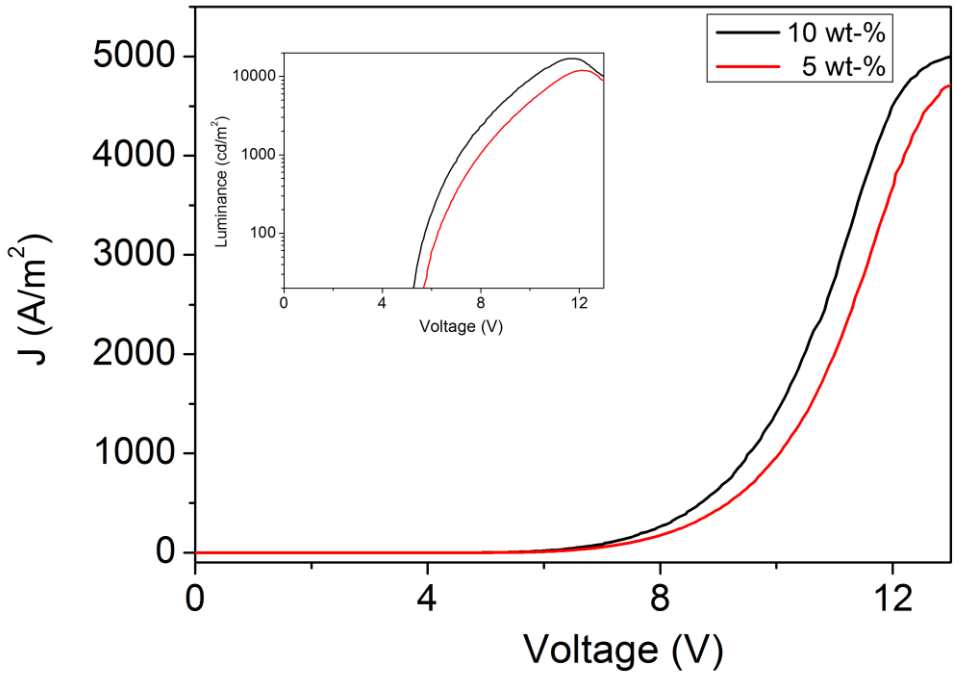

Figure S13. *Current density-voltage characteristics of sublimation processed OLEDs with different doping concentrations of complex* ***C2****. The inset shows the corresponding brightness-voltage curves of the devices.*

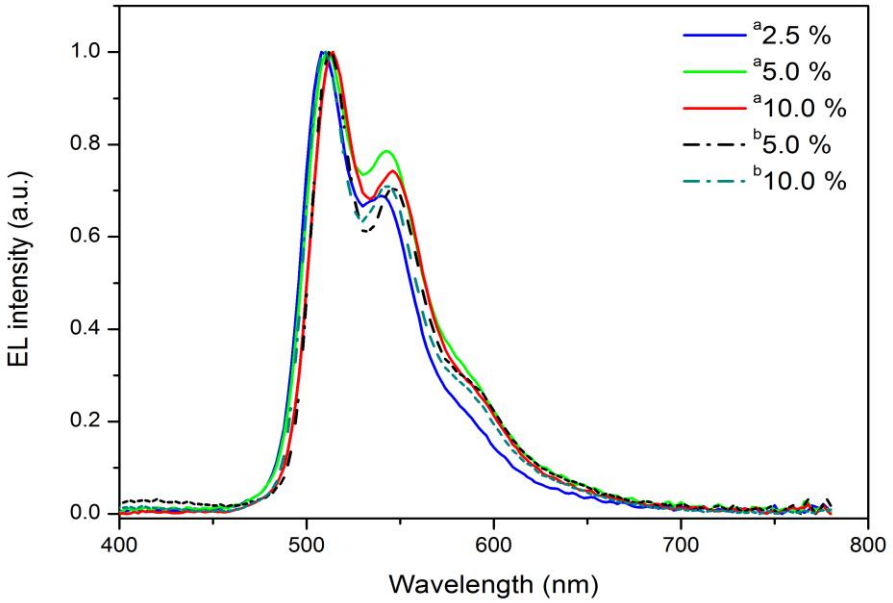

Figure S14. *EL spectra of* [a]*spin coated (solid) and* [b]*thermal evaporation (dashed) processed OLEDs with different doping concentrations of complex* ***C2****.*

wt - %	$V_{turn-on}$ / V	$h_{L,max}$ / cd A^{-1}	EQE (%)	l_{em} / nm	CIE (*x*, *y*)
2.5[a]	6.6	3.28	0.99	508	(0.27, 0.62)
5 [a]	6.7	4.75	1.47	512	(0.21, 0.55)
10 [a]	7.3	4.85	1.89	514	(0.30, 0.62)
15 [a]	10.2	3.67	1.12	514	-
5 + TPBI [a]	6.3	21.86	6.86	512	(0.29, 0.61)
5[b]	6.3	6.13	1.93	511	(0.30, 0.59)
10 [b]	5.7	10.01	3.18	510	(0.29, 0.60)

Table S8. *Electrical characteristics of [a]spin-coated or [b]sublimation processed devices based on complex **C2** for with different doping concentrations*